



VCU

Virginia Commonwealth University
VCU Scholars Compass

Theses and Dissertations


Graduate School

2019

Examination of Strain-Dependent Differences in *S. sanguinis* Virulence and Growth

Shannon Baker
Virginia Commonwealth University

Follow this and additional works at: <https://scholarscompass.vcu.edu/etd>

 Part of the [Bacteria Commons](#), [Bacterial Infections and Mycoses Commons](#), [Cardiovascular Diseases Commons](#), [Disease Modeling Commons](#), and the [Oral Biology and Oral Pathology Commons](#)

© The Author

Downloaded from

<https://scholarscompass.vcu.edu/etd/5707>

This Dissertation is brought to you for free and open access by the Graduate School at VCU Scholars Compass. It has been accepted for inclusion in Theses and Dissertations by an authorized administrator of VCU Scholars Compass. For more information, please contact libcompass@vcu.edu.

**© Shannon Paige Baker (2019)
All Rights Reserved**

Examination of strain-dependent differences in *S. sanguinis* virulence and growth
A dissertation submitted in partial fulfillment of the requirements for the degree of Doctor
of Philosophy at Virginia Commonwealth University

By

SHANNON BAKER

B.S., Clemson University, 2013

Director: TODD KITTEN, PH.D.

PROFESSOR, PHILIPS INSTITUTE, SCHOOL OF DENTISTRY

Virginia Commonwealth University

Richmond, Virginia

February, 2019

Table of Contents

| | |
|--|-------------|
| Acknowledgements | i |
| List of Tables | iii |
| List of Figures | iv |
| List of Abbreviations | vi |
| Abstract | viii |
| CHAPTER 1 | 1 |
| Introduction | 1 |
| The Human Oral Microbiome..... | 1 |
| The Streptococci..... | 2 |
| Infective Endocarditis..... | 3 |
| <i>Streptococcus sanguinis</i> | 6 |
| Virulence..... | 8 |
| Model of Infective Endocarditis | 10 |
| Research Objective | 11 |
| CHAPTER 2 | 13 |
| General Material and Methods | 13 |
| Bacterial Strains and Growth Conditions | 13 |
| DNA Manipulation..... | 13 |
| Transformation | 14 |
| Rabbit Model of IE | 15 |
| ICP-OES..... | 16 |
| Statistical Analyses..... | 17 |
| CHAPTER 3 | 18 |
| Genomic, phenotypic, and virulence analysis of <i>Streptococcus sanguinis</i> oral and infective endocarditis isolates..... | 18 |
| Materials and Methods | 20 |
| Sequence Information | 20 |
| Bioinformatic Analyses | 20 |
| Strain Construction | 21 |
| Modification of Rabbit Model | 24 |
| DNA Isolation..... | 24 |
| Barcode Sequencing and Quantitation..... | 25 |
| Bacteriocin Assays | 25 |
| Biofilm Assay | 26 |
| <i>In vitro</i> strain competition assays | 26 |
| Rationale | 18 |
| Introduction | 18 |
| Results | 20 |
| Genomic Overview | 28 |
| Phylogenetic Analyses..... | 29 |
| Identification of Putative Virulence Genes and their Examination <i>In Vivo</i> | 30 |
| Strain Identification and Construction | 34 |
| Pooled virulence analysis by Bar-seq..... | 38 |

| | |
|---|------------|
| Phenotypic Assays | 43 |
| Bacteriocin Production | 43 |
| Biofilm Formation..... | 44 |
| Cell-Associated Manganese Content | 45 |
| Virulence Analysis of ATCC 10556..... | 46 |
| Virulence Analysis of SK330..... | 48 |
| Discussion | 52 |
| CHAPTER 4..... | 55 |
| Loss of an integral membrane protein restores serum growth to manganese-deficient <i>Streptococcus sanguinis</i> | 55 |
| Materials and Methods | 58 |
| DNA Isolation and Whole-Genome Sequencing | 58 |
| Bioinformatic Analyses | 60 |
| RNA Preparation and RNA-seq Analysis | 60 |
| Rationale | 55 |
| Introduction | 55 |
| Results | 61 |
| Complementation of manganese-transport deficient <i>S. sanguinis</i> | 61 |
| Spontaneous Δ <i>ssaACB</i> Reversion Mutants..... | 63 |
| Suppressor Mutant Isolation and Whole-Genome Sequencing | 63 |
| SSA_0696 Is Responsible for the Suppressor Phenotype..... | 65 |
| Investigation of SSA_0696 Suppression Mechanism | 69 |
| Discussion..... | 76 |
| Chapter 5..... | 83 |
| General Discussion | 83 |
| Literature Cited:..... | 87 |
| Vita..... | 101 |

Acknowledgements

I'd like to thank Dr. Todd Kitten, who has truly been a remarkable mentor. From our first formal lab interactions reviewing data to our now informal discussions across the lab from his office and my desk chair, I'm incredibly appreciate of his adaptability, advice and general willingness and interest in my graduate experience, both in lab and beyond. His patience and kind support has been integral in my development as a scientist and as a person.

I am also grateful for the support of my committee, who have helped guide my graduate education, focused my research plan, and provided letters of support in all of my many funding endeavors. Additional faculty and staff have been instrumental in maintaining my research momentum. Our lab manager Seon-Sook has always tirelessly ordered everything I asked for, Nicai Zollar has always loaned me any reagents I may need and helped with all of our rabbit surgeries, and Dr. Turner has always been available to help train and re-train me on each iteration of the ICP-OES and ICP-MS equipment within the Chemistry department. I would also like to thank the faculty and staff of the Philips Institute and Microbiology and Immunology, especially Martha VanMeter and Margaret Poland for making sure I did any and all pesky administrative paperwork on time.

Lastly, I would like to acknowledge my family who has spent countless hours listening to me talk about my progress in the graduate program and my various projects over the years. I am so grateful to my mother, Wanda Baker, and father, Wilbur Wise, who instilled in me both a powerful work ethic and desire to learn. Without the strong foundations they provided, my quest for a PhD would not have been possible. My

fiancé, Ryan Green, has been instrumental in helping me to accomplish so much. His support and encouragement has shown me that I really can overcome immunology and biochem class and that I really need someone to tirelessly edit my papers for conciseness. Additionally, I'd like to thank Ryan's parents, RC and Lisa Green for their support, especially with regards to dinner. Without them, there would have been many more unappetizing dinners of cereal, as trips to the grocery store gave way to extra hours in lab.

For everyone here and those that I may not have mentioned by name, I thank you. It truly takes a village to raise a PhD.

List of Tables

Table 3.1 Strains used in this study.

Table 3.2 Bioinformatic sort based on strain origin

Table 3.3 Raw and normalized Bar-seq data

Table 3.4 Plate counts of each strain present in inoculum

Table 3.5 Candidate virulence genes.

Table 4.1 Strains used in this study.

Table 4.2 Strain genealogy and SNP-related information

List of Figures

FIG 3.1 Cluster analysis of 19 genomes by PGAP in GF mode.

Fig. 3.2 Graphical representation of core genome and unique genes.

FIG 3.3 Pan-genome based phylogram

FIG 3.4 Selection of a conserved intergenic region (CIR) for insertion of exogenous DNA into *S. sanguinis* strains.

FIG 3.5 Examination of SK36 derivatives in a rabbit model of IE.

FIG 3.6 Examination of SK36 and SK405 derivatives in a rabbit model of IE.

FIG 3.7 Use of a conserved intergenic region for barcode insertion.

FIG 3.8 Misidentified GenBank WGS sequences as determined by our analysis.

Fig 3.9 Growth of *S. sanguinis* parent and marked strains in rabbit serum in 12% O₂.

FIG 3.10 Examination of marked strains in a rabbit model of IE.

Fig 3.11 Bacteriocin production by agar overlay assay.

FIG 3.12 *S. sanguinis* biofilm production.

FIG 3.13 Cell-associated manganese content of *S. sanguinis* strains.

FIG 3.14 SK1.

FIG 3.15 Competition studies in pooled serum and on blood agar.

FIG 3.16 Schematic of a RM system and identified iterations found in SK330.

Fig 4.1 Investigations of an Δ *ssaACB* mutant and its complemented derivative.

Fig 4.2 Growth of suppressor mutants and parental strains

Fig 4.3 The role of individual SNPs identified by WGS on the suppressor phenotype.

Fig 4.4 Graphical representation of SSA_0696 in the suppressor phenotype.

Fig 4.5 The contribution of SSA_0695 and SSA_0696 to serum growth.

Fig 4.6 The role of SSA_0696 in SK49.

Fig 4.7 Metal content of an Δ SSA_0696 mutant.

Fig 4.8 The role of an ECF transport system in the suppressor phenotype.

Fig 4.9 Examination of an Δ SSA_0696 mutant in a rabbit model of IE.

Fig 4.10 Effect of aging serum on the suppressor phenotype.

Fig 4.11 Predicted topology and location of suppressing mutations in SSA_0696.

List of Abbreviations

| | |
|-----------------|----------------------------------|
| % | percentage |
| °C | degrees Celsius |
| µg | microgram |
| µl | microliter |
| ml | milliliter |
| x <i>g</i> | times gravity |
| A | absorbance |
| ABC | ATP-binding cassette |
| ANOVA | analysis of variance |
| BHI | brain heart infusion |
| BM | biofilm media |
| bp | base pair |
| CFU | colony forming units |
| Cm ^r | chloramphenicol resistance |
| Sc ^r | spectinomycin resistance |
| Tc ^r | tetracycline resistance |
| Km ^r | kanamycin resistance |
| CSP | competence stimulating peptide |
| C-terminus | carboxyl-terminus |
| CV | crystal violet dH ₂ O |
| DNA | deoxyribonucleic acid |
| h | hour |

| | |
|---------|--|
| min | minute |
| HS | horse serum |
| IE | infective endocarditis |
| NVE | native valve endocarditis |
| PCR | polymerase chain reaction |
| PBS | phosphate buffered saline |
| RT | room temperature |
| SOEing | splicing by overlap extension |
| WT | wild-type |
| ICP-OES | inductively coupled plasma optical emission spectroscopy |
| RM | restriction modification |
| MT | methyltransferase |
| MLSA | multi-locus sequence analysis |
| ECF | energy coupling factor |
| BHT | butylated hydroxytoluene |

Abstract

Examination of Strain-Dependent Differences in *S. sanguinis* Virulence and Growth

By: Shannon Baker, B.S.

A dissertation submitted in partial fulfillment of the requirements for the degree of Doctor
of Philosophy at Virginia Commonwealth University

Clemson University, 2013

Major Director: Todd Kitten, PH.D.

Professor, Philips Institute, School of Dentistry

Streptococcus sanguinis, an abundant and benign inhabitant of the oral cavity, is an important etiologic agent of infective endocarditis, particularly in people with pre-disposing cardiac valvular damage. Although commonly isolated from patients with IE, little is known about the factors that make any particular *S. sanguinis* isolate more virulent than another or, indeed, whether significant differences in virulence exist among isolates. To investigate the virulence of multiple isolates, a variation of the Bar-seq (barcode sequencing) method was employed. A conserved chromosomal site was identified for subsequent insertion of a barcode identifier, unique for each strain. Barcode insertion did not affect growth *in vitro* or in a rabbit model of endocarditis. Pooling of these strains and inoculation into rabbits demonstrated that all strains were capable of causing disease; however, virulence varied widely among strains. Genomic comparisons of the more virulent strains versus less virulent strains failed to conclusively identify any single gene responsible for virulence. Given this result, we continued our examination of the manganese transport system SsaACB, which is present in every strain of *S. sanguinis* examined. Although its contribution to virulence has not been confirmed in any strain other than SK36, it has been shown to be required for virulence in multiple species of streptococci, making it a candidate for emerging targeted therapies. In *S. sanguinis* strain SK36, previous studies have confirmed that loss of the manganese transport protein SsaB is tantamount to loss of virulence. Moreover, *ssaB*-deficient mutants are deficient for serum growth—a phenotype we have previously found to be associated with virulence. Our *in vitro* studies of manganese transporter-deficient strain SK36 supported this, but also revealed the emergence of suppressor mutants. In each suppressor mutant that was isolated, mutations were identified that mapped to a common gene, SSA_0696. Deletion of SSA_0696 resulted

in restored *in vitro* growth in the *ssaACB*-deficient background, unearthing a novel mechanism for bacterial growth under manganese limitation. Fortunately, the suppressor mutant phenotype was not maintained *in vivo*; however, the combined results of these experiments suggest the efficacy of future therapeutics may require consideration of virulence at the species level and the incorporation of multiple targets.

CHAPTER 1

Introduction

The Human Oral Microbiome

The term “microbiome”, established by Nobel laureate Joshua Lederberg, refers to a community of microbial residents and is usually associated with a particular anatomical location. Of the microbiomes, the oral cavity is estimated to be the second most complex (1), and is comprised of viruses, protozoa, fungi, archaea and bacteria. Interestingly, the composition of oral fauna has co-evolved with humans. Major milestones in human history such as the advent of agriculture and increased industrial output have ushered in bacterial species better suited to diets high in sugar and acid (2, 3), whereas societal awareness of oral hygiene has more recently led to positive selection for antibiotic-resistant organisms (3). Within the mouth, the bacterial population is incredibly heterogeneous, with an estimated 1000 species present (2), although many have remained uncultivated by current methods (4). Many of these organisms reside on the teeth and back of the tongue, or dorsum. At these sites accumulation can be up to 10^{11} organisms per gram weight (5); however, this density depends on factors including host response, oral hygiene, and food consumption (6).

Although characterized by its diversity, there is a definitive disparity in species diversity and presence between a healthy oral cavity and a dysbiotic one. A dysbiotic profile is characterized by comparatively low species diversity and increased prevalence of species such as *Porphyromonas gingivalis*, *Treponema denticola*, and *Prevotella intermedia* (7). Indeed, the diseased state is most readily identifiable as the environment typically undergoes large changes. For example, the shift from Gram-positive to Gram-

negative organisms is a trademark of periodontitis, inflammation of the gums and supporting structures, and a lower pH is indicative of *Streptococcus mutans* and *Lactobacillus* species. Indicators of good oral health include *Streptococcus sanguinis*, *Streptococcus gordonii*, *Streptococcus intermedius*, and *Streptococcus oralis* (7). In the case of *S. sanguinis* it has been argued that the health benefit is associated with its antagonistic role against *Streptococcus mutans* (8-10), a causative agent of dental caries (11).

The Streptococci

Of all the organisms present within the oral cavity, the genus *Streptococcus* is considered to be best represented (12, 13), especially at early stages of colonization (14). Generally considered to be pioneers (15) and commensals (14) of the oral cavity, these bacteria are Gram-positive, microaerobic, catalase-negative, non-motile and coccoid in form. Early attempts to differentiate the species were based on their hemolytic ability (16). Species that had been thought to partially hydrolyze red blood cells are considered alpha-hemolytic and have a characteristic green halo on blood agar plates; beta-hemolytic species fully lyse red blood cells resulting in a zone of clearance on the plate, whereas gamma-hemolytic species are unable to lyse red blood cells at all. Subsequent studies in *Streptococcus gordonii* however, have dispelled the colorimetric changes in “alpha-hemolytic” streptococci as being attributable to hemolytic activity; instead, hydrogen peroxide has been shown to account for the green color that is observed (17). The Lancefield classification (18), a later attempt to further parse the species, groups based on antigenic differences in cell wall components including carbohydrates, pili-associated proteins and capsule. Subsequent isolation and

identification of numerous new species has made reliance on these classifications less common and current methods have begun to focus on DNA sequencing for reliable identification.

Sequencing of 16S rRNA genes is one such method for species identification; however, many species such as *Streptococcus mitis*, *Streptococcus oralis* and *Streptococcus pneumoniae* are almost identical by this method (19). Therefore, as may be inferred, a robust system of classification of these organisms has remained difficult and has only recently begun to improve. Combining multiple technologies and analyses including: multi locus sequence analysis (MLSA) (20), average amino acid identity (21), codon usage (21), tRNA intergenic lengths (22), and DNA hybridization (23), to name a few, has expanded the known number of streptococcal species from approximately 40 (24) to 99 (21) in a little over a decade.

Infective Endocarditis

Due to the proximity of *S. sanguinis* and other organisms to the oral mucosa, dissemination into the bloodstream is inevitable. This transient bacteremia is the result of traumatic injury to the oral mucosa, caused by oral surgery, eating, and daily oral hygienic practices (25-31). Typically this is not a cause for concern as this bacteremia is usually promptly eliminated by the immune system, hence its transient nature. However, in certain groups, including those with pre-existing heart damage (32), congenital or induced, those with prosthetic heart valves (33), and even neutropenic patients (34), events that may result in bacteremia require prophylactic measures. In these populations, bacterial invasion of the bloodstream can cause disease.

In those with pre-existing cardiac damage or prostheses, bacterial inoculation into the bloodstream can cause the disease infective endocarditis (IE). Characterized as an inflammation of the endocardium due to infection, consequences can be quite severe, with a mortality rate exceeding 30% (35, 36), and can include events such as embolism or stroke (37-39). Despite earlier diagnoses and improved treatment options the mortality rate has not changed over the past 20 years and exceeds that of many common cancers (40). Each year in the US approximately 15,000 new cases of IE are reported (41) and the incidence of disease is increasing (40). A higher incidence of disease is associated with males (42) and the elderly (41), likely due to advances in medicine and increased longevity (43).

Infective endocarditis can be subdivided into separate groups based on cause or area affected: native-valve endocarditis (NVE), prosthetic-valve endocarditis, nosocomial or community acquired endocarditis (44), and intravenous drug use-mediated endocarditis. Further classification, subacute versus acute, distinguishes between a slow or aggressive progression of disease respectively. Of these classifications, subacute NVE is most common (45).

NVE presentation relies on a series of basic steps, the first of which is typically a requirement of pre-existing valvular damage. Although rare, NVE cases where no pre-existing damage was present have occurred (46). The second step necessitates bacteremia, followed by bacterial adherence to the damaged site, initially referred to as the sterile vegetation or nonbacterial thrombotic endocarditis lesion (47). Initially, the sterile vegetation is comprised of platelets and thrombin, but after bacterial attachment, inflammatory immune cells and activated fibrinogen bind to the bacteria. This stabilizes

the vegetation and provides the bacteria with a protected space in which to proliferate (48). Dissemination of these emboli can result in secondary disease manifestations (49, 50) and fatality (51).

Most NVE cases are associated with the mitral or aortic valves, and are classified as left-sided. Infections are almost exclusively monomicrobial (52), with staphylococci being the most common etiologic agent at 44% (49); however, the streptococci constitute approximately one-third of the remaining cases reported (49) and have been argued to be the most common etiological agent in persons of Asiatic descent and in pediatric patients (53). Of the streptococci, *S. sanguinis* is most often identified as the causative agent (54). Initial symptoms, such as malaise, low-grade fever, fatigue, or development of a heart murmur may induce a health care professional to diagnose IE. Peripheral signs can include petechiae, Osler's nodes (painful, erythematous subcutaneous nodules on the tips of the hands and feet) and Janeway lesions (lesions on the palms and soles of the feet) (43, 55).

Diagnosis of IE is based on a combination of subjective symptom descriptions, objective organism identification and diagnostic testing known as the Duke criteria. A positive, blood-based diagnostic result can be met in three ways: typical infective endocarditis organisms are isolated (1) from two separate locations, (2) from the same site on two occasions and separated by at least twelve hours, (3) from three separate blood draws from the same location within one hour. Additional imaging by echocardiography may be ordered to assess valvular dysfunction, vegetation location or damage after a positive blood result. Established in 1994 at Duke University (56), the criteria have since been revised to account for additional species and negative blood

cultures (57). With the revisions and emerging technologies, the sensitivity and specificity of these criteria in correctly diagnosing IE is now greater than 90% (35).

Treatment of IE is challenging and is typically antimicrobial in nature (41, 58, 59); however, surgery may be incorporated to help remove infected material and shorten the timeline of treatment. In a mature streptococcal vegetation, over 90% of the bacteria are metabolically inactive or non-growing (60). In combination with the protected, biofilm-like nature of the infected vegetation, this encourages the use of bactericidal regimens as they are more effective than bacteriostatic ones (61, 62). Drug resistance is of concern, and most recommendations for treatment of NVE suggest 2-6 weeks of antibiotic therapy and greater than 6 weeks for treatment of prosthetic valve IE (63). Regarding antibiotic-sensitive streptococcal IE, the cure rate following recommended regimens is greater than 95% (63).

No vaccines or other prophylactic measures are currently clinically available for prevention of IE. However, several groups have found some success with vaccines in animal models of endocarditis (64-66), and others have begun exploring alternative therapeutic approaches (67, 68). The American Heart Association recommends that high-risk patients practice good oral hygiene and make health care professionals aware of their increased risk of contracting IE. Antibiotic prophylaxis is encouraged and should be administered prior to or within two hours after undergoing procedures that may exacerbate their risk of contracting IE (69).

Streptococcus sanguinis

Of particular interest to the work described herein is the oral commensal *S. sanguinis*. Sequenced in 2006, *S. sanguinis* has a circular chromosome that is both

larger and has a higher G+C content than many other streptococci (70). It is an adaptable organism, having numerous pathways for fermentation and energy production, amino acid production, lipid biosynthesis and cell wall biosynthesis (70). Interestingly, some studies suggest approximately 12% of the genome may be a result of horizontal gene transfer (70). Of note, the *eut* locus appears to have been obtained in this manner. Related to the utilization of ethanolamine as a carbon and energy source, this locus is present in few other streptococci; however, when present, it is more common to oral pathogens (70). Further supporting the genetic plasticity of the species, a recent study identified 35 instances of up to 9 different phage ranging in size from 7.5 to 51.6 kb in the genomes of 19 examined *S. sanguinis* strains (71).

In the oral cavity, *S. sanguinis* is a pioneer species whose colonization is correlated with the arrival of the first tooth, typically by 9 months of age (72). Although predominantly associated with the tooth surface (73), it is also present on the oral mucosa (74) and in saliva (75). After eruption of the tooth it binds to salivary proteins, IgA and α -amylase, and glycoproteins that coat the tooth surface (72, 76). As *S. sanguinis* proliferates, it secretes H_2O_2 as a byproduct of its metabolism. This serves as a deterrent to the colonization of several other species, including the cariogenic *S. mutans* (10, 77, 78). In fact, studies have shown that when *S. sanguinis* colonization precedes *S. mutans*, it can delay the deleterious effects of *S. mutans* (79) by 6 months (72). In spite of its defensive capability, numerous species are able to colonize the tooth surface and *S. sanguinis* itself, establishing the oral biofilm.

Virulence

Surface-exposed proteins that mediate bacterial attachment to the sterile vegetation have been suggested as the first virulence factors for IE pathogenesis. In fact, they are thought to account, at least in part, for the prevalence of bacterial induced IE (80). This has been attributed to the ability of these proteins, namely SrpA in *S. sanguinis*, to bind exposed sialylated proteins on platelets that have accumulated at the sterile vegetation site. Of note, it is this same interaction (binding sialylated proteins on the tooth surface) that contributes to successful colonization of *S. sanguinis* in the oral cavity (81). Interestingly however, unlike the surface proteins of other streptococci and notable IE pathogens like *Staphylococcus aureus*, individual adhesins in *S. sanguinis* were demonstrated to only moderately affect virulence in a rabbit model of IE (82). This has been attributed to differences in structure (83) and perhaps, functional redundancy, as *S. sanguinis* is predicted to have more of these proteins than other related species (82).

The next step in the progression of IE relies on the ability of *S. sanguinis* to evade the immune system and proliferate. To this end, *S. sanguinis* stimulates platelet aggregation (84-88). In effect, this provides the bacteria with a platelet cloak of invisibility, as they no longer resemble a foreign invader, but rather the host itself. Beyond immune evasion, platelet aggregation has been implicated in clinically severe cases of IE, as resulting infectious vegetations tend to be larger and the risk for associated comorbidities increases (89).

After colonization, the most well characterized virulence factors are related to the manganese requirement of *S. sanguinis*. Unlike many other pathogens, *S. sanguinis* is

a manganese-centric, as opposed to iron-centric, organism (90). Therefore, the deleterious effects of disruptions of manganese homeostasis reflect this manganese preference. Several proteins relating to manganese have been particularly well characterized, including the manganese transport protein SsaB, the manganese-dependent enzyme SodA, and the manganese dependent aerobic ribonucleotide reductase system, comprised of NrdHEKF and NrdI.

In a screen of 52 predicted lipoproteins, SsaB was found to be singularly important for virulence (91). The substrate binding protein in an ATP-binding cassette (ABC) transport system, SsaB and orthologous proteins belong to the Lipoprotein Receptor Antigen I (Lral) family of metal transporters (92, 93). They have universally been demonstrated to transport manganese (94-96) and play a role in streptococcal virulence (96-101). Early hypotheses speculated that the virulence defect associated with loss of manganese was due to impaired function of the manganese-dependent enzyme superoxide dismutase.

As with SsaB, SodA is known to have a role in virulence in a number of streptococcal species (102-104). SodA is an important enzyme in oxidative stress defense that converts superoxide to hydrogen peroxide and oxygen. When this activity is impaired or absent, superoxide accumulates and can damage iron-containing proteins, resulting in the release of free iron. This further propagates oxidative stress, as newly available Fe^{2+} reacts with hydrogen peroxide, present as a byproduct of aerobic growth, to produce the highly reactive hydroxyl radical (105). Beyond this intrinsic benefit, superoxide dismutase activity has also been linked to resistance to phagocytic killing (103, 104). For *S. sanguinis*, the link between manganese and superoxide

dismutase activity was validated in a study wherein deletion of *ssaB* resulted in a mutant that was both manganese deficient and impaired for superoxide dismutase activity (90). Neither the *ssaB* mutant nor a *sodA* mutant was more sensitive to phagocytic killing by polymorphonuclear leukocytes (90). Interestingly, virulence was more attenuated in the *ssaB* mutant than the *sodA* mutant. This suggested an alternative role for manganese in the cell, possibly via interaction with an alternate virulence factor.

Concurrent with these studies, the same group identified a manganese-requiring aerobic ribonucleotide reductase (106, 107). These enzymes convert ribonucleotides to deoxyribonucleotides, required for DNA replication and repair, and are essential in most organisms (108). In their study, they demonstrated that mutants deficient in this enzyme were not recovered in a rabbit mode of endocarditis (106). Although they did not directly address whether ribonucleotide reductase activity is impaired in an *ssaB* mutant, it is quite plausible that the reduced virulence of this mutant may be explained, in part, by deficiencies of this enzyme and others.

Model of Infective Endocarditis

With regards to *in vivo* examination of pathogen virulence and endocarditis pathogenesis there have been two models, rat and rabbit, that have been routinely used (60, 109). Both models approximate native valve endocarditis effectively, as they require cardiac damage for disease manifestation (109, 110). Of additional note, in the rabbit model, symptoms and extracardiac pathologies mirror those of humans (111, 112). In the context of the work that will be discussed within this text, the rabbit model was exclusively used. Previous studies demonstrated that the rabbit model is more

permissive for infection (113) and has a lower incidence of a bottleneck effect than the rat model (114-117). Additionally, introduction of cardiac damage is technically easier in the rabbit model.

One shortcoming of the model is the rate of progression of disease. Our model is limited to three days of strain incubation after inoculation, for reasons discussed in further detail later. This is not characteristic of streptococcal-mediated NVE, which is usually chronic and subacute. Incubations that last much longer than this amount of time are typically fatal (118); therefore, this model is only intended to mimic early IE.

Although variations of the model exist, our method calls for retention of the catheter within the carotid artery for the duration of the experiment, no sonication of cells before inoculation and an inoculum level of approximately 10^7 CFU/ml. The former is a lab preference as we have empirically determined that resulting vegetations and bacterial output are more robust and reliable. The lack of sonication is taken as a precaution against undesired removal of outer surface proteins, such as adhesins, that may be important in bacterial colonization of the sterile vegetation or other unidentified processes (82, 113). The specified inoculum was previously defined as ensuring infection without being immediately fatal (118).

Research Objective

S. sanguinis is a bacterium with a dual nature. In the mouth, it is considered to be benign or even beneficial, whereas in the bloodstream it is an opportunistic pathogen and etiologic agent of the disease infective endocarditis. Until now, studies have focused on characterizing a single virulence determinant, SsaB, within a single strain, SK36. While this has been useful, the goal of this work was to expand our knowledge of

S. sanguinis virulence by examining additional strains and by investigating the mechanism by which these bacteria could potentially circumvent therapies designed to target the manganese acquisition protein, SsaB. In Chapter 3, a collection of *S. sanguinis* isolates was analyzed using bioinformatic and phenotypic methods and virulence was assessed in a well-established rabbit model of endocarditis. In Chapter 4, I investigated suppressor mutants that arose from strains that were deficient in manganese acquisition due to deletion of the *ssaB* gene. The mechanism by which these strains circumvented the need for SsaB and the implications of our findings were addressed. Together, these studies have reshaped our understanding of endocarditis virulence in *S. sanguinis*.

CHAPTER 2

General Material and Methods

Bacterial Strains and Growth Conditions

Bacterial strains used are listed in tables as described within each chapter. For growth studies, strains were inoculated from frozen single-use aliquots at a thousand-fold dilution into brain heart infusion (BHI) broth (BD) and grown utilizing the Anoxomat™ Mark II jar-filling system (AIG, Inc.) at 37°C and 6% O₂ (6% O₂, 7% H₂, 7% CO₂, and 80% N₂) for 18 h. The next day, cultures were diluted and plated onto BHI supplemented with 1.5% (w/v) agar and incubated at 37°C for 24 h in 0% O₂ (0.2% O₂, 9.9% H₂, 9.9% CO₂, and 80% N₂) with additional O₂ removal by palladium catalyst. These same cultures were also used to inoculate pooled rabbit serum (Gibco) at a 10⁶-fold dilution that was then incubated at 37°C at 12% O₂ (12% O₂, 4.3% H₂, 4.3% CO₂, and 80% N₂). After 24 h, 1 ml of the serum cultures was removed, sonicated by an ultrasonic homogenizer (BioLogics, Inc.) for 1.5 min at 50% power, diluted, plated onto BHI agar and incubated at 0% O₂ (0.2% O₂, 9.9% H₂, 9.9% CO₂, and 80% N₂) for 1 d. Bacterial enumeration was determined by counting colonies from plated cultures.

DNA Manipulation

Chromosomal DNA was isolated from all strains as previously described (116). PCR was routinely performed in a MyCycler (Bio-Rad) or an MJ Research PCT-200 thermal cycler (Bio-Rad). PCR amplification was performed using Q5 2x High Fidelity Master Mix (NEB). PCR reaction mixtures typically included primers at a final concentration of

0.5 μM , and 10 ng of *S. sanguinis* SK36 chromosomal DNA or PCR amplicon as template. Plasmid DNA as PCR template was used at 0.1 ng μl^{-1} . Integrated DNA Technologies synthesized most of the primers used. Purification of DNA from agarose was performed using the QIAquick Gel Extraction Kit (Qiagen). PCR purifications were performed using the MinElute PCR Purification kit (Qiagen). When required for selective growth, erythromycin (Em), chloramphenicol (Cm), spectinomycin (Sc), kanamycin (Kn) and tetracycline (Tet) were used at 10, 5, 200, 500, and 5 $\mu\text{g ml}^{-1}$, respectively.

Many strains referenced within this work were created using overlap extension PCR (119). In brief, knockout mutants were generated by amplifying left and right flanking sequences, adjoining the gene to be deleted, that contained sequences specific to the strain in which the fragment would be transformed. Typically, an antibiotic cassette was amplified that contained extra bases at either end that could be used to create an overlap with the left and right flanking sequences. In some instances, variations of this fragment included additional unique barcode sequences, used for later strain identification. In all cases, after purification, these fragments were combined in an additional PCR reaction and gel purified before utilization in our transformation protocol.

Transformation

Transformation was used in mutant generation as described previously (113). In brief, 50 μl of overnight cultures were diluted in 10 ml of Todd-Hewitt broth containing horse serum. These cultures were incubated at 37°C until an OD_{600} of 0.05-0.08 was reached. At this time, 330 μl of the diluted culture was added to a 0.7 ml microcentrifuge tube containing the appropriate DNA and 2 μl of competence stimulating peptide (CSP). If

the DNA construct contained a selectable marker, the culture was incubated for 1.5-2 h. Constructs with no selectable marker were incubated for approximately 5 h. Cultures were then sonicated, serially diluted and plated onto BHI agar \pm antibiotics as appropriate. Plates were incubated overnight and colony counts were determined the following day by counting visible colonies. PCR screening of DNA from resulting colonies followed by sequencing (Eurofins) was used to verify mutant identity.

Rabbit Model of IE

Specific-pathogen-free New Zealand White rabbits (2–4 kg; RSI Biotechnology) were utilized in the previously described endocarditis model (90, 106) to assess virulence. Prior to surgery, the rabbits were sedated and anesthetized. Insertion of a 19-gauge catheter, to reach the aortic valve by way of the right carotid artery, was used to induce minor damage to the endocardium. Each catheter was trimmed and sutured in place. All incisions were closed with staples. The following afternoon, all strains to be inoculated into animals were cultured in BHI for overnight growth in 6% O₂. For all studies, except where otherwise identified, sample preparation, inoculation and quantification of bacteria from harvested tissue were performed as described previously (90). In brief, cells were subcultured in BHI for 3 h before adjustment to an OD₆₀₀ of 0.8. Samples were washed twice to remove excess BHI and then 0.5 ml of culture, either single strain or equal parts of a strain mix, was inoculated into the right peripheral ear vein. Approximately 20 h after inoculation, rabbits were sacrificed via intravenous injection of Euthasol. Catheter placement was verified upon necropsy. Harvested cardiac vegetations were placed into PBS, homogenized and plated onto BHI agar containing the appropriate antibiotics.

ICP-OES

For each strain, 10 ml of BHI containing appropriate antibiotics was inoculated at a 1:1000 dilution and incubated overnight at 37°C and 6% O₂. Two additional 50-ml conical tubes containing 38 ml BHI (unless otherwise indicated) were also incubated under the same conditions for each strain. The next day, 3 ml of the overnight culture was used to inoculate each 38-ml BHI tube. These subcultures were placed back in the incubator at 12% O₂ for 3 h. Cells were then harvested by centrifugation at 3740 x g for 10 min at 4°C. The supernatant was discarded and 5 ml cold, Chelex-treated (BioRad) PBS was added and the sample was resuspended. Centrifugation and resuspension of cells in 5ml Chelex-treated PBS was repeated as before. The two 5-ml tubes were combined into a single 15-ml metal free conical tube (VWR). At this point, 1 ml was removed for protein determination using the Pierce BCA Protein Assay Kit (ThermoFisher). The remaining sample was centrifuged as before and the supernatant discarded. The pellet was resuspended by adding 4.5 ml Chelex-treated de-ionized water, followed by 1.5 ml of concentrated (67-70%) trace metal grade nitric acid. The mixture was then placed into modified PTFE (TFM) digestion vessels in a Multiwave Go Microwave Digestion System (Anton Paar) and digested at 20 bar using a modification of the Organic B template. The temperature of the first hold step was increased to 120°C and the second hold was increased to 180°C for 20 min. After cooling, each sample was transferred to a new 15-ml metal-free conical tube. Each vessel was rinsed with 1 ml Chelex-treated water that was then added to the sample in the 15-ml metal-free tube. Samples were diluted 1:3 in Chelex-treated water, yielding a final acid concentration of 5%. Samples were analyzed on an Agilent 5110 ICP-VDV OES using a

CMS-5 metal standard (Inorganic Ventures, Inc.) for reference and a Pb internal standard (MSPB-10PPM; Inorganic Ventures). Final values were determined by normalizing the sample concentrations to the protein amounts obtained by BCA assay.

Statistical Analyses

All statistical tests were performed using InStat (GraphPad Software, Inc.). Significance was determined by paired t-test or ANOVA (paired or unpaired) as indicated in the figure legends. For ANOVA, a post-hoc test was employed when differences among groups were indicated as significant. P-values ≤ 0.05 were considered significant.

CHAPTER 3

Genomic, phenotypic, and virulence analysis of *Streptococcus sanguinis* oral and infective endocarditis isolates

Rationale

Many strains of *S. sanguinis* have been isolated from patients confirmed to have IE; however, investigations into what makes these strains better able to cause disease, relative to counterpart strains in the oral cavity, have not been conducted. The goal of this project was to analyze a collection of strains comprised of blood and oral isolates of *S. sanguinis*, using both bioinformatic and microbiological-based techniques, to determine if blood isolates had identifiable and testable genetic elements that contribute to their virulence.

Introduction

A wide range of *S. sanguinis* isolates are currently used and identified in the literature. With the oral cavity, references to SK150 (an oral isolate) are common for studies examining composition and interactions of species within the biofilm (8, 126, 127). In contrast, strains SK36 and the type strain ATCC 10556 (also known as SK1 or NCTC 7863), an oral and blood isolate respectively, dominate virulence studies and have been used to expand our knowledge of processes including adherence (128, 129), immune evasion (130-132), manganese uptake (91), oxidative stress resistance (90), and synthesis of deoxyribonucleotides (106, 107).

These studies have been crucial components in understanding the physiology of *S. sanguinis*. However, a species cannot be fully understood through examination of

one or two strains. In fact, recent work in *S. pneumoniae* has demonstrated that interpretations of results can be biased and oversimplified when too few strains are examined (133-135). Fortunately for those who study *S. sanguinis*, a number of isolates are available for study along with complementary information such as strain origin, multi-locus sequence analysis (MLSA), and draft or complete genome sequences (NCBI) (70). Therefore, assimilation and further characterization of these strains into the research pipeline is not only feasible, but is also desirable, if the species as a whole is to be understood.

For this study, a mixed collection of 20 oral and blood *S. sanguinis* isolates underwent vigorous bioinformatic and phenotypic analyses to identify factors that might contribute to the ability of an individual strain, or perhaps, certain groups of strains (ex: oral vs. blood), to cause IE. Bioinformatic analyses identified several candidate genes that upon further investigation failed to correspond to virulence. Later investigations using a pooled inoculum approach known as Bar-seq established the incredible range (~4 orders of magnitude) in virulence, but failed to identify a relationship between increased virulence and strain and origin. Additional phenotypic assays also did not provide insight into virulence, but did further uncover the heterogeneity of the species. Of note, an unintended byproduct of these studies was the identification of several egregious errors in GenBank.

Specific Materials and Methods

Sequence Information

The complete genome sequence of *S. sanguinis* strain SK36 and the latest RefSeq draft assemblies for the nineteen remaining *S. sanguinis* isolates were downloaded from NCBI's ftp site on December 13, 2017.

Bioinformatic Analyses

Sequence Processing

Nucleotide, protein, and corresponding protein function files required for PGAP input were created from available RefSeq assembly files, downloaded from NCBI. Files were formatted using custom Python scripts and UNIX commands. Nucleotide files were generated from `Assembly_cds_from_genomic.fna` files, protein files were generated from `Assembly_protein.faa` files and function files were created from the `Assembly_feature_table.txt` files. Minor alterations were made to draft assembly files to meet requirements of the PGAP program for exact translation from nucleotide to protein sequences.

Pan and Core-Genome Analysis

The GF method of PGAP version 1.12 (120) with default settings was utilized for pan and core genomes analysis, variant detection in coding sequences, and for generation of single-nucleotide polymorphism (SNP) and pan-based neighbor-joining trees. Pan and SNP-based neighbor-joining trees were visualized using UGENE (121) version v1.16.1.

Phage Analysis

The PHASTER program (122) was used to identify phage-like elements within SK36 and the RefSeq scaffold genomic.fna files of the other strains.

Bacteriocin Analysis

Bacteriocin analysis was performed using BAGEL4 (123) with RefSeq assembly accessions used as input for all strains except SK1, which was not accepted by the program. Instead, FASTA files for SK1 scaffolds 1, 2, 3, and 4 were used as input.

Selection of a Conserved Chromosomal Insertion Site

UGENE was used for identification of convergent genes. MEGA 6 and BLASTN were used for alignment and identification of conservation among strains, respectively.

ARNOLD was used to identify putative terminator sequences.

Strain Construction

All mutant strains were generated using overlap-extension PCR (119) with the primers listed in Table 3.1. In all cases, left and right flanking PCR products were generated that contained sequences specific to the strain into which the fragment would be transformed adjoined to sequences complementary to the DNA to be inserted so as to generate the overlap necessary for the overlap extension step. For the knockout mutants, these flanking sequences were on either side of the gene(s) to be deleted. For SK405-Spc^r and subsequent barcoded mutants, the flanking sequences were located in a conserved region between two convergent genes identified using MEGA 6 and BLASTN. For creation of the barcoded mutants, one primer was modified to include both an additional conserved sequence and unique 10-bp barcode. All fragments were gel purified before proceeding to the overlap extension step. The final PCR reaction

employed 10 ng of each fragment as template. The resulting product was gel purified before incorporation into the transformation mixture.

| Table 3.1 Primers used in strain construction | | | |
|---|----------------------|---|--|
| # | Primer Name | Sequence (5' --> 3') | Purpose |
| | | | Generate SK36 Sc^r by overlap extension PCR |
| 1 | spcUP | CCGCTCTA GAACTA GTGGATCC | <i>aad9</i> with native promoter |
| 2 | spcDO | CAATTTTTTAA TAA TTTTTTAA TCTG | <i>aad9</i> with native promoter |
| 3 | MJY1 | CCAGACGATCACTTCATCC | left fragment |
| 4 | MJY5-R | GGA TCCACTAGTTCTAG A GCGGGAA TAGAGGTTTTTAAAGAA TATTGACAAC | left fragment |
| 5 | MYJ6-F | CAGATTA AAAAAATTA TAAAAAAATGCTAGATAAACTTCTGTTCTAC | right fragment |
| 6 | MYJ2-R | TGTA TAGCATTTCAATTCAAG | right fragment |
| | | | Generate SK36 ΔssaACB Tc^r by overlap extension PCR |
| 7 | Tet-F2 | ATGAAAATTA TTAATATTGGAGT | <i>tetM</i> |
| 8 | Tet-R2 | TCACTAAGTTATTTTATTGAACAT | <i>tetM</i> |
| 9 | 0262-F1 | GCA CGATGATAAGCTCCTG | left fragment |
| 10 | 0262T-R1 | CCAATA TTAATAA TTTTCA TCTCATACACCTCTATAGT | left fragment |
| 11 | 0260T-F3 | CAATAAAA TAACTTAGTGATAA TAAAAGGTTAGGAA GACA | right fragment |
| 12 | 0260-R3 | CGTTTTCTCAA TATTATCAA TCCA | right fragment |
| | | | Generate SK36 ΔssaACB Km^r by overlap extension PCR |
| 13 | Kan-F2 | ATGGCTAAAATGAGAAATCAACC | <i>apha-3</i> |
| 14 | Kan-R2 | CTAAAACAAATTCATCCAGTA | <i>apha-3</i> |
| 15 | 0262-F1 | GCA CGATGATAAGCTCCTG | left fragment |
| 16 | 0262-R1S | TCTCATTTTATGCCATCTCATACCTCTATAGT | left fragment |
| 17 | 0260-F3 | GATGAA TTGTTTTA GTAA TAAAAGGTTAGGAA GACA | right fragment |
| 18 | 0260-R3 | CGTTTTCTCAA TATTATCAA TCCA | right fragment |
| | | | Generate SK405 Sc^r by overlap extension PCR |
| 19 | spcUP-short | CCGCTCTA GAACTA GTGGATCC | <i>aad9</i> with native promoter |
| 20 | spcDO-long | GAAGTTATCTAGCAATTTTTTAA TTTTTTAA TCTG | <i>aad9</i> with native promoter |
| 21 | MJY1 | CCAGACGATCACTTCATCC | left fragment |
| 22 | MJY5-R | GGA TCCACTAGTTCTAG A GCGGGAA TAGAGGTTTTTAAAGAA TATTGACAAC | left fragment |
| 23 | MYJ6-F | CAGATTA AAAAAATTA TAAAAAAATGCTAGATAAACTTCTGTTCTAC | right fragment |
| 24 | MYJ2-R | TGTA TAGCATTTCAATTCAAG | right fragment |
| | | | Generate SK405 Δlipo by overlap extension PCR |
| 25 | TetProm | CTAGGTTGATTTTCGTTCTG | <i>tetM</i> with native promoter |
| 26 | Tet_R1 | GAGTTAAAATTTTTTAGACACTAAGTTATTTTATTGAACATATATC | <i>tetM</i> with native promoter |
| 27 | SK405_lipo_Lflank_L1 | ACGCTGCTGGATTTTGA TAC | SK405 Δ lipo |
| 28 | SK405_lipo_Lflank_R1 | TATTCACGACGAAAA TCAACCTAGTTGCACTCTCTTATGGAA C | SK405 Δ lipo |
| 29 | SK405_lipo_Rflank_L1 | AAA TAACTTAGTGCTAAAAA TTTTTAACTCTGTCAA G | SK405 Δ lipo |
| 30 | SK405_lipo_Rflank_R1 | GAAAAA ACGGGACATAC | SK405 Δ lipo |
| | | | Generate SK405 Δtel by overlap extension PCR |
| 31 | kan F2p | GATAAA CCCAGCGAA CCA TTTGA | <i>apha3</i> with native promoter |
| 32 | Kan-R2Med | AGGTA CTA AAA CAA T TCA TCCA GT | <i>apha3</i> with native promoter |
| 33 | SK405-F1 | TGGCCA GTTCGATA GCTTCA | SK405 Δ tel |
| 34 | SK405-R1 | GCTCAA CTGTCACTTTA TACTTCA | SK405 Δ tel |
| 35 | SK405-F3 | ACACACGCA T TAAA AACTGAA CT | SK405 Δ tel |
| 36 | SK405-R3 | CTCCTTA TCGGGACATCGCT | SK405 Δ tel |
| | | | Generate BC strains by overlap extension PCR |
| 37 | Spec_Bseq_L1 | CCGCTCTAGAACTAGTGG | <i>aad9</i> with native promoter |
| 38 | Spec_Bseq_R1 | CGGCGCCTTA TAA TTTTTTAA TCT | <i>aad9</i> with native promoter |
| 39 | Lflank_36Bseq_L1 | ATTAACA CTCTATGAGTAAAC | BC strains: SK36, SK49, VMC66, SK115, SK160, SK330, SK340, SK405, SK408, SK678, SK1056, SK1057, SK1058, SK1059 |

| | | | |
|----|--------------------|--|--|
| 40 | Lflank_36Bseq_R1 | TCCACTAGTCTAGACGCG GACTGACTAC A GTTGCTATCACAGGTGGACGAA TAGAGGTTTTTAAAGAA T | BC strains: SK36, |
| 41 | Rflank_36Bseq_L1 | GATTA A A A A A A T T A T A A G G C C G C C G C T A G A T A A A C T T C T G T T C T A C A C | BC strains: SK36, SK353, SK150, SK160, SK330, SK405, SK408, SK1056, SK1057 |
| 42 | Rflank_36Bseq_R1 | AAAAATTCAC TCCAAAGTTAG | BC strains: SK36, SK353, SK115, SK678, SK1058 |
| 43 | Lflank_49Bseq_R1 | GATCCACTAGTCTAGACGCG TAAACCACT AGTTGCTATCACAGGTGGACGAA TAGAGGCTTTTAAAGAA | BC strains: SK49 |
| 44 | Rflank_49Bseq_L1 | GATTA A A A A A A T T A T A A G G C C G C C G C T A G A T A A A C T T C T G T T C T A C T C | BC strains: SK49, VMC66 |
| 45 | Lflank_66Bseq_R1 | GATCCACTAGTCTAGACGCG CCAAATCCGT AGTTGCTATCACAGGTGGACGAA TAGAGGCTTTTAAAGAA | BC strains: VMC66 |
| 46 | Rflank_72Bseq_R1 | AAAAATTCAC TCCAAAGG | BC strains: SK160, SK405, SK408, SK1056, SK1057 |
| 47 | Lflank_115Bseq_R1 | GATCCACTAGTCTAGACGCG CCCATATGTC AGTTGCTATCACAGGTGGACGAA CAGAGGTA TTTAAAGGCT | BC strains: SK115, |
| 48 | Rflank_115Bseq_L1 | GATTA A A A A A A T T A T A A G G C C G C C G A T A G A T A A A C T T C T G T T C T A C T C | BC strains: SK115, |
| 49 | Lflank_150Bseq_L1 | ATTGAACACTCAATGAGTAAAC | BC strains: SK150, SK355 |
| 50 | Lflank_150Bseq_R1 | GATCCACTAGTCTAGACGCG TTGCTAGTTA AGTTGCTATCACAGGTGGACGAA TAGAGGCTTTTAAAGAA | BC strains: SK150, |
| 51 | Rflank_150Bseq_R1 | CTTTGGAGTGT TTTT T T A T C T A A A A T T T G | BC strains: SK49, VMC66, SK150, SK355, SK1059 |
| 52 | Lflank_160Bseq_R1 | GATCCACTAGTCTAGACGCG GACACATCC AGTTGCTATCACAGGTGGACGAA TAGAGGCTTTTAAAGAA | BC strains: SK160, |
| 53 | Lflank_330Bseq_R1 | GATCCACTAGTCTAGACGCG CTATAACTGA AGTTGCTATCACAGGTGGACGAA TAGAGGCTTCTAAAGAA | BC strains: SK330, |
| 54 | Rflank_330Bseq_R1 | AAAAATTCAC TCCAAAGG | BC strains: SK330, |
| 55 | Lflank_340Bseq_R1 | GATCCACTAGTCTAGACGCG CTACCCATAT AGTTGCTATCACAGGTGGACGAGTAGAGGTTTTTAAAGAA | BC strains: SK340, SK678 |
| 56 | Rflank_340Bseq_L1 | GATTA A A A A A A T T A T A A G G C C G C C G C T A G A T A A A C T T C T T T C A A C A C G | BC strains: SK340, SK1058 |
| 57 | Rflank_340Bseq_R1 | CTTTGGAGT TTTT T T A T C T A A A A T T T G | BC strains: SK340 |
| 58 | Lflank_353Bseq_L1 | ATTAAACAATCTATGGGTAAACC | BC strains: SK353, |
| 59 | Lflank_353Bseq_R1 | GATCCACTAGTCTAGACGCG GTGTTGT AGTTGCTATCACAGGTGGACGAA TAGAGGCTTCTAAAGAA T | BC strains: SK353, |
| 60 | Lflank_355Bseq_R1 | GATCCACTAGTCTAGACGCG CCCACAAGAG AGTTGCTATCACAGGTGGACGAA TAGAGGCTTTTAAAGAA | BC strains: SK355, |
| 61 | Rflank_355Bseq_L1 | GATTA A A A A A A T T A T A A G G C C G C C G C T A G A T A A A C T T C T G T T C T A C A A G | BC strains: SK355, |
| 62 | Lflank_405Bseq_R1 | GATCCACTAGTCTAGACGCG GCAACTTTGA AGTTGCTATCACAGGTGGACGAA TAGAGGTTTTTAAAGAA | BC strains: SK405 |
| 63 | Lflank_408Bseq_R1 | GATCCACTAGTCTAGACGCG CATTGACTAC AGTTGCTATCACAGGTGGACGAA TAGAGGCTTTTAAAGAA | BC strains: SK408 |
| 64 | Lflank_678Bseq_R1 | GATCCACTAGTCTAGACGCG CGCACCAATG AGTTGCTATCACAGGTGGACGAA TAGAGGCTTCTAAAGAA | BC strains: SK678 |
| 65 | Rflank_678Bseq_L1 | GATTA A A A A A A T T A T A A G G C C G C C G C T A G A T A A A C T T C T G T T C T A C A C | BC strains: SK678 |
| 66 | Lflank_1056Bseq_R1 | GATCCACTAGTCTAGACGCG GTATAAAGCG AGTTGCTATCACAGGTGGACGAA TAGAGGCTTTTAAAGAA | BC strains: SK1056 |
| 67 | Lflank_1057Bseq_R1 | GATCCACTAGTCTAGACGCG GTGAGCCCAA AGTTGCTATCACAGGTGGACGAA TAGAGGTTTTTAAAGAA | BC strains: SK1057 |
| 68 | Lflank_1058Bseq_R1 | GATCCACTAGTCTAGACGCG GTACTCTGGC AGTTGCTATCACAGGTGGACGAGTAGAGGTTTTTAAAGAA | BC strains: SK1058 |
| 69 | Lflank_1087Bseq_R1 | GATCCACTAGTCTAGACGCG CTTAGTCGCC AGTTGCTATCACAGGTGGACGAA TAGAGGTTTTTAAAGAA | BC strains: SK1059 |
| 70 | Rflank_1087Bseq_L1 | GATTA A A A A A A T T A T A A G G C C G C C G C T A G A A A A C T T C T G T T C T A C A C | BC strains: SK1059 |
| | | | Amplification of BC strains for Illumina Sequencing Using Staggered Primers |
| 71 | Bseq-quant1L | TCGTCGGCAGCGTCA GATGTGTA TAA GAGACAGCCA CCTGTGATAGCAACT | Total DNA: inocula and homogenized rabbit tissue |
| 72 | Bseq-quant2L | TCGTCGGCAGCGTCA GATGTGTA TAA GAGACAGTCCA CCTGTGATAGCAACT | Total DNA: inocula and homogenized rabbit tissue |
| 73 | Bseq-quant3L | TCGTCGGCAGCGTCA GATGTGTA TAA GAGACAGGTCCA CCTGTGATAGCAACT | Total DNA: inocula and homogenized rabbit tissue |
| 74 | Bseq-quant4L | TCGTCGGCAGCGTCA GATGTGTA TAA GAGACAGCA CCA CCTGTGATAGCAACT | Total DNA: inocula and homogenized rabbit tissue |
| 75 | Bseq-quant1R | GTCTCGTGGGCTCGGAGATGTGTA TAA GAGACAGTAT TCAAATATA TCCTCCTCAC | Total DNA: inocula and homogenized rabbit tissue |
| 76 | Bseq-quant2R | GTCTCGTGGGCTCGGAGATGTGTA TAA GAGACAGATAT TCAAATATA TCCTCCTCAC | Total DNA: inocula and homogenized rabbit tissue |
| 77 | Bseq-quant3R | GTCTCGTGGGCTCGGAGATGTGTA TAA GAGACAGTCTAT TCAAATATA TCCTCCTCAC | Total DNA: inocula and homogenized rabbit tissue |
| 78 | Bseq-quant4R | GTCTCGTGGGCTCGGAGATGTGTA TAA GAGACAGCTAT TCAAATATA TCCTCCTCAC | Total DNA: inocula and homogenized rabbit tissue |
| | **NOTE** | Boldface lettering within sequences is indicative of the unique barcode included in the primer design | |

Table 3.1 Primers and strains used in this study.

Modification of Rabbit Model

For the pooled barcode mutant virulence study, strains were not subcultured as in our typical model. Instead duplicate inoculum pools were prepared directly from the overnight culture. In both cases, 2 ml of each strain was removed from each overnight culture. The first ml was sonicated, diluted in PBS and plated to determine the relative abundance of each strain in the inoculum. The second ml for each strain was combined into a 50 ml conical tube and vortexed. The combined cells were washed twice in PBS and diluted to give a concentration of $\sim 10^8$ cfu/ml. A portion of the inoculum pool was withheld for DNA purification and amplification using primers specific for the conserved region and *spc* cassette. After harvesting of the cardiac vegetation, DNA was isolated and amplified as in the inoculum.

DNA Isolation

DNA was isolated from 1 ml of each pooled inoculum and 1 ml homogenized vegetations with the Qiagen DNeasy Blood and Tissue kit, following the protocol for Gram-positive organisms. Samples was pelleted by centrifugation, resuspended in 180 μ l enzymatic lysis buffer (20 mM Tris-Cl, 2 mM EDTA, 1.2% (v/v) Triton X-100) supplemented with lysozyme (20mg/ml) and mutanolysin (150 U/ml), and incubated at 37 °C for 1 hour. Twenty-five μ l of proteinase K was added to samples. The samples were vortexed and incubated overnight. The next morning samples were vortexed again, vigorously and 4 μ l RNase A (100 mg/ml) was added. Samples were incubated for 2 min at room temperature, followed by 15 seconds of vortexing. Two-hundred μ l Buffer AL was added and the sample was vortexed. One hundred μ l ethanol (96-100%)

was added and samples were once again vortexed. Samples were column purified per the manufacturer's instructions.

Barcode Sequencing and Quantitation

After isolation of DNA from the two inocula and homogenates, products with Illumina adapters were obtained using PCR. These amplicons were purified and sent to the VCU Nucleic Acid Research Facility for multiplexed paired-end sequencing on a MiSeq instrument (Illumina) with a Phi-X spike. Barcode counts were quantified using the Geneious R10 (version 10.2.3) program. Within Geneious, reads were trimmed using the BBDuk plugin and sorted using the "separate reads by barcode" tool. Inoculum levels of each strain were determined as total number of reads per strain divided by total number of reads from all strains. Output values were each normalized to the inoculum by dividing the percent relative abundance of each strain in the output by the percent relative abundance in the corresponding inoculum.

Bacteriocin Assays

Bacteriocin assays were based on the procedure described by Perry et al (124). Cultures were grown for 18 h in BHI in 6% O₂. The next day all strains were stabbed into 18-replicate BHI agar plates using pipet tips dipped in the overnight cultures. Stabbed plates were incubated overnight anaerobically. The next day, newly grown overnight cultures of each strain were diluted 20-fold into fresh BHI and incubated until an OD₆₀₀ of 0.2 was reached. Five-ml of each diluted culture was separately added to 10 ml of 1% molten low melting point agarose, gently mixed and then poured on top of a stabbed plate. After solidification of the overlays, plates were

incubated overnight in 6% O₂. Bacteriocin production was recorded as presence or absence of zones of inhibition. *S. mutans* strain UA159 was used as a positive control.

Biofilm Assay

Strains were inoculated at a 1000-fold dilution into BHI and grown in 6% O₂ overnight at 37°C. The next day, cultures were used to inoculate 96-well plates containing biofilm medium (BM) (125) with 1% added sucrose or glucose at a 1:100 dilution. Plates were incubated in either 0% or 12% O₂ overnight. Planktonic cells were removed and the wells were allowed to dry. Wells were washed with 200 µl of distilled water followed by staining with 50 µl of 0.4% crystal violet (CV) for 30 min at room temperature after which the CV was removed by pipette and the biofilms were washed twice with 200 µl of distilled water. Three-hundred µl of 30% acetic acid was added and allowed to sit for 30 min to solubilize the biofilm. The resulting supernatant was diluted 1:8 and assayed for absorbance at 560 nm.

***In vitro* strain competition assays**

Strains were grown overnight in BHI in 6% O₂ as is typical. For the culture-based assay, cells were diluted as normal and 50 µl of one strain or 50 µl of each of two strains was added to a single tube containing 5 ml of rabbit serum. These cultures were incubated overnight at 12% O₂ before dilution plating and later bacterial enumeration of the plated cultures. For the blood agar studies, 500 µl of each strain was obtained directly from the BHI overnight culture and centrifuged. The pellet was resuspended in 50 µl of PBS and was then pipetted onto a blood agar plate. The plates were incubated overnight in 12% O₂. For pairwise comparisons, 500 µl of both strains were combined,

centrifuged and resuspended in 100 μ l of PBS. As before, 50 μ l of this mixed sample was pipetted onto a blood agar plate and incubated. The next day, the resulting growth was scraped from the plate and placed into 1 ml of PBS. Each sample was sonicated, diluted, plated, incubated and enumerated as before.

Results

Genomic Overview

Tara Nulton performed most of the bioinformatic analyses for this work. When she compared genome sequences for 19 out of 20 isolates in our possession, of which 10 were oral and 9 were blood, she identified GC contents ranging from 42.8% to 43.4% and protein-coding sequences ranging from 2298 (SK340) to 2166 (SK49). The 20th strain was not incorporated into these analyses for reasons that will be described in detail later. Utilization of the gene family (GF) mode of PGAP identified *S. sanguinis* as having an “open”, or ever-increasing pan-genome (Fig 3.1). Identification of 4051 clusters of orthologous alleles was consistent with this classification, but was less than

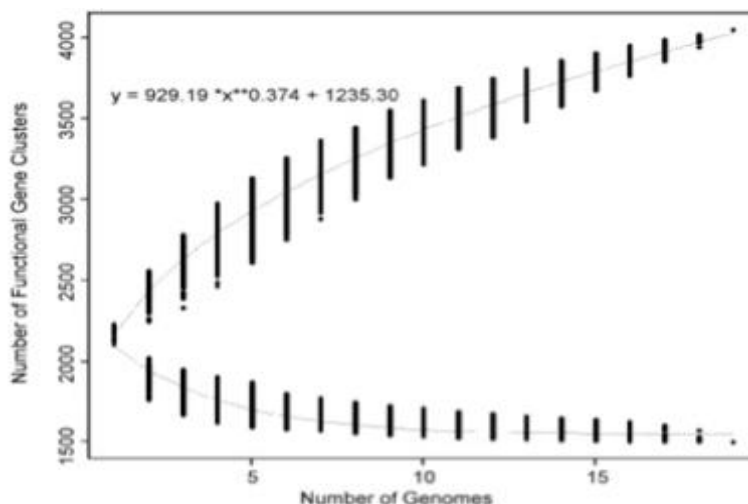


Fig 3.1 - Cluster analysis of 19 genomes by PGAP in GF mode. Upper curve, pan-genome calculation; lower curve, core genome calculation.

the 5100 clusters previously identified by Zheng et al. (136). Our identification of 1499 core clusters, shared by all strains, was also less than that identified by Zheng (136). The core clusters identified in this study account for 68% of the genes in SK36, our lab wild-type (WT) strain. For each strain, variable numbers of unique gene clusters were also identified (Fig 3.2)

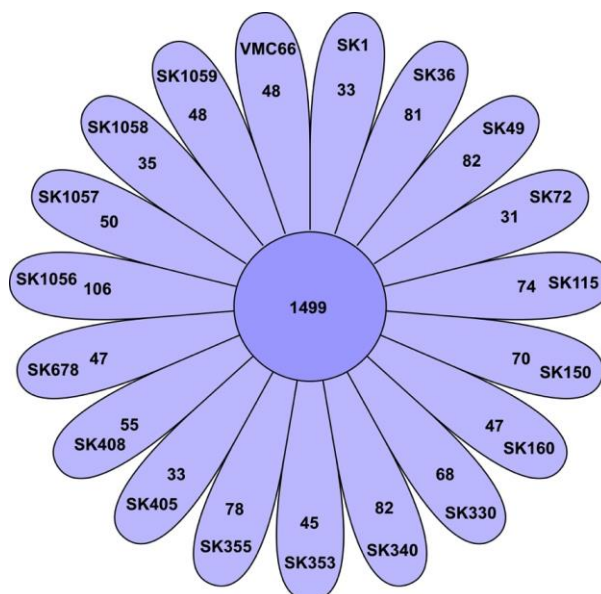


Fig 3.2 - Graphical representation of core genome and unique genes.

Phylogenetic Analyses

A neighbor joining phylogram was used to investigate the phylogenetic relationship of strains of similar and differing origin (Fig 3.3A). This phylogram determines relatedness based on the presence or absence of genes, previously identified in our examination of the pan-genome. Three clades were identified in this analysis, one large clade containing five blood isolates, and two smaller, mixed, clades. Although this method did not fully resolve strains by origin it is interesting to note that half of the blood isolates do present as a single, well-defined clade. Utilization of a SNP-based neighbor joining phylogram, which accounts for variations due to mutations, insertions and deletions, identified two distinct clades (Fig 3.3B). Of note, clades one and two are very similar to clades one and three previously identified in Fig 3.3A.

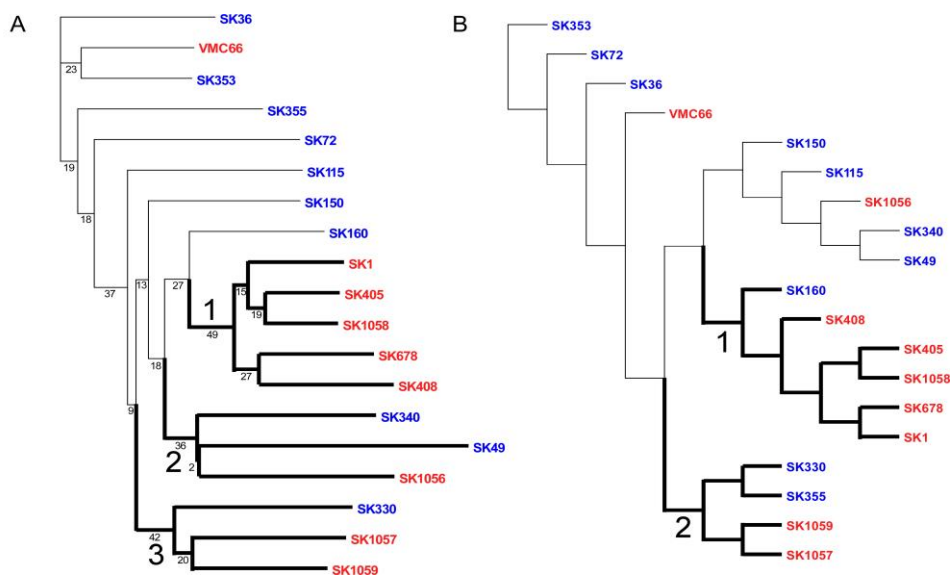


Fig 3.3 - (A) Pan-based phylogram. The phylogram was computed by PGAP using the neighbor-joining method of clustering. Red indicates blood isolate, blue denotes oral isolate. Clades are numbered and accentuated by darker branches emanating from clade's most basal node. The pan-based tree is created using a gene distance matrix approach built upon gene presence or absence in each strain. **(B)** SNP-based phylogram. The phylogram was computed by PGAP using the neighbor-joining method of clustering and the tree was visualized using UGENE. Red indicates blood isolate, blue denotes oral isolate. Clades are labeled and accentuated by darker branches emanating from the clade's most basal node.

Identification of Putative Virulence Genes and their Examination *In Vivo*

Culling the total genes for those present only in blood isolates distinguished several genes that could potentially have explained these strains' ability to cause IE (Table 3.2). From these, a putative lipoprotein (HMPREF9390_RS07860) and a ~12-kb genomic island (HMPREF9390_RS08320 through HMPREF9390_RS08365) containing a tellurite resistance gene were chosen for further investigation.

| SK405 Locus_Tag | Predicted Function | Oral Blood | |
|--------------------|--|------------|---|
| HMPREF9390_RS07860 | hypothetical lipoprotein | 2 | 8 |
| HMPREF9390_RS08320 | Phosphoribosyl transferase (PRT)-type I domain protein | 2 | 6 |
| HMPREF9390_RS08325 | Phosphoribosyl transferase (PRT) | 2 | 6 |
| HMPREF9390_RS08330 | YceG family protein | 2 | 6 |
| HMPREF9390_RS08335 | TelA | 2 | 6 |
| HMPREF9390_RS08340 | TerD3 family protein | 2 | 6 |
| HMPREF9390_RS08345 | TerD2 family protein | 2 | 6 |
| HMPREF9390_RS08350 | TerD family protein | 2 | 6 |
| HMPREF9390_RS08355 | calcium-translocating P-type ATPase, PMCA-type | 2 | 6 |
| HMPREF9390_RS08360 | haloacid dehalogenase-like hydrolase | 2 | 6 |
| HMPREF9390_RS08365 | ATP/GTP-binding protein | 2 | 6 |

Table 3.2 - Bioinformatic sort based on strain origin.

Ten oral and nine blood isolates were used in the sort.

In *Bacillus anthracis*, deletion of the tellurite resistance genes *yceGH*, rendered strains that were more sensitive to oxidative stress and cathelicidin-mediated killing and were attenuated in murine models of infection (137). Therefore, we hypothesized this locus might play a role in *S. sanguinis* virulence. The lipoprotein was chosen based on previous findings that established the importance of lipoproteins on virulence (90, 91, 106) and because it was one of a limited number of genes that were almost exclusively found in blood isolates.

To explore the putative role for these genes in virulence, two strains were chosen. The first, SK36, is an oral isolate that is prevalent in the literature and lacks both the *tel* locus and the lipoprotein. The second, SK405, is a blood isolate that contains both loci. Traditionally, strains marked with antibiotic resistance cassettes have been utilized to investigate virulence in our rabbit model of IE (90, 106, 138). Insertions of these cassettes into the hypothetical gene SSA_0169 have been found not to affect a number of phenotypes, including virulence (138). Unfortunately, the SSA_0169 site is not conserved among all of the isolates in our collection, and was not present in SK405. Therefore, we searched for a conserved locus that could be used to facilitate future

genetic manipulation of SK405 and the strains in our collection. Search parameters included finding a site that would be between convergent genes, would be flanked by a terminator sequence and whose subsequent manipulation would not cause apparent pleiotropic effects. Information incorporated from several programs identified a candidate in a conserved intergenic region (CIR) between genes encoding a hypothetical protein, SSA_1217 and a DNA repair protein, RadC.

To test the viability of this site for genetic manipulation, a construct with a spectinomycin resistance cassette (138, 139), containing the *aad9* gene and its native promoter, was created using overlap extension PCR(120) and transformed into SK36 (140) (Fig 3.4). Growth of this marked strain was assessed, and determined to be unaffected, 24 h after inoculation into pooled rabbit serum that was set to an initial O₂ concentration of 12% (data not shown). This models the oxygen concentration of arterial blood flow at the site of an aortic vegetation (141) and has been previously determined to recapitulate *in vivo* results (90).

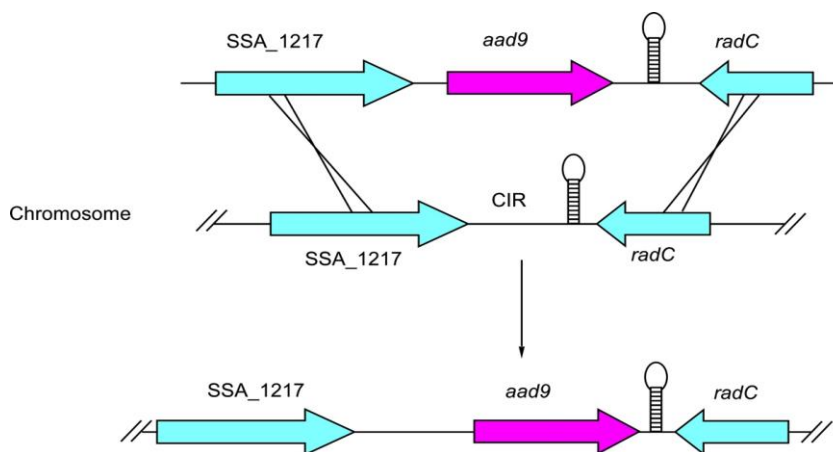


Fig 3.4 - Selection of a conserved intergenic region (CIR) for insertion of exogenous DNA into *S. sanguinis* strains. The spectinomycin resistance cassette is denoted as *aad9*. The stem and loop structure represents the terminator sequence.

With these positive results we transitioned to testing *in vivo*. The spectinomycin-marked SK36 and a strain of SK36 containing an erythromycin cassette in SSA_0169 (138), were co-inoculated into catheterized rabbits (Fig 3.5). Two additional, differently marked, *ssaACB* deletion mutants were co-inoculated at this time to reduce animal use. As desired, there was no difference between recovery of the spectinomycin-resistant (Sc^r) SK36 and the erythromycin-resistant (Em^r) derivative and growth of the two-*ssaACB* deletion mutants was equally attenuated, as expected (90, 113). We thus concluded neither the antibiotic insertion site (SSA_0169 vs. CIR) nor the choice of resistance gene (*ermB* vs. *aad9* or *tetM* vs. *aphA-3*) affected the results of our *in vivo* investigations.

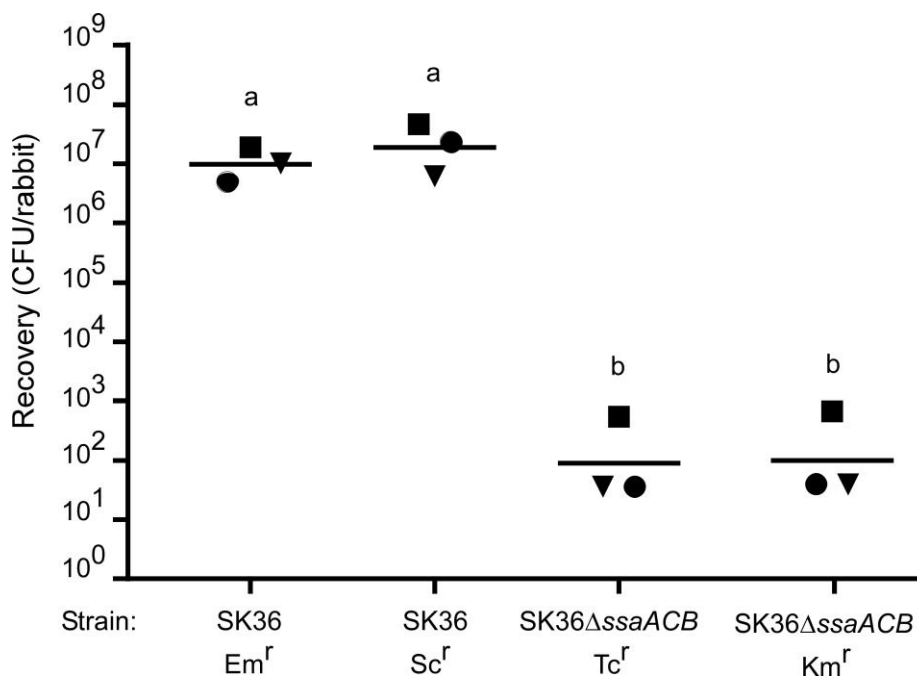


Fig 3.5 - Examination of SK36 derivatives in a rabbit model of IE. Rabbits were co-inoculated with the strains indicated. Like shapes indicate values obtained from the same rabbit in a single experiment. Geometric means are indicated by horizontal bars. Significance was determined by repeated measures ANOVA with Tukey-Kramer post hoc test. Samples that do not share a letter are significantly different; $P < 0.001$.

With a viable site for genetic manipulation available we proceeded with the creation of a Sc^r derivative of SK405. The *tel* and lipoprotein mutants of SK405 were created by insertion of *aphA-3* or *tetM*, encoding kanamycin resistance (138) or tetracycline resistance (138), respectively. As with SK36, growth of the Sc^r SK405 was indistinguishable from WT SK405 when grown in rabbit serum. Co-inoculation of Em^r SK36, as a reference, Sc^r SK405, and both the *tel* and lipoprotein mutant into rabbits failed to identify a role for either locus in virulence (Fig 3.6). Of interest, the SK405 reference strain and both mutants were significantly more virulent than the marked SK36 strain.

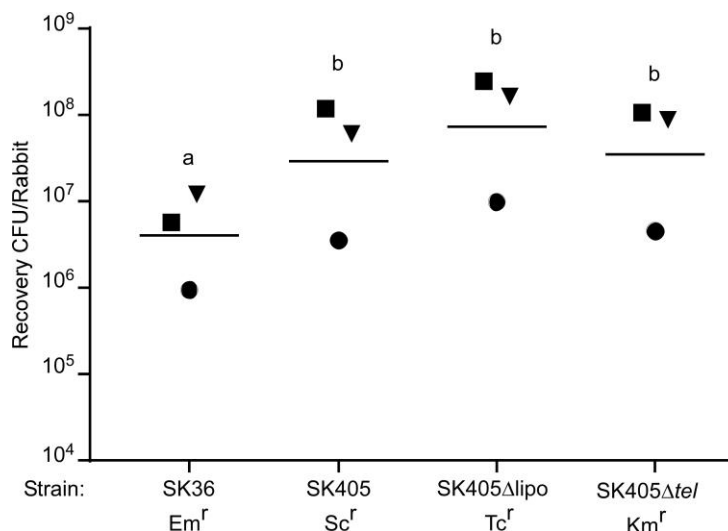


Fig 3.6 - Examination of SK36 and SK405 derivatives in a rabbit model of IE. Rabbits were co-inoculated with the strains indicated. Like shapes indicate values obtained from the same rabbit in a single experiment. Geometric means are indicated by horizontal bars. Significance was determined by repeated measures ANOVA with Tukey-Kramer post hoc test. Samples that do not share a letter are significantly different; ** $P < 0.01$.

Strain Identification and Construction

We questioned whether our failure to identify virulence factors was because the IE isolates were not uniformly more virulent than the oral isolates. Perhaps, if given more time or under different circumstances, an “oral” isolate might have been isolated

from the blood and would have thus been considered virulent. The inclusion of such a strain would have likely altered the conclusions we could make about genes that were common to more virulent strains. To address this possibility, we decided to create marked derivatives of all of our strains and test them *in vivo*.

The traditional rabbit model can accommodate 4 differently marked strains; however, we had significantly more than this. Therefore, we modified a previous technique, Bar-seq, that interrogates mutant fitness by sequencing transposon insertions that contain random and unique barcode sequences (142). For each strain, an 879-bp cassette that contained a common upstream (P1) primer binding site, a unique 10-bp barcode (BC) identifier, and the *aad9* gene was inserted into the CIR by transformation. The inclusion of a common primer-binding site, allowed for later PCR amplification and quantification of all barcodes present in a sample (Fig 3.7).

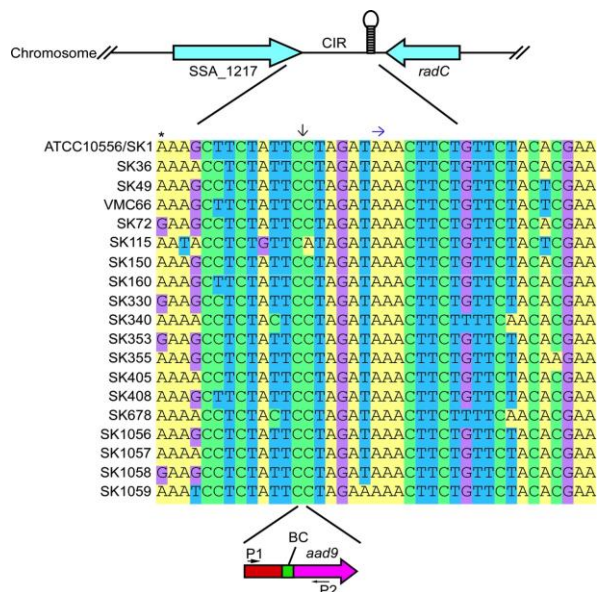


Fig 3.7 - Use of a conserved intergenic region for barcode insertion. Stem and loop structure indicates terminator sequence. * indicates last bp of stop codon in SSA_1217. Downward arrow indicates barcode (BC) insertion site. Right arrow indicates start of terminator sequence. P1 and P2 designate primers used to amplify DNA from inoculum cells and from harvested rabbit vegetations for Illumina sequencing.

During the creation of these marked strains, we found we were unable to successfully generate three strains—SK1, SK72, and SK1087—each for differing reasons. By the time this study began, we realized that SK1 was not actually in our collection. We did obtain ATCC 10556, which is considered equal to SK1 (143) at a much later date; however, construction and assessment of its marked derivative would have caused significant delays and thus, was not included in this experiment. Regarding SK72, repeated attempts at transformation were unsuccessful for reasons we could not determine, as the SK72 draft genome sequence indicated that every gene shown previously to be required for transformation of SK36 was present and intact (144). The final strain, SK1087, was excluded here, and previously in the bioinformatic analysis, primarily because we were initially unable to amplify its CIR. During the construction of this, and several other marked strains, we realized the sequences we were amplifying were in conflict with the sequences recorded in GenBank. The sequences we amplified did match other *S. sanguinis* strains in our collection, however. We concluded either our strain stocks had been mislabeled or the GenBank WGS sequences were misidentified.

To formally investigate this, we sequenced several housekeeping genes and compared our sequences to those from a previously published multi-locus sequence analysis (MLSA) available for all strains except VMC66 (20). Although not available for download from GenBank, they are available for download from the authors' website (viridans.emlsa.net/). In all cases, the sequences of our strains were consistent with the MLSA results (data not shown). When we used these housekeeping sequences as a query for a BLASTN of the WGS database, and against the nr database for SK36, our sequences were once again in conflict. Moreover, comparisons of the MLSA sequences

themselves against those in GenBank were in conflict. To ensure our findings were accurate, we obtained new stocks of three of the strains in conflict from Dr. Mogens Kilian (University of Aarhus, Denmark). He is the original provider of all of the “SK” strains for our lab, the Human Microbiome Project, and the MLSA study. Again, all sequences we obtained were in agreement with the MLSA findings and our earlier sequences, and were in conflict with information available from GenBank. Our four conclusions are summarized in Fig 3.8. First, the sequences for SK678 and SK1058 are reversed in GenBank. Second, the GenBank sequence identified as SK1087 is actually SK1059. Third, the GenBank sequence that is identified as SK1059 actually belongs to SK340, as does the sequence identified as SK340. In short, we affirm that there are two versions of the SK340 sequence in GenBank. Finally, we conclude there is no WGS sequence in GenBank for strain SK1087, which may explain our earlier obstacle in amplifying the CIR of this strain. At the conclusion of this rigorous investigation, we were left with 17 strains, 9 oral isolates and 8 blood isolates, which were successfully barcoded. All strains identifications included here are in agreement with our sequence results and the MLSA data, as opposed to the GenBank identifications.

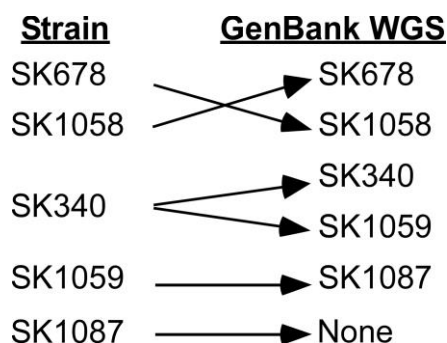


Fig 3.8 - Misidentified GenBank WGS sequences as determined by our analysis.

After sequence verification of the BC strains, growth of these strains and each of their parents was assessed in pooled rabbit serum. Results indicate that no strain was affected by insertion of the barcode (Fig 3.9). The validation of these strains enabled us to progress to testing in our rabbit model.

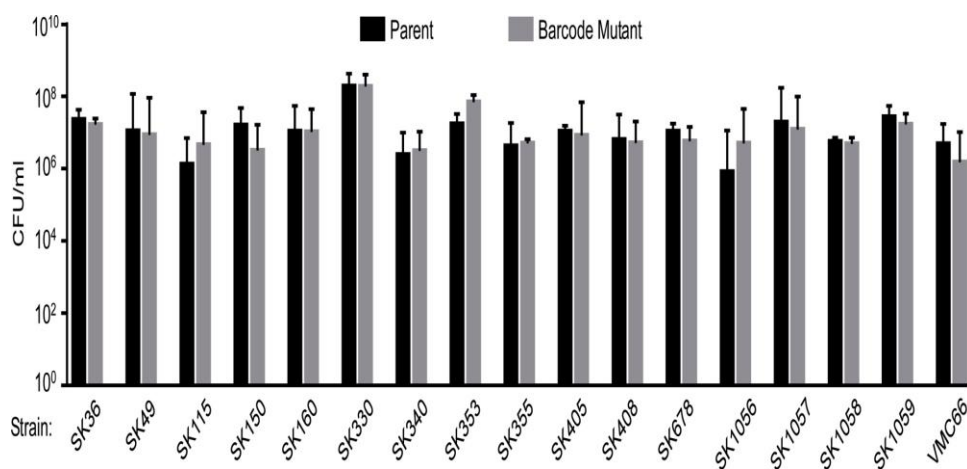


Fig 3.9 - Growth of *S. sanguinis* parent and marked strains in rabbit serum in 12% O₂. The strains indicated were grown for 24 h at 37°C before serial dilution for bacterial enumeration. The means and standard deviations are shown for n=3 experiments. There was no significant difference between any parent vs. marked strain as determined by paired t test.

Pooled virulence analysis by Bar-seq

For this study, we used Bar-seq to monitor strain fitness by quantifying barcodes in harvested tissues (output) versus those in an inoculum (input) using Illumina short-read sequencing (142). Barcodes for each strain were detected at near-equal levels in the inoculum pool before (Table 3.3) and after normalization (Fig 3.10). CFU counts obtained by dilution plating each strain prior to pooling of the inocula showed similar trends, although a greater variability in strain recovery was seen (Table 3.4).

In contrast to the equally distributed barcodes in the inoculum, barcodes counts recovered from harvested cardiac homogenates were highly variable, covering

approximately four logs (Table 3.3 and Fig 3.10). Of the seventeen included strains, three were more abundant in the output than in the inocula. Two of the three strains were blood isolates (SK405 and SK678); however statistical analysis did not identify an association between strain source and virulence (unpaired t-test, $P=0.1234$).

Interestingly, several strains were recovered in low abundance. Of these, SK330 is of special interest. SK330 had the fewest CFU in the inoculum as determined by plating, although the averaged counts were still within a log of SK115, the strain closest to SK330 in terms of cardiac recovery. The lower levels of SK330 in the inoculum were surprising, as the protocol for rabbit inoculation was adjusted to account for the slow growth of SK330 in BHI that we had observed in pilot studies. The poor growth of SK330 in BHI was also surprising given that this strain consistently grew to higher levels than any of the other strains tested in rabbit serum (Fig. 3.9).

| Raw Counts | Barcode Counts | | | | | | | | | | | | | | | | Total | |
|----------------------------------|----------------|---------------|---------------|---------------|----------------|----------------|----------------|---------------|---------------|----------------|---------------|----------------|---------------|---------------|----------------|---------------|----------------|--------------|
| | SK36 | SK49 | SK115 | SK150 | SK160 | SK330 | SK340 | SK353 | SK355 | SK405 | SK408 | SK678 | SK1056 | SK1057 | SK1058 | SK1059 | | VMC66 |
| Inoculum-1 | 26,028 | 22,147 | 18,432 | 22,568 | 24,654 | 22,677 | 19,230 | 14,959 | 25,160 | 19,065 | 22,685 | 24,882 | 20,186 | 24,268 | 24,773 | 22,011 | 19,298 | 373,023 |
| Inoculum-2 | 26,373 | 24,878 | 19,953 | 23,823 | 29,103 | 24,285 | 22,029 | 15,540 | 28,005 | 20,159 | 25,457 | 28,485 | 23,102 | 27,395 | 30,402 | 21,777 | 20,005 | 410,771 |
| Rabbit #731 | 2,805 | 76 | 49 | 8,841 | 3,060 | 3 | 2,886 | 1,223 | 552 | 35,857 | 6,216 | 25,555 | 752 | 1,099 | 526 | 565 | 1,533 | 91,598 |
| Rabbit #732 | 14,288 | 1,142 | 192 | 30,105 | 67,303 | 9 | 28,953 | 1,944 | 580 | 333,611 | 40,458 | 143,989 | 7,133 | 3,828 | 2,919 | 8,230 | 16,223 | 700,907 |
| Rabbit #733 | 32,107 | 236 | 214 | 10,899 | 27,094 | 97 | 22,669 | 4,788 | 1,152 | 205,191 | 29,296 | 226,287 | 4,135 | 6,058 | 3,103 | 1,694 | 5,273 | 580,293 |
| Rabbit #734 | 9,158 | 103 | 28 | 9,742 | 38,809 | 3 | 4,942 | 1,162 | 192 | 86,453 | 11,739 | 42,782 | 1,168 | 2,177 | 2,038 | 1,139 | 7,385 | 219,020 |
| Rabbit #735 | 9,046 | 99 | 26 | 5,783 | 30,697 | 24 | 16,142 | 4,745 | 1,153 | 41,145 | 5,635 | 60,575 | 2,405 | 1,807 | 6,114 | 3,714 | 8,302 | 197,412 |
| Rabbit #736 | 18,343 | 184 | 109 | 46,152 | 37,697 | 64 | 21,965 | 7,106 | 2,064 | 322,303 | 36,366 | 165,120 | 1,512 | 4,550 | 2,348 | 6,818 | 10,350 | 683,051 |
| % of Total | SK36 | SK49 | SK115 | SK150 | SK160 | SK330 | SK340 | SK353 | SK355 | SK405 | SK408 | SK678 | SK1056 | SK1057 | SK1058 | SK1059 | VMC66 | Total |
| I1 | 6.98% | 5.94% | 4.94% | 6.05% | 6.61% | 6.08% | 5.16% | 4.01% | 6.74% | 5.11% | 6.08% | 6.67% | 5.41% | 6.51% | 6.64% | 5.90% | 5.17% | 100.00% |
| I2 | 6.42% | 6.06% | 4.86% | 5.80% | 7.08% | 5.91% | 5.36% | 3.78% | 6.82% | 4.91% | 6.20% | 6.93% | 5.62% | 6.67% | 7.40% | 5.30% | 4.87% | 100.00% |
| C731 | 3.06% | 0.08% | 0.05% | 9.65% | 3.34% | 0.00% | 3.15% | 1.34% | 0.60% | 39.15% | 6.79% | 27.90% | 0.82% | 1.20% | 0.57% | 0.62% | 1.67% | 100.00% |
| C732 | 2.04% | 0.16% | 0.03% | 4.30% | 9.60% | 0.00% | 4.13% | 0.28% | 0.08% | 47.60% | 5.77% | 20.54% | 1.02% | 0.55% | 0.42% | 1.17% | 2.31% | 100.00% |
| C733 | 5.53% | 0.04% | 0.04% | 1.88% | 4.67% | 0.02% | 3.91% | 0.83% | 0.20% | 35.36% | 5.05% | 39.00% | 0.71% | 1.04% | 0.53% | 0.29% | 0.91% | 100.00% |
| C734 | 4.18% | 0.05% | 0.01% | 4.45% | 17.72% | 0.00% | 2.26% | 0.53% | 0.09% | 39.47% | 5.36% | 19.53% | 0.53% | 0.99% | 0.93% | 0.52% | 3.37% | 100.00% |
| C735 | 4.58% | 0.05% | 0.01% | 2.93% | 15.55% | 0.01% | 8.18% | 2.40% | 0.58% | 20.84% | 2.85% | 30.68% | 1.22% | 0.92% | 3.10% | 1.88% | 4.21% | 100.00% |
| C736 | 2.69% | 0.03% | 0.02% | 6.76% | 5.52% | 0.01% | 3.22% | 1.04% | 0.30% | 47.19% | 5.32% | 24.17% | 0.22% | 0.67% | 0.34% | 1.00% | 1.52% | 100.00% |
| % of Total/ % of Inoculum | SK36 | SK49 | SK115 | SK150 | SK160 | SK330 | SK340 | SK353 | SK355 | SK405 | SK408 | SK678 | SK1056 | SK1057 | SK1058 | SK1059 | VMC66 | |
| C731 | 47.70% | 1.37% | 1.10% | 166.43% | 47.15% | 0.06% | 58.75% | 35.29% | 8.84% | 797.66% | 109.50% | 402.32% | 14.60% | 17.99% | 7.76% | 11.63% | 34.37% | |
| C732 | 31.75% | 2.69% | 0.56% | 74.06% | 135.53% | 0.02% | 77.03% | 7.33% | 1.21% | 969.86% | 93.14% | 296.25% | 18.10% | 8.19% | 5.63% | 22.15% | 47.53% | |
| C733 | 86.18% | 0.67% | 0.76% | 32.38% | 65.90% | 0.28% | 72.84% | 21.81% | 2.91% | 720.51% | 81.46% | 562.34% | 12.67% | 15.65% | 7.22% | 5.51% | 18.66% | |
| C734 | 136.54% | 56.68% | 23.90% | 46.08% | 530.41% | 41.82% | 71.62% | 39.74% | 14.55% | 100.83% | 78.98% | 70.01% | 64.96% | 82.84% | 162.04% | 84.31% | 201.47% | |
| C735 | 149.64% | 60.44% | 24.62% | 30.35% | 465.46% | 371.20% | 259.52% | 180.02% | 96.92% | 53.24% | 42.06% | 109.98% | 148.39% | 76.29% | 539.33% | 305.00% | 251.28% | |
| C736 | 87.69% | 32.47% | 29.83% | 70.00% | 165.20% | 286.08% | 102.06% | 77.92% | 50.14% | 120.54% | 78.45% | 86.65% | 26.96% | 55.52% | 59.86% | 161.82% | 90.54% | |
| Average | 89.92% | 25.72% | 13.46% | 69.88% | 234.94% | 116.58% | 106.97% | 60.35% | 29.10% | 460.44% | 80.60% | 254.59% | 47.61% | 42.75% | 130.31% | 98.40% | 107.31% | |

Table 3.3- Raw and normalized Bar-seq data. Raw counts were determined using the program Geneious to count the incidence of each barcode. The “% of total” was calculated by dividing the barcodes for each strain by the total barcodes in the inoculum or output respectively. The “% of Total/% of Inoculum” was calculated by taking the previous section and dividing by the % of strain representation in the inoculum.

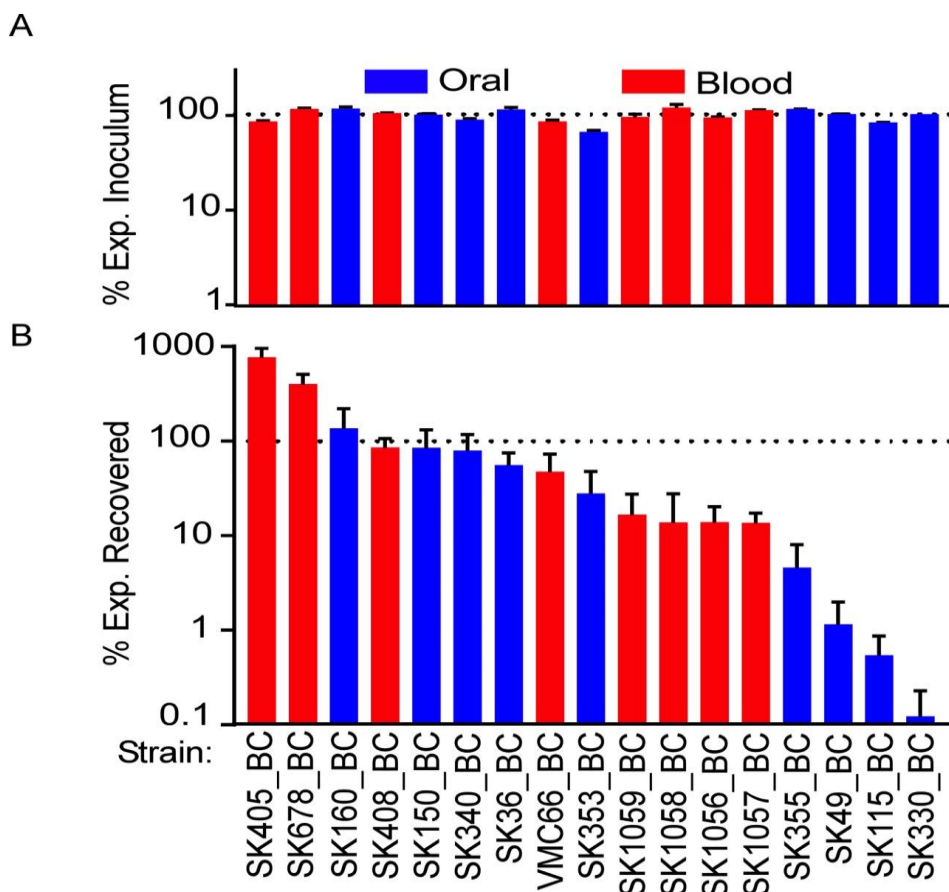


Fig 3.10 - Examination of marked strains in a rabbit model of IE.

Six rabbits were co-inoculated with 17 barcoded strains in one of two duplicate pools. Blue and red indicate oral or blood isolates respectively. % Exp., Percent expected. **(A)** The % Exp. Inoculum for each strain was determined by dividing the BC counts for each strain by the total BC counts for that inoculum, then multiplying by 17. **(B)**, The % Exp. Recovered was determined similarly by the equation (% each strain in the total recovered counts for each rabbit)/(% each strain in the total inoculum counts). The dashed line represents 1/17th of total bacterial burden in each inoculum **(A)** and % abundance in each rabbit **(B)** relative to its abundance in the corresponding inoculum. There was no significant association between strain source (blood of IE patient vs. oral cavity) and virulence (unpaired t test, $P=0.1234$).

| Strain | Plate Counts | |
|--------|--------------|------------|
| | Inoculum 1 | Inoculum 2 |
| SK36 | 203 | 169 |
| SK49 | 120 | 77 |
| VMC66 | 168 | 73 |
| SK115 | 49 | 39 |
| SK150 | 39 | 27 |
| SK160 | 169 | 68 |
| SK330 | 7 | 3 |
| SK340 | 140 | 77 |
| SK353 | 127 | 105 |
| SK355 | 106 | 71 |
| SK405 | 155 | 119 |
| SK408 | 85 | 78 |
| SK678 | 60 | 40 |
| SK1056 | 143 | 54 |
| SK1057 | 114 | 62 |
| SK1058 | 137 | 110 |
| SK1059 | 74 | 42 |

Table 3.4- Plate counts of each strain present in inoculum.

Plate counts obtained for each strain before pooling all strains in one of two duplicate inocula.

With experimental evidence of more virulent strains available, we reevaluated our strains bioinformatically, comparing the more virulent strains to the less virulent ones, as opposed to the previous blood versus oral sort. This approach identified 30 genes exclusive to the more virulent strains (Table 3.5). Interestingly, ten of these belonged to the previously investigated *tel* locus. Many of the remaining genes have no known ties to virulence. Further investigations of these genes are warranted.

| SK405 Locus_Tag | Predicted Function | Less Virulent ¹ | More Virulent ² |
|--|--|----------------------------|----------------------------|
| HMPREF9390_RS00505 | hypothetical protein | 0 | 3 |
| HMPREF9390_RS01040 ³ | zinc-binding dehydrogenase family oxidoreductase | 0 | 3 |
| HMPREF9390_RS01045 | TetR family transcriptional regulator | 0 | 3 |
| HMPREF9390_RS01515 | molecular chaperone HscC | 0 | 3 |
| HMPREF9390_RS01520 | hypothetical protein | 0 | 3 |
| HMPREF9390_RS03570 | ABC transporter ATP-binding protein | 0 | 3 |
| HMPREF9390_RS03575 | ABC transporter permease | 0 | 3 |
| HMPREF9390_RS03635 | membrane protein | 0 | 3 |
| HMPREF9390_RS06090 | hypothetical protein | 0 | 3 |
| HMPREF9390_RS06105 | N-acetyltransferase | 0 | 3 |
| HMPREF9390_RS06115 | alpha/beta hydrolase | 0 | 3 |
| HMPREF9390_RS06500 | glycosyl transferase family 1 | 0 | 3 |
| HMPREF9390_RS06505 | von Willebrand factor A | 0 | 3 |
| HMPREF9390_RS07665 | hypothetical protein | 0 | 3 |
| HMPREF9390_RS07670 | alpha/beta hydrolase | 0 | 3 |
| HMPREF9390_RS07780 | hypothetical protein | 0 | 3 |
| HMPREF9390_RS08320 | Phosphoribosyl transferase (PRT)-type I domain protein | 0 | 3 |
| HMPREF9390_RS08325 | Phosphoribosyl transferase (PRT) | 0 | 3 |
| HMPREF9390_RS08330 | YceG family protein | 0 | 3 |
| HMPREF9390_RS08335 | TelA | 0 | 3 |
| HMPREF9390_RS08340 | TerD3 family protein | 0 | 3 |
| HMPREF9390_RS08345 | TerD2 family protein | 0 | 3 |
| HMPREF9390_RS08350 | TerD family protein | 0 | 3 |
| HMPREF9390_RS08355 | calcium-translocating P-type ATPase, PMCA-type | 0 | 3 |
| HMPREF9390_RS08360 | haloacid dehalogenase-like hydrolase | 0 | 3 |
| HMPREF9390_RS08365 | ATP/GTP-binding protein | 0 | 3 |
| HMPREF9390_RS09105 | hypothetical protein | 0 | 3 |
| HMPREF9390_RS09160 | hypothetical protein | 0 | 3 |
| HMPREF9390_RS09535 | TIGR01741 family protein | 0 | 3 |
| HMPREF9390_RS11625 | hypothetical protein | 0 | 3 |
| ¹ Less virulent strains include SK330, SK115, SK49 and SK355. | | | |
| ² More virulent strains include SK405, SK678 and SK 160. | | | |
| ³ Highlighting indicates contiguous genes. | | | |

Table 3.5- Candidate virulence genes.

Based on a bioinformatics sort comparing the top three most virulent strains to the four least virulent strains.

Phenotypic Assays

The range in virulence of the Bar-seq study was surprising. Considering the lack of genes identified by our virulence sort, we wondered if our results could have been biased by the pooled-inoculum method, and if not, whether we could correlate our Bar-seq results with other well characterized multi-gene systems that might contribute, in part, to virulence.

Bacteriocin Production

Regarding the former, we specifically questioned whether competition between the strains at the damaged cardiac site might have masked the individual capabilities of each strain and biased our bioinformatic sort and interpretation of the results. One known mechanism of competition is bacteriocin production (145). A BAGEL (123) analysis of all strains, searching for bacteriocins, identified a single putative lantibiotic encoded by HMPREF9391_RS05365 in strain SK408. This bacteriocin is homologous to the “streptin” of *Streptococcus pyogenes* M1GAS (146). When considering SK408 in the context of the virulence results, it is among the most virulent strains. It is therefore possible that this strain could have used this putative lantibiotic to gain a competitive advantage over other nearby strains. To test this possibility we used an assay previously employed by others (147, 148). The premise is that each strain is stabbed into an agar plate and then subjected to an overlay containing an indicator strain the following day. If the stabbed strain secretes an inhibitory product, the indicator strain in the overlay will not grow around the stabbed strain. This presents as a zone of inhibition and is a positive result for bacteriocin production. There was no inhibition by any *S. sanguinis* strain of any other *S. sanguinis* strain in our analysis (Fig 3.11); however, as

expected, all strains displayed sensitivity to one or more bacteriocins produced by *Streptococcus mutans* UA159.



Fig 3.11 - Bacteriocin production by agar overlay assay. The strains indicated were stabbed into an agar plate and incubated anaerobically overnight at 37°C. Low-melting point agarose containing a single strain was overlaid and cultures were allowed to grow as before. A clear zone surrounding a stab indicates a positive result. Representative picture of n=3 experiments with an SK36 overlay; the experiment was also performed 3 times with each of the other strains listed in the overlay.

Biofilm Formation

In vitro biofilm formation does not correlate with virulence for *S. sanguinis* strain SK36 (149); however, this is not true for all streptococci (150, 151). We questioned whether a relationship between biofilm formation and virulence of our other *S. sanguinis* strains existed or if, in fact, they each would resemble that of SK36. To investigate this, each strain was grown in biofilm medium supplemented with either sucrose (125) or glucose (152) to model oral (153, 154) and cardiac conditions, respectively. As seen in

Fig 3.12, there was no association, in either media, with biofilm formation and virulence (sucrose, Pearson correlation, $P=0.2392$; glucose, Pearson correlation, $P=0.5686$) or with strain origin (sucrose, unpaired t-test, $P=0.6493$; glucose, unpaired t-test, $P=0.3029$).

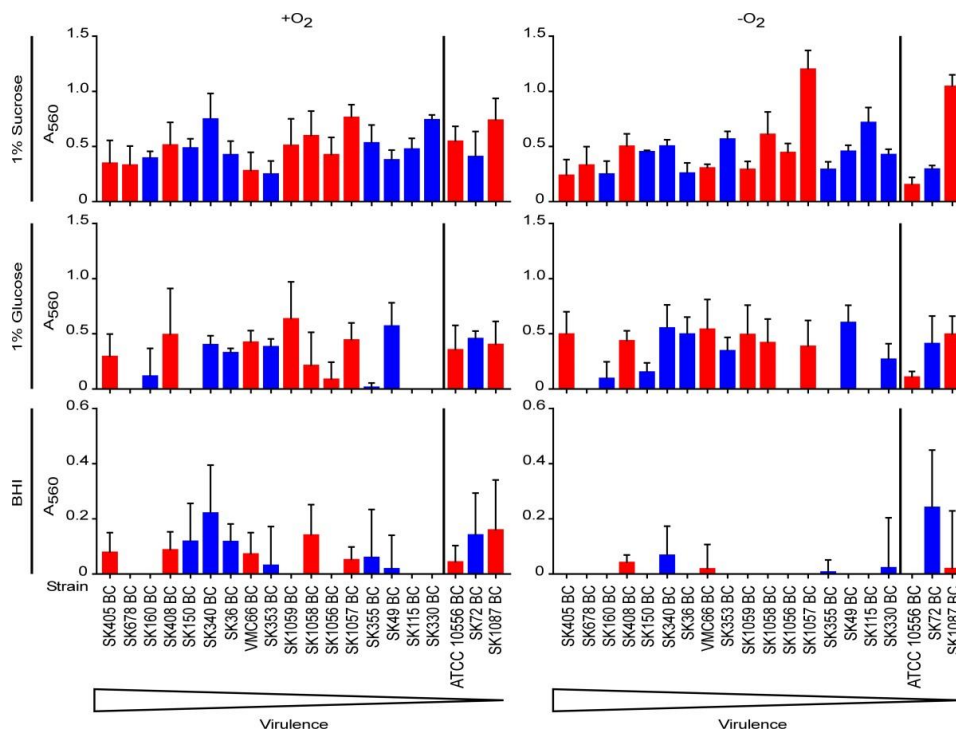


Fig 3.12 *S. sanguinis* biofilm production. Strains were grown in biofilm medium supplemented with either (A), 1% sucrose or (B), 1% glucose and grown under anaerobic or aerobic conditions, respectively. Biofilm formation was determined by absorbance at 560nm. Blue indicates oral isolates while red indicates blood isolates. Results are from $n=4$ experiments. There was no significant correlation between biofilm formation and virulence as determined by Pearson correlation in (A), $P=0.2392$ or in (B), $P=0.5686$. There was no significant relationship between biofilm formation and strain origin as determined by unpaired t test in (A), $P=0.6493$ or in (B), $P=0.3029$. Strains SK1, SK72 and SK1087 were not included in statistical testing, as virulence data was determined separately or was not available.

Cell-Associated Manganese Content

As previously mentioned, metal deficiencies can have dire effects on streptococcal physiology and virulence (90, 155). In the context of manganese, we did

not expect these strains to be manganese deficient, as bioinformatic analyses indicated the presence of the manganese transport system, *ssaACB* (90). Additionally, two strains (VMC66 and SK408) have an NRAMP-family (natural resistance-associated macrophage protein) transporter, which has been associated with manganese (156, 157). Although studies have investigated manganese deficiency and attenuation of virulence, none have explored whether elevated manganese levels may correlate with increased virulence. To investigate this possibility, strains were grown aerobically in BHI and subjected to inductively coupled plasma optical emission spectrometry (ICP-OES). No correlation between cellular manganese content and virulence was identified (Fig 3.13) (Pearson correlation, $P=0.9350$). Of note however, was the finding that blood isolates possessed significantly higher manganese levels than their oral counterparts (unpaired t-test, $P=0.0124$), which is more readily appreciated when strains are sorted by manganese content (Fig 3.13B). Also of interest, is the finding that the strains with the most manganese were, in fact, VMC66 and SK408, both of which have the extra NRAMP system for manganese transport.

Virulence Analysis of ATCC 10556

As mentioned previously, SK1 was not included in the Bar-seq study and subsequent bioinformatic analysis as it was not available until after the conclusion of these experiments. However, we later obtained and successfully marked ATCC 10556 (considered an SK1 equivalent (143)) with a kanamycin resistance cassette at the CIR, used for the barcode insertions in the other strains. We also tested this mutant for virulence. The results are included here as an addendum because, as will be demonstrated, not only do they provide additional phenotypic information, they also

encompass data that may have significant implications for the interpretation of the Bar-seq virulence results; however, these data are preliminary and as such, cannot encompass a separate chapter.

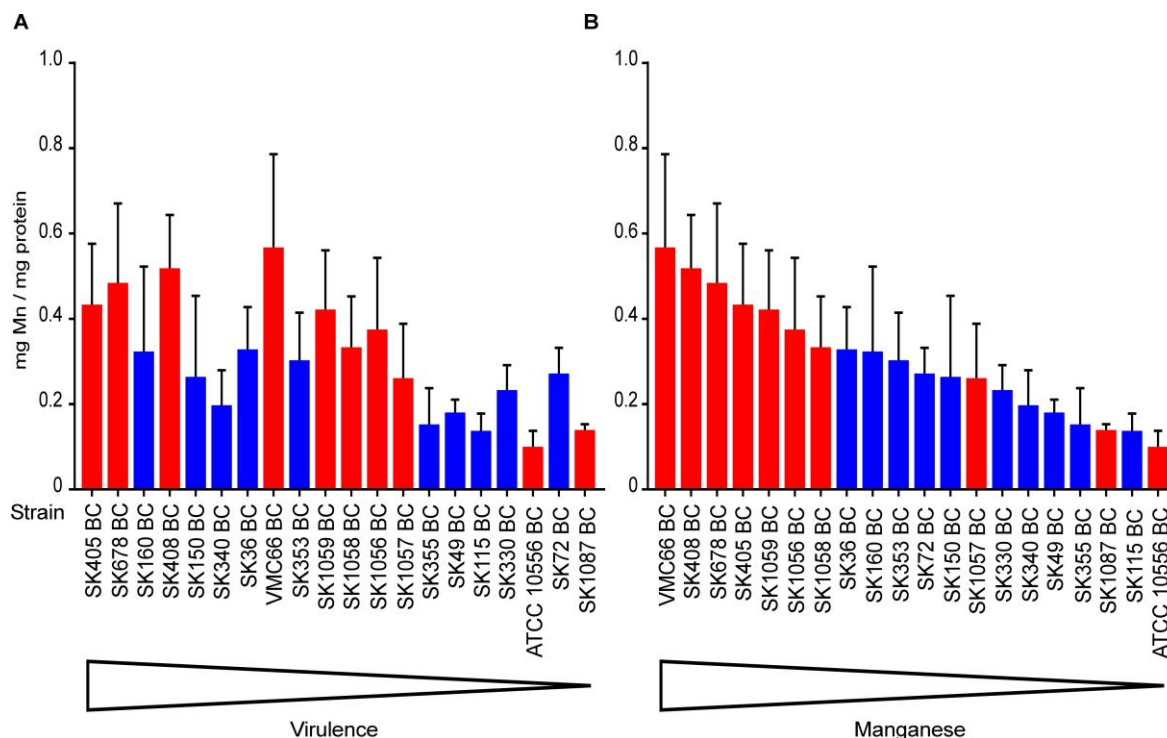


Fig 3.13 Cell-associated manganese content of *S. sanguinis* strains. Strains were grown in 12% O₂ and analyzed by ICP-OES displayed in order of (A), decreasing virulence or (B), decreasing Mn content. Means and standard deviations from n=4 independent experiments are shown. There was no significant correlation between virulence and Mn content in (A) as determined by Pearson correlation, $P = 0.9350$. There was significant correlation between strain origin and Mn content in (B) as determined by unpaired t test, $P = 0.0124$. For statistical analysis, strains SK1, SK72 and SK1087 were not included as in Fig 3.12.

ATCC 10556 was tested *in vivo* alongside Em^r SK36 and the barcoded, Sc^r SK330. SK330 was incorporated, as it was the poorest performer in the Bar-seq virulence study. Its inclusion allowed for assessment of whether the large inoculum pool biased our results. As can be seen in Fig 3.14, ATCC 10556, a blood isolate, was recovered at numbers approximately a log lower than SK36 and SK330; however, when

comparing the recoveries of SK36 and SK330 they were not significantly different, a finding in contrast to the results of the Bar-seq experiment. This led us to once again consider that competition among strains may have been present in the Bar-seq inoculum that was not at play in an inoculum with fewer strains.

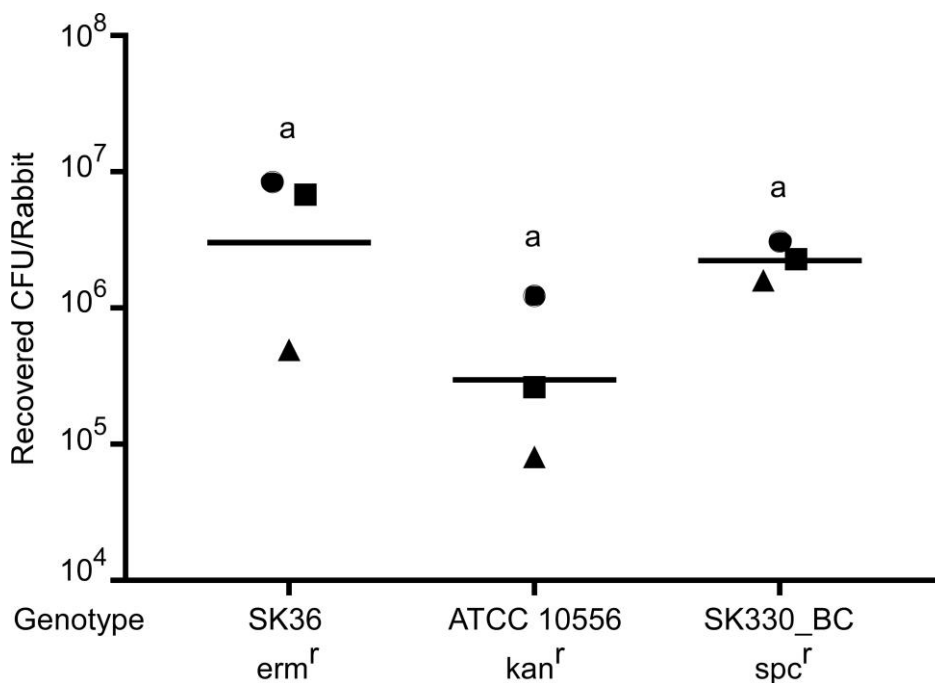


Fig 3.14 Examination of SK1 in a rabbit model of IE. Rabbits were co-inoculated with the strains indicated. Like shapes indicate values obtained from the same rabbit in a single experiment. Geometric means are indicated by horizontal bars. Significance was determined by ANOVA with Tukey-Kramer post hoc test. Samples that do not share a letter are significantly different. $P > 0.05$

Virulence Analysis of SK330

As we already ruled out bacteriocin production as a factor, we wondered if perhaps, a strain or several strains might outcompete SK330 for nutrients at the site of attachment to the sterile vegetation. To explore this, we co-inoculated two strains onto either blood agar or into pooled rabbit serum and allowed for 24 h of growth. Fig 3.15 demonstrates that in a pairwise comparison against Em^r SK36 (i.e., JFP36), SK330

growth was variable depending on the media used for culture incubation. On blood agar (Fig 3.15A), there appeared to be no difference in strain growth, whereas in serum, SK330 significantly outperformed SK36 (Fig 3.15B). Additionally, although SK330 was not directly compared against other strains in this assay, it had a higher final CFU in serum and a lower CFU count in BHI than SK115, SK405, or SK678, a finding that was consistent with results seen previously in Fig 3.9. The variability in growth of SK330 was also observed in later studies in which SK330 was competed against differing pools of strains used in the Bar-seq study (data not shown), and when grown with differing starting densities relative to SK36 (data not shown).

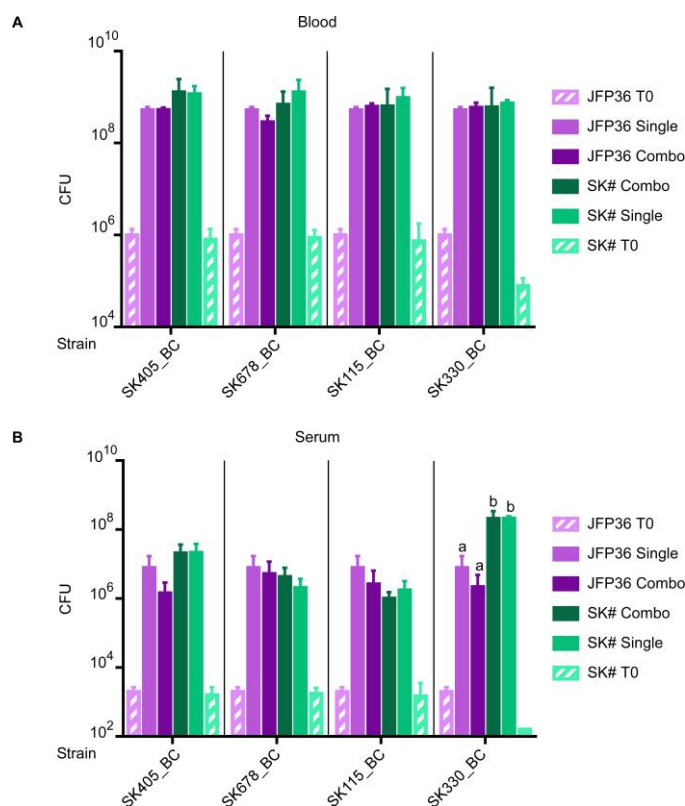


Fig 3.15 Pairwise *S. sanguinis* strain competition assay. Strains were co-inoculated onto **A)** blood agar plates or into **B)** pooled rabbit serum and growth was assessed after 24 h. The means and standard deviations are shown for n=3 experiments. Statistical significance for the 24 h samples was assessed by ANOVA with a Tukey-Kramer post-hoc test for each strain pair (delineated by black vertical bars): $P < 0.01$.

One possible explanation for these results is restriction modification (RM) system methyltransferase (MTase) activity. In *S. pneumoniae*, RM system MTase activity has been shown to be responsible for the long-observed switching of cells between an opaque colony morphology, associated with abundant capsule production and increased systemic virulence, and a smooth colony phenotype that has less capsule, enhanced nasopharyngeal colonization, and reduced virulence (158-160). This system has also been shown to be involved in transcriptional regulation, phenotypic phase variation, DNA repair, and population evolution (161, 162).

Within the draft sequences of *S. sanguinis* there are multiple homologous RM systems. The Type I system, present in at least 9 of the 20 strains, contains a nearby recombinase gene, along with a methyltransferase and specificity subunit. The MTase and S subunits are both necessary and sufficient for methylation activity and the REase is required for restriction. The S subunit includes two target recognition domains (TRDs) that impart target sequence specificity to both the restriction and modification activities of the natural multi-subunit complex. Recombination events include switching among or within the S- subunits, which results in phase variation. SK330 is one of the nine strains that have this system. We hypothesized that this system may play a role in growth of the strain in rabbit serum when grown singly versus in competition with other strains.

We tested this in SK330 by growing the strain in differing media, with and without competition, and assaying the arrangement of the RM system using a previously described PCR-based method (160). In brief, primer sets (a forward and reverse) are designed within each region of the RM site and used with a cognate primer for amplification. Depending on which of the sets, forward or reverse, gives a product,

information is obtained on the directionality of that particular subunit. In effect, this can discriminate between subunits that may have undergone an inversion. Additionally, products that are a different size than expected may indicate a subunit has recombined or switched with an adjacent subunit. Both possibilities have been shown to affect virulence. Fig 3.16 summarizes the results of these PCR reactions. Cells that were grown in BHI were primarily of the “parental” genotype (first map in Fig. 3.16), but at least two different recombination events were also apparent—the inversion of the second domain of the full-length S.1 subunit, and the switching of that same domain with S.3 (Fig. 3.16). In contrast, only the parental genotype was detected in serum-grown cells. No cardiac homogenate was available for testing to determine the RM profile of SK330 that had undergone selective pressure in the blood; however, it is plausible that in the Bar-seq experiment where SK330 was 1/17th of the inoculum, it likely found itself in competition with other strain. This may have induced or selected for subunit switching, whereas in Fig 3.14, SK330 was 1/3 of the inoculum, and may have been separated from the other two strains, removing pressure to change the RM subunit configuration.

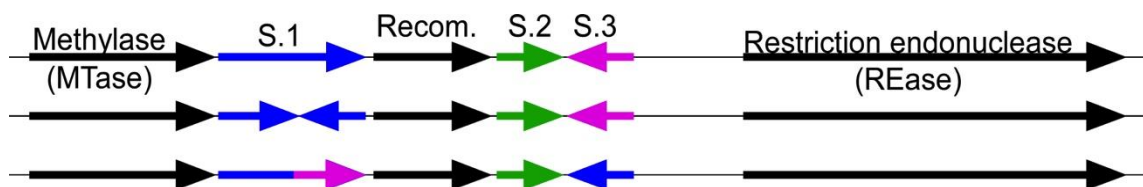


Fig 3.16 The SK330 rearranging Type I RM system. RM= site-specific recombinase.

Discussion

Combining powerful bioinformatic analysis with a novel Bar-seq method allowed us to better interrogate the virulence of the *S. sanguinis* species as a whole while minimizing animal use.

Through the identification of a conserved intergenic region, we were able to insert unique barcode sequences into 17 *S. sanguinis* isolates that we could then use to track the growth of each respective strain in a rabbit model of endocarditis. This premise proved successful methodologically, as evidenced by the near-equal recovery of each barcode in duplicate inoculum pools and practically, as seen in the wide growth variability in harvested cardiac homogenates.

No correlation between virulence and strain origin was seen in this assay, and is in agreement with a conclusion reached previously using data derived solely from MLSA of isolates of differing origin (163). This is, perhaps, not surprising when considering the incidence of IE is relatively low, in spite of the relative ease of access that *S. sanguinis* has to the bloodstream. It has been suggested that other considerations, such as cardiac risk factors (164), may play a more important role in IE pathogenesis.

In spite of this, it is interesting to note that many of the most virulent strains cluster in the phylogenetic tree, a phenomena which suggests there may be lineages that may be better able to cause disease. The results of the phylogenetic tree may also inform our bioinformatic virulence sort, which did not identify many genes with known ties to virulence. The SNP-based tree focuses on evolution of core genes, which, in effect, may offer a hypothesis that allelic differences account for virulence. This would

not have been accounted for in the virulence sort, which was more similar to the Pan-based tree approach in that it was based on presence or absence of genes.

We considered our Bar-seq results might have been influenced by external factors relating to the pooled inoculation method. One unlikely possibility that was seen in previous studies using a 40-strain pooled inoculum was a bottleneck effect, where differences in recovery are due to chance rather than differences in virulence (114). In fact, it would appear that this was not a factor in our results as the reads for each barcode were similar between animals, in spite of being variable from strain to strain. Our next hypothesis was bias due to inter-strain competition. We chose to examine bacteriocin production as *S. sanguinis* is incredibly competent (165), and may use bacteriocin production as a mechanism to kill cells that are not competent (145, 166, 167). This process is beneficial as it makes DNA available for uptake and increases the genetic plasticity population. It may also function to limit the maintenance of social cheaters (168). However, our bacteriocin assay saw no evidence for killing by *S. sanguinis*-mediated bacteriocin production. Finally, we considered our previous and subsequent data where several of the Bar-seq strains were co-inoculated into rabbits in smaller pools. These results were conflicting, with some strains (SK405 vs. SK36) appearing to corroborate their Bar-seq relationship and recovery levels, and other strains (SK330 vs. SK36) appearing to exhibit a completely different phenotype. Although the reasons for this have not been thoroughly investigated, preliminary studies suggest that the differences may be accounted for by RM systems present in some strains that may alter virulence profiles when stimulated. In this context, we hypothesize that competition might be provide the stimulus for this phenomenon.

A comparison of the virulence and the phylogenetic trees suggested subtle differences in genetic composition could explain the variability in strain recovery of the Bar-seq experiment. We wondered if strains might cluster together in other biologically relevant assays in a manner similar to the virulence study. Together, small improvements in multiple assays could explain an overall more virulent phenotype. Subsequent investigations into biofilm formation (oral and cardiac simulated) found there was no similar strain pattern to that seen with virulence. We were hopeful there would be differences in manganese content, as manganese-deficient strains have several known defects and, while there is no *in vivo* information on strain performance when manganese is plentiful, perhaps strains with higher manganese would be better able to adapt to life in the bloodstream. Unfortunately, similar results were found when the strains were assayed for metal content, where there was no correlation between manganese content and virulence. Interestingly, there was an association with isolates of blood origin.

Although no specific conclusions regarding virulence were obtained in this study, we are happy to provide this compilation of bioinformatic and phenotypic data to the streptococcal community. Indeed, the rigor of this study not only expanded the total knowledge of *S. sanguinis*, but also aided in the identification of strains that had been mislabeled in GenBank. Although these errors may persist in GenBank for some time (169, 170), as NCBI has not yet attempted to address these errors, the scientific community is now aware of the implications of these findings. As such, further propagation of incorrect information and continued misallocation of resources can be avoided.

CHAPTER 4

Loss of an integral membrane protein restores serum growth to manganese-deficient *Streptococcus sanguinis*

Rationale

While working with manganese-deficient SsaB mutants, which are severely attenuated in growth, we identified suppressor mutants that were able to circumvent manganese limitation and grow in pooled serum through a heretofore unknown mechanism. Subsequent investigations revealed that the suppressor mutant phenotype was not maintained in a rabbit model of endocarditis. The reasons for the discrepancy between growth in pooled serum versus *in vivo* are not known; however, these findings highlight the need for continued refinement of our *in vitro* model and serve to remind the scientific community that bacterial circumvention of therapeutics is possible.

Introduction

Metals are an essential component of bacterial physiology, serving as cofactors and providing structural support for a number of proteins that, in turn, are key components in bacterial processes including metabolism and defense (176). Metal acquisition is therefore tantamount to survival. For pathogens, obtaining metals necessitates expression of high-affinity metal transport systems, as metals are typically limited within a host. This shortage is attributed to specialized host proteins, such as ferritin and calprotectin, whose sole purpose is metal sequestration for the prevention of pathogen invasion (177-180) and otherwise harmful redox reactions (181, 182).

One well-characterized method of metal procurement by bacteria is the Lral (Lipoprotein Receptor Antigen I) family of ABC-type metal-transport proteins, specifically those belonging to the A-I group (92, 93, 155). Present throughout the streptococci, this group has been implicated in manganese transport in all cases (94-96), and iron in some circumstances (101, 117, 183, 184). In turn, the relationship between manganese and virulence has been thoroughly examined, with findings highlighting how loss of these transport proteins is equivalent to loss of virulence in multiple models of infection (96, 98-101, 115). In these cases and others, manganese loss has been demonstrated to disrupt a number of manganese-centric processes including superoxide dismutase activity (90), deoxyribonucleotide synthesis (106), and degradation of the alarmone (p)ppGpp (185, 186). Loss of any one of these systems is detrimental to bacterial virulence as it renders the bacteria sensitive to oxidative stress tolerance (90), impaired in DNA replication and repair (108), and unable to maintain the cellular balance between growth and survival (187) respectively.

Some bacteria are able to circumvent the loss of this transport family through the use of alternative metal uptake systems. For manganese, and iron to some extent, one such alternative system is the NRAMP family of metal transporters. These transporters are common, present in both eukaryotes and prokaryotes, and play an important role at the host-pathogen interface. They are pH dependent, and similar to the Lral-family, have been demonstrated to be important in bacterial pathogenesis and resistance to oxidative stress (101, 157, 188).

Because the inability to acquire metals is so tightly associated with loss of virulence, and as metal transporters are typically highly conserved, they have become

the focus for targeted therapeutics (67, 68) and vaccines (65, 189). The efficacy of this approach has been suggested as vaccination studies against the Lral family of lipoproteins (64, 65) and inhibition of ZnuABC-mediated zinc transport in *Salmonella* Typhimurium through the use of a small-molecule inhibitor (190) have been successful in a basic laboratory setting. However, as of yet, there are no currently available commercial therapeutics.

In *S. sanguinis* strain SK36, there is a single annotated manganese transport system that belongs to the Lral-family. Loss of this protein, SsaACB, results in severely diminished aerobic growth in serum and loss of virulence in a rabbit model of endocarditis. Two strains of *S. sanguinis*, SK408 and VMC66—characterized in the previous chapter, have an additional NRAMP-family transporter that provides redundancy in manganese uptake. In fact, recent studies in *E. faecalis* have shown that deletion of the Lral transporter, does not result in the severe attenuation of virulence characteristic of SsaB-deficient *S. sanguinis* SK36 (157). Similar virulence deficiencies are only seen when the NRAMP transporter is deleted in addition to the Lral transport system (157). This finding is significant in that infections with these strains may be more difficult to treat, as they may be more resistant to SsaB-targeting therapeutics.

Specific Materials and Methods

DNA Isolation and Whole-Genome Sequencing

Strains (Table 4.1) were grown overnight in BHI in 6% O₂. DNA was isolated using a modification of the Qiagen DNeasy Kit protocol. In brief, cells were diluted and harvested from a logarithmic-phase culture. Enzymatic lysis buffer containing 20 mg/ml lysozyme was freshly prepared and added to each sample. Then the Qiagen DNeasy kit protocol was followed as directed. The eluate was concentrated by addition of 10mg of oyster glycogen, 0.1 volumes of 3M sodium acetate and 2.5 volumes of 100% ethanol, followed by incubation for 30 minutes at room temperature, and centrifugation at 15,000 RPM for 20 minutes at 20°C. The pellet was washed with 1 ml 70% ethanol by gently inverting the tube. The supernatant was discarded and the pellet was dried by speedvac until no visible liquid remained. The pellet was resuspended in 50 µl elution buffer. DNA was electrophoresed for 2 hours at 70 volts on a 2% agarose gel. Samples were quantified by spot densitometry and sent to the VCU Nucleic Acid Research Facility for 300-bp paired-end whole-genome sequencing on the Illumina Mi-seq. Results were analyzed using the Geneious R10 (version 10.2.3) program.

Table 4.1 Primers and Strain Construction

| # | Primer | Sequence | Strain Creation |
|--|-------------------------|--|--|
| WT (SK36) ΔssaACB Km^r by overlap extension PCR | | | |
| 1 | Kan-F2 | ATGGCTAAAAATGAGAATATCACC | <i>apha-3</i> |
| 2 | Kan-R2 | CTAAAACAATTCATCCAGTA | <i>apha-3</i> |
| 3 | 0262-F1 | GCACGATGATAAGCTCCTG | left fragment |
| 4 | 0262-R1S | TCTCATTTTAGCCATCTCATACACCTCTATAGT | left fragment (short) |
| 5 | 0262-R1L | TCTCATTTTAGCCATTTAAAATAAAAAATAAGTCAAGT | left fragment (long) |
| 6 | 0260-F3 | GATGAATTGTTTTAGTAATAAAAGGTTAGGAAGACA | right fragment |
| 7 | 0260-R3 | CGTTTTCTCAATATTAATCAATCCA | right fragment |
| Complemented ΔssaACB Km^r by overlap extension PCR | | | |
| 8 | ssaACB-Asc | GTTGCGAGCGCGCCTCATCTTCTCTCACTTTCATGC | <i>ssaACB</i> |
| 9 | ssaACB-Not | AGAGCGGGCGGCCGCGGATTTGTCTTCCCTAACCTTTT | <i>ssaACB</i> |
| 10 | 0170 | TCGACTGTCTATGGTGGACAGCG | left fragment |
| 11 | pJFP96-Asc | GGCGCGCCTGCGAACACATGG | left fragment |
| 12 | pJFP96-Not | GCGCGCCCGCTCTAGAACT | right fragment |
| 13 | Frag Reverse | TCGACTCGTGACGGAAGCAGACTTGG | right fragment |
| SNP mutants by direct amplification and subsequent transformation | | | |
| 14 | ssa_0696_MC_L1 (679610) | CATGCCTGAGGACACAGAGAACTTGTC | positions: 679,285; 679,340; 679,563; 679,610; 679,709 |
| 15 | ssa_0696_MC_R1 (679610) | GGAGTAAAAGTTGGCAGAGGCTCAAATCAAACCTATTCT | positions: 679,285; 679,340; 679,563; 679,610; 679,709 |
| 26 | ssa_0916_MC_L1 | GGATGTCAACCGAGTTTTGGGAAC | position 928,775 |
| 27 | ssa_0916_MC_R2 | TAATGGCATCATCTGCCTCAATGATTTG | position 928,775 |
| 28 | ssa_1044_MC_L1 | GGAACCTGAACTGGCTGGTC | position 1,060,699 |
| 29 | ssa_1044_MC_R2 | TCCTTCTCCAGCTCGAAATTAATAT | position 1,060,699 |
| 30 | 1217844_MC_L1 | AAGTCACGGTGGCCATTATC | position 1,217,844 |
| 31 | 1217844_MC_R2 | ATCCGACAGACACTGCATGA | position 1,217,844 |
| WT (SK36) ΔSSA_0696 Sc^r and ΔssaACB ΔSSA_0696 by overlap extension PCR | | | |
| 32 | Spec_L1 | TCATGGAGGATTTGTGAGGAGGATATATTTGAATACATACG | <i>aad9</i> fragment |
| 33 | spec_R1 | GAAGTGAATGACGCGGAATGGATCCAAT | <i>aad9</i> fragment |
| 34 | ssa_0696_MC_L1 (679610) | CATGCCTGAGGACACAGAGAACTTGTC | left fragment |
| 35 | 0696_Lflank | TATCCTCTCACAAAATCCTCCATGAGATAATTAAGTTAGG | left fragment |
| 36 | ssa_0696_MC_R2 (679610) | GGAGTAAAAGTTGGCAGAGGCTCAAATCAAACCTATTCT | right fragment |
| 37 | 0696_Rflank | GGATCCATTCCGGTCAATCACTTCGAATTTGTAGCTCCTG | right fragment |
| Complemented ΔssaACB ΔSSA_0696 | | | |
| 38 | 679_709_L1 | TGGCTATTGCTCAAGCCTTT | SSA_0696 |
| 39 | ssa_0696_MC_R2 (679709) | AAAGTTGGCAGAGGCTCAAA | SSA_0696 |
| ΔssaACB ΔSSA_0696 ΔSSA_0695 by overlap extension PCR | | | |
| 40 | spec_Lf_F1_0695 | GGGAACCTAGGAGGTGAGGAGGATATATTTGAATACATACGAAC | <i>aad9</i> fragment with native promoter |
| 41 | spec_Rf_R1_0695 | CTCCATGAGATAATGACGCGGAATGGATCCAATTTTTTTTATAATTTTTTAATC | <i>aad9</i> fragment with native promoter |
| 42 | 679709_L1 | TGGCTATTGCTCAAGCCTTT | left fragment |
| 43 | spec_Lf_R1_0695 | ATATCCTCCTCACCTCCTAGGTTCCATTCTAATATAAG | left fragment |
| 44 | spec_Rf_F1_0696 | CCATCCCGCTCATTCACCTCGAAATTTGTAGCTCC | right fragment |
| 45 | ssa_0696_MC_R2 (679709) | AAAGTTGGCAGAGGCTCAAA | right fragment |
| ΔssaACB ΔECF | | | |
| 46 | New_ECF_F1 | AACAGTAGCTGTTGATCC | left fragment |
| 47 | ECF-R1 | AGATTAATAAAAAATTAAGGCCGCGCTGCTGTTAAAGTGT | left fragment |
| 48 | Spec_Bseq_L1 | CCGCTTAGAACTAGTGG | <i>aad9</i> fragment with native promoter |
| 49 | Spec_Bseq_R1 | CGGCGCCTTATAATTTTTTAATCT | <i>aad9</i> fragment with native promoter |
| 50 | ECF-F2 | CCAAGTCTTAGAGCGGATCCAGAAATAATCGTAAAGATTAAG | right fragment |
| 51 | New_ECF_Rev | CTTATCTCTGAAAAATCAAGCC | right fragment |
| SK49 ΔssaACB ΔSSA_0696 | | | |
| 52 | SK49-0696-F1 | AGACCAGTTTGAACAGCTG | left fragment |
| 53 | SK49-0696-R1 | ATATCCTCCTCACAAAATCCTCCATGAGATGATTAG | left fragment |
| 54 | SK49-spec-F1 | TCATGGAGGATTTGTGAGGAGGATATATTTGAATAC | <i>aad9</i> fragment |
| 55 | SK49-spec-R1 | AATTTAAAGTGAATGACGCGGAATGGATCCAATTTTTTTTATAATTTTTTAATC | <i>aad9</i> fragment |
| 56 | SK49-0696-F3 | CCATCCCGCTCATTCACCTTAAATTTATAGCTCCTGTC | right fragment |
| 57 | SK49-0696-R3 | CATTTTCCCGACTCTCGG | right fragment |

Bioinformatic Analyses

TMHMM v.2.0 was used for protein topology prediction (171, 172). Signal peptide prediction was determined with SignalP 3.0 (173). Structural comparisons were determined using Phyre V 2.0 (174). Protter provided the basis for graphical representation of SSA_0696 within the membrane (175).

RNA Preparation and RNA-seq Analysis

Strains were inoculated into BHI containing appropriate antibiotics and placed in 1% O₂ (1% O₂, 9.5% H₂, 9.5% CO₂, and 80% N₂) for overnight growth. Additional tubes containing 19.5 ml and 6 ml of rabbit serum were also placed under these conditions for each included strain. Two additional 6 ml tubes of rabbit serum were placed in an incubator with lids loose. All tubes were incubated overnight at 37°C. The following day all 1% O₂ tubes were transferred to an anaerobic chamber. The overnight culture was vortexed and 500 µl was added to the tube containing 19.5 ml of rabbit serum. The 20 ml culture was incubated for 3.5 hours before 6 ml was removed and added to each 6 ml serum tube. The anaerobic sample was immediately dipped for 30 seconds in a dry ice bath and then centrifuged. This was repeated with the aerobic samples at 10 minutes and 30 minutes following transfer from the anaerobic chamber. The supernatants were discarded and the pellets were resuspended in 700 µl RLT buffer (Qiagen RNeasy Kit) containing 7 µl β-mercaptoethanol and vortexed vigorously for 10 seconds. The suspension was transferred to 2-ml tubes of lysing matrix b beads (MPBio) followed by disruption with a Fast Prep 24 instrument for 45 seconds at level 6. The suspension was centrifuged for 3 minutes and the supernatant was transferred to a new tube. The standard Qiagen RNeasy Kit protocol was then followed, beginning with

addition of an equal volume of ethanol. RNA was quantified with a NanoDrop spectrophotometer and sequenced with 300 bp paired-end reads on the Illumina Mi-Seq. Results were analyzed using the DE-Seq module in the Geneious R10 (version 10.2.3) program.

Results

Complementation of manganese-transport deficient *S. sanguinis*

Studies in *S. sanguinis* SK36 have shown that disruption of the lipoprotein SsaB results in growth attenuation in pooled rabbit serum and attenuation in virulence in a rabbit model of endocarditis (90, 113). Manganese addition restored growth (90), which is consistent with the role of the SsaACB protein complex in manganese transport. This result also suggested an alternative manganese transport system is present and capable of supporting growth in a high-manganese environment in the event of an SsaACB system failure. Efforts to complement this mutant genetically, by placing a WT copy of the mutated gene in a plasmid or an ectopic expression site (113, 138) have met with limited success, however (90). This is likely due to one of two possibilities, the first being an ineffective complementation construct (90, 116, 191). Separation of the *ssaB* gene from the rest of the complex might have disrupted the normal stoichiometry and created artificial differences in expression levels or disjointed the translation and secretion of the component proteins in space and time. The second possibility is that disruption of SsaB could have had a polar effect on *tpx*, a downstream gene that has been shown to be co-transcribed with the *ssaACB* operon in some cases (192, 193). To test these possibilities, a strain was created in which the entire *ssaACB* operon was deleted. The strain was complemented by replacing the operon, including its native

promoter, in the same ectopic chromosomal site used in the attempted complementation of the *ssaB* mutant.

Aerobic growth in pooled rabbit serum of the Δ *ssaACB* mutant resembled the *ssaB* mutant(91)(Fig 4.1A). Growth was fully restored in the complemented strain, both in pooled rabbit serum (Fig 4.1A) and *in vivo* (Fig 4.1B). Fig 4.1B used the Tc^r Δ *ssaACB* _1 strain, as opposed to the Km^r Δ *ssaACB* strain used elsewhere. This allowed for later strain differentiation by plating. Additionally, metal levels for the Δ *ssaACB* strain were comparable to those in the *ssaB* mutant, while the complemented strain had WT levels of metals and also of SsaB expression (Fig 4.1C-D).

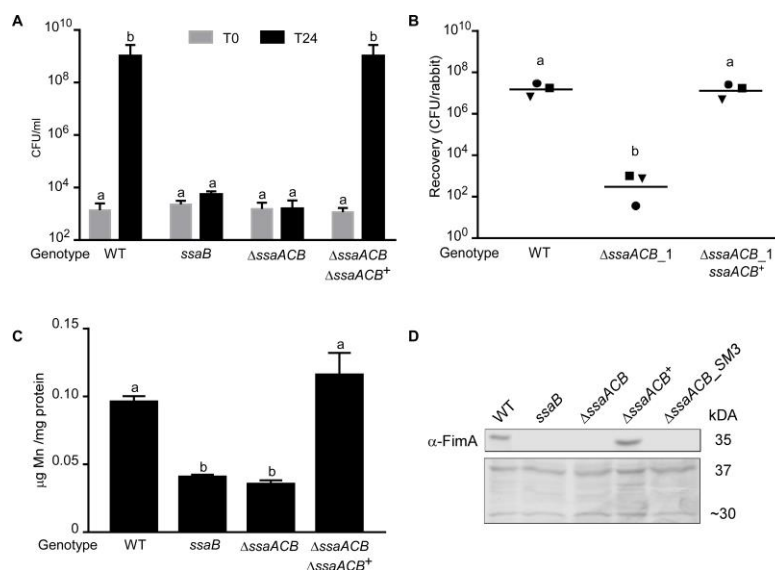


Fig 4.1 Investigation of an Δ *ssaACB* mutant and its complemented derivative. (A) Growth in pooled rabbit serum. All strains were incubated for 24 h in rabbit serum in 12% O₂. Bacteria were enumerated by dilution plating. Colony counts are shown for both T₀ h and T₂₄ h. The means and standard deviations from a minimum of 3 independent experiments are indicated. Statistical significance was assessed by ANOVA with a Tukey-Kramer post-hoc test; $P < 0.001$. **(B)** Virulence testing in a rabbit model of IE. Rabbits were co-inoculated with WT, the Δ *ssaACB*, and complemented Δ *ssaACB* strains and sacrificed at 20 h post-infection. Individual values and geometric means of recovered bacteria from 3 rabbits are shown. Shared symbols indicate different strains recovered from the same rabbit. Statistical significance was determined by repeated-measures ANOVA with a Tukey-Kramer post-hoc test; $P < 0.01$. **(C)** Metal analysis. Strains were grown in BHI in 12% O₂. Metal levels for Mn, Fe, Co and Zn are indicated. Statistical significance was assessed by ANOVA with a Tukey-Kramer post-hoc test; $P < 0.001$. **(D)** SsaB expression in a complemented *ssaACB* mutant and a representative suppressor mutant. SsaB expression was determined by probing with anti-FimA. In A, B, and C, samples that do not share a letter are significantly different

Spontaneous $\Delta ssaACB$ Reversion Mutants

During the above studies, there were several instances when the $\Delta ssaACB$ strain grew well beyond expectations. In each circumstance, colonies were saved for later testing. Initially, we wondered whether our mutant stock was contaminated with WT cells. However, after reaffirming that these cells were kanamycin resistant as expected, we assayed for SsaB expression. For both the WT and complemented mutant, a robust SsaB signal was detected when probing with antiserum raised against FimA, an ortholog of SsaB found in *Streptococcus parasanguinis* (66, 90, 113); however, for the *ssaB* mutant and these spontaneous mutants, no signal was detected (Fig 4.1C). Additionally, when grown in aerobic rabbit serum, these spontaneous mutants continued to grow significantly better than the $\Delta ssaACB$ parent strain (Fig 4.2). Taken together, these results suggested that we had true spontaneous, or suppressor, mutants, as opposed to a contaminated stock culture.

Suppressor Mutant Isolation and Whole-Genome Sequencing

We next attempted to isolate additional suppressor mutants. To our knowledge, suppressor mutants have never arisen in a manganese-deficient *S. sanguinis* background, and we wondered whether the mutants we obtained thus far were representative of a single mechanism for circumvention of a manganese requirement, or whether they encompassed multiple possibilities. Obtaining and sequencing additional suppressor mutants could help to answer this question. To promote the possibility for suppressor mutant growth, we serially passaged the *ssaB* and $\Delta ssaACB$ mutants in serum over two days with the idea that this would allow additional time for outgrowth of any mutants that may arise. Indeed, this was the case, as two additional suppressor

mutants were obtained from each parent background, bringing our total collection to seven strains—five obtained from independent experiments and two possible siblings chosen from the same plate (Table 4.2). Interestingly, all of the isolates had similar levels of growth restoration when assessed in our typical serum growth study (Fig 4.2), suggesting, perhaps, that a mutation in a common gene or pathway was responsible.

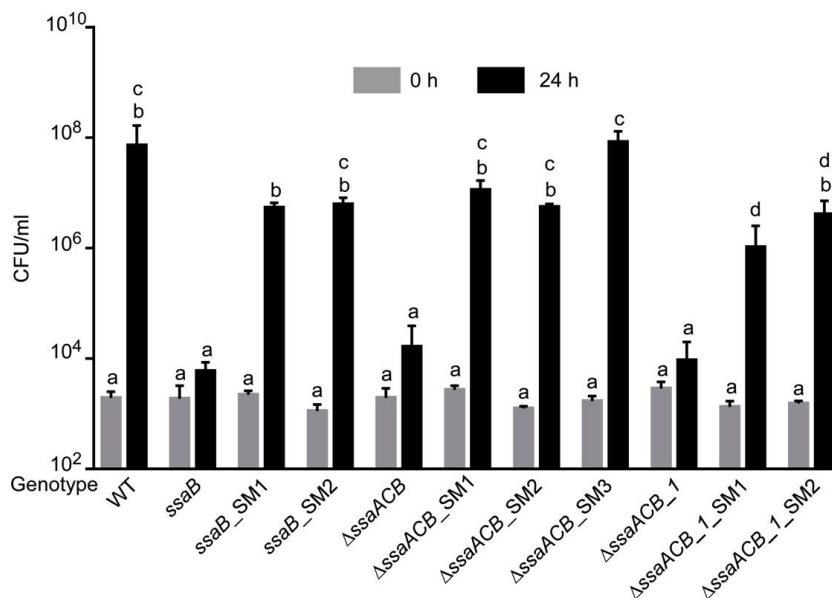


Fig 4.2 Growth of suppressor mutants and parental strains. Serum growth was examined as in Fig 1A. Statistical significance was assessed by ANOVA with a Tukey-Kramer post-hoc test. Samples that do not share a letter are significantly different; $p < 0.05$.

Whole-genome sequencing of the suppressor mutants, the *ssaB* mutant and both Δ *ssaACB* parents, revealed eight, high-confidence, unique single nucleotide polymorphisms (SNPs) across three genes and two non-coding regions (Table 4.2). Additional SNPs (excluded from Table 4.2) were identified, but were low-confidence calls and appeared to represent a minority of the population, at most. In Table 4.2, missense mutations account for the majority of SNPs; however, one resulted in a frame shift and another may have disrupted a ribosome-binding site. Interestingly, although

SNPs were identified across multiple genes, each suppressor strain sequenced had an SNP associated with a single gene, SSA_0696.

Table 2 Strain genealogy and SNP-related information

| WT | Strain Genealogy | | SNP-Related Information | | | |
|------------------------------|--|--|-----------------------------------|--|---------------------------------------|--|
| | Generation 1 | Generation 2 | SNP Position | Amino Acid Change | Affected Location | Putative Function |
| SK36 (human oral isolate) | <i>ssaB</i> (Cm ^R ; <i>ssaB</i> :: <i>mariner2</i>) | <i>ssaB</i> _SM1 | 679,610; 1,217,844 | A106E; N/A | SSA_0696; 96 bp before SSA_1189 | integral membrane protein; non-coding |
| | | <i>ssaB</i> _SM2 | 679,610; 1,217,844 | A106E; N/A | SSA_0696; 96 bp before SSA_1189 | integral membrane protein; non-coding |
| | Δ <i>ssaACB</i> (Km ^R ; <i>ssaACB</i> :: <i>aphA</i>); | Δ <i>ssaACB</i> _SM1 | 679,709 | S139T | SSA_0696 | integral membrane protein |
| | | Δ <i>ssaACB</i> _SM2 | 679,340 | S16L | SSA_0696 | integral membrane protein |
| | | Δ <i>ssaACB</i> _SM3 | 679,563; 928,775; 1,060,699 | D90 --> Frameshift; M160T; G235D | SSA_0696; SSA_0916; SSA_1044 | integral membrane protein; α/β hydrolase; <i>thrB</i> |
| | Δ <i>ssaACB</i> _1 ¹ (Km ^R ; <i>ssaACB</i> :: <i>aphA</i>); | Δ <i>ssaACB</i> _1_SM1 ² | 679,285 | N/A | 9 bp before SSA_0696 | non-coding |
| | | Δ <i>ssaACB</i> _1_SM2 ² | 679,285 | N/A | 9 bp before SSA_0696 | non-coding |

¹A second Δ *ssaACB* clone.

²Two clones chosen from the same suspected suppressor mutant plate. Every other isolate was obtained from different experiments.

Table 4.2 Strain genealogy and SNP-related information.

SSA_0696 Is Responsible for the Suppressor Phenotype

SSA_0696 is annotated as a 26-kDa putative integral membrane protein of uncharacterized function. *In silico* analyses predicted six transmembrane domains, notable structural homology (~50%) to an ECF-type folate transporter, and no recognizable signal sequence. There is a paralog immediately upstream, SSA_0695. Beyond this, very little is known.

To conclusively implicate SSA_0696 in the suppressor mutant phenotype and thereby eliminate the other SNPs present, we generated PCR amplicons containing each individual SNP identified by WGS. Transformation of each of these SNPs into the background in which they were first identified established a library of 8 single-SNP strains. Aerobic growth of these strains was tested. Only the strains with SNPs related to SSA_0696 displayed the suppressor phenotype (Fig 4.3).

Within the gene, the mutations were widely dispersed. This, combined with the frame shift mutation that was present in the first half of the gene, suggested the phenotype likely resulted from gene inactivation (Fig 4.4). This was confirmed by

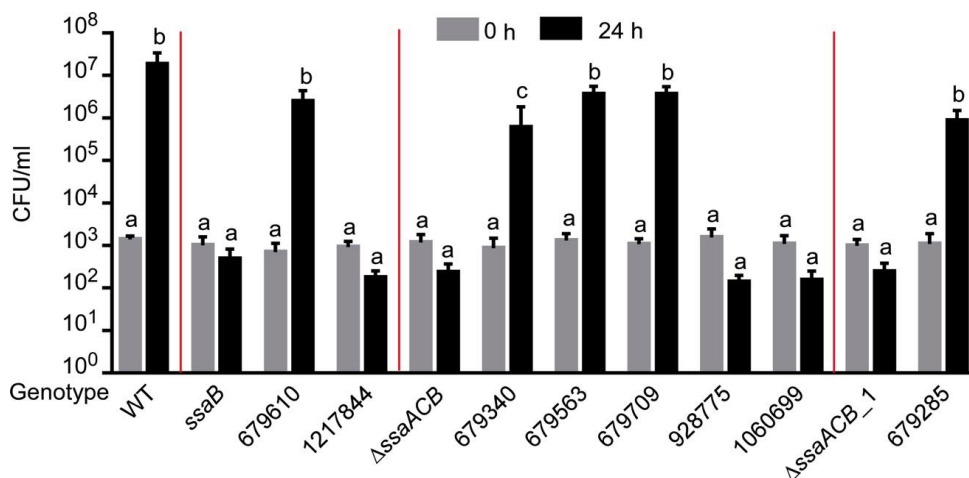


Fig 4.3. The role of individual SNPs identified by WGS on the suppressor phenotype. Names reflect the coordinate of the SNP mutation identified in Table 2. Red lines indicate different strain families, as in Fig. 2. Serum growth was examined as in Fig 1A. Statistical significance was assessed by ANOVA with a Tukey-Kramer post-hoc test. Samples that do not share a letter are significantly different; $P < 0.05$.

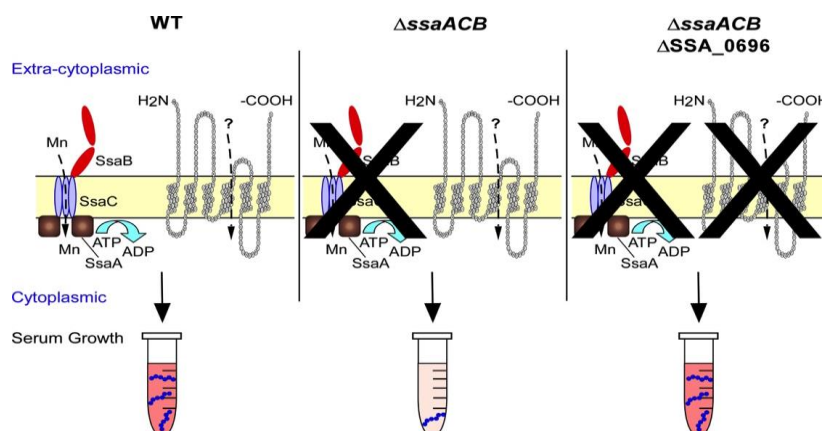


Fig 4.4. Graphical representation of SSA_0696 in suppressor phenotype.

deletion of SSA_0696 from both a WT and Δ ssaACB background. The gene was replaced with a spectinomycin resistance gene under control of the native SSA_0696 promoter and ribosome-binding site. In both cases, deletion of SSA_0696 resulted in a significant improvement in growth (Fig 4.5). Of interest, although growth was complemented when SSA_0696 was deleted, neither Δ SSA_0696 strain resembled their parent strain when examined microscopically. In fact, they were opposite morphologically, with the SSA_0696 mutant typically forming clumps as opposed to chains when grown in BHI, and chains as opposed to clumps when grown in pooled rabbit serum (data not shown). The role of SSA_0696 was confirmed when the growth of the Δ ssaACB Δ SSA_0696 strain was successfully complemented by introducing the

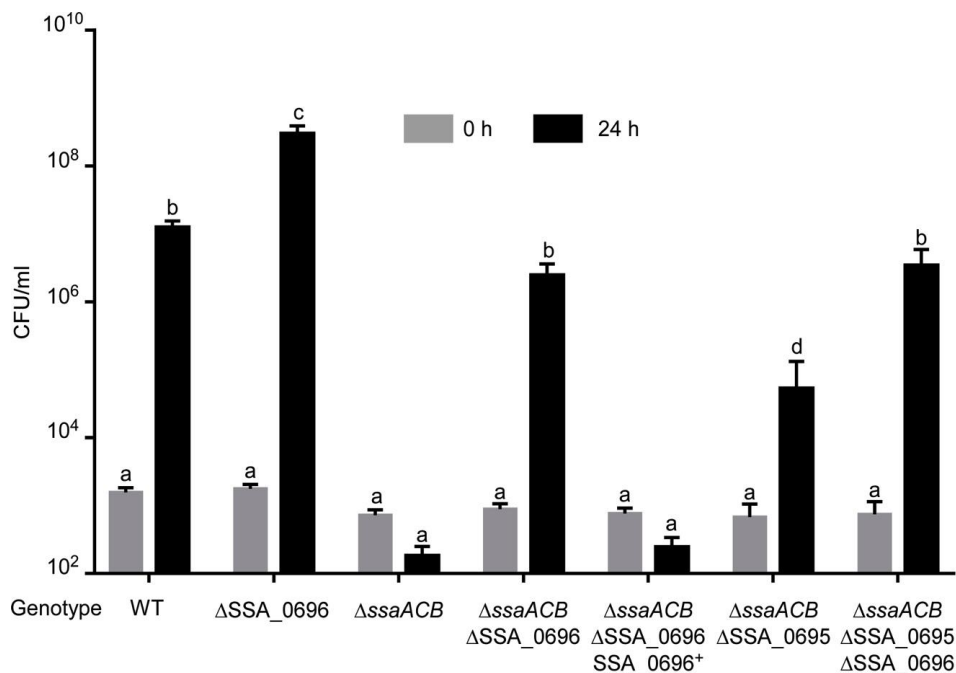


Fig 4.5. The contribution of SSA_0695 and SSA_0696 to serum growth. Serum growth was examined as in Fig 1A. Statistical significance was assessed by repeated measures ANOVA with a Tukey-Kramer post-hoc test. Samples that do not share a letter are significantly different; $P < 0.01$.

SSA_0696 gene into its native site on the chromosome (Fig 4.5).

Previous studies by our lab and others have established the importance of characterizing a species rather than a specific strain, as strain-specific phenotypes are not uncommon (71, 158-160). In consideration of this, we removed the SSA_0696 equivalent, HMPREF9380_0754, from a derivative of the *S. sanguinis* strain SK49 in which the *ssaACB* operon had been deleted. As for the SK36 version, this gene was replaced with a spectinomycin-resistance cassette under control of the native SK49 promoter. Like SK36, this strain is also an oral isolate; however, in a study examining virulence by sequencing barcodes recovered from cardiac homogenates, this strain was appreciably less virulent than SK36 (71). Results of growth in pooled rabbit serum were surprising, as loss of SSA_0696 suppressed the poor-growth phenotype of an Δ *ssaACB* mutant; however, not to the extent that it was indistinguishable from WT (Fig 4.6). This suggests SK36 may have a capacity to overcome a manganese-deficiency that is not

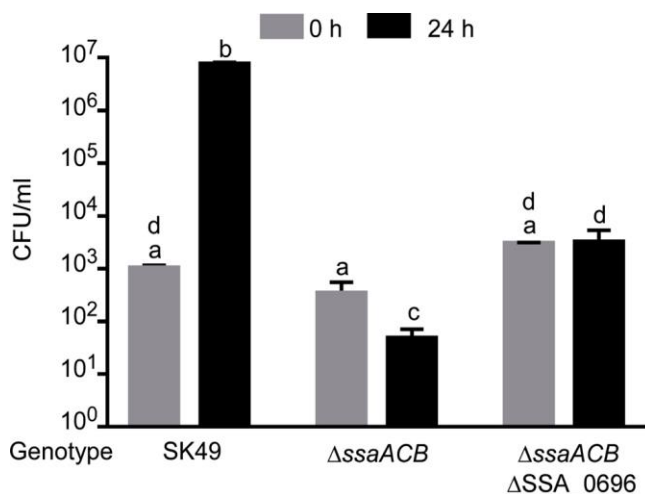


Fig 4.6. The role of SSA_0696 in SK49. All strains were grown for 24 h in rabbit serum in 12% O₂. Strains were enumerated by plating serial dilutions and counting resulting colonies. Colony counts are shown for both T0 h and T24 h. The means and standard deviations of 3 independent experiments are indicated. Statistical significance was assessed by ANOVA with a Tukey-Kramer post-hoc test. Samples that do not share a letter are significantly different; $p < 0.05$.

shared by other strains.

Together SSA_0696 and SSA_0695, a paralog located upstream, are predicted to constitute an entire operon. Because of this, we hypothesized the two proteins might serve redundant functions. To test this, we created two strains: one deleted for $\Delta ssaACB \Delta SSA_0695$ and the other for $\Delta ssaACB \Delta SSA_0695-0696$ and assessed their growth in serum. As indicated in Fig 4.5, deletion of SSA_0695 only, results in a partial restoration of growth. This is not enough to be indistinguishable from the WT or $\Delta ssaACB \Delta SSA_0696$ strain, but is enough to be significantly different from its $\Delta ssaACB$ parent. Removal of SSA_0695 in the $\Delta ssaACB \Delta SSA_0696$ background did not improve the growth relative to the $\Delta ssaACB \Delta SSA_0696$ strain, indicating that these genes do not function additively or synergistically (Fig 4.5).

Investigation of SSA_0696 Suppression Mechanism

As these mutants emerged from a manganese-deficient background and in manganese-limited serum, we wondered if their restored growth indicated that these strains had developed a novel mechanism of maintaining manganese homeostasis, either through metal regulation or acquisition. To test this, the WT, $\Delta ssaACB$, and ΔSSA_0696 strains from both backgrounds were grown aerobically in BHI and metal content was assessed by ICP-OES. No significant difference was found for Mn, Fe, Zn or Co that could be attributed to SSA_0696 (Fig 4. 7).

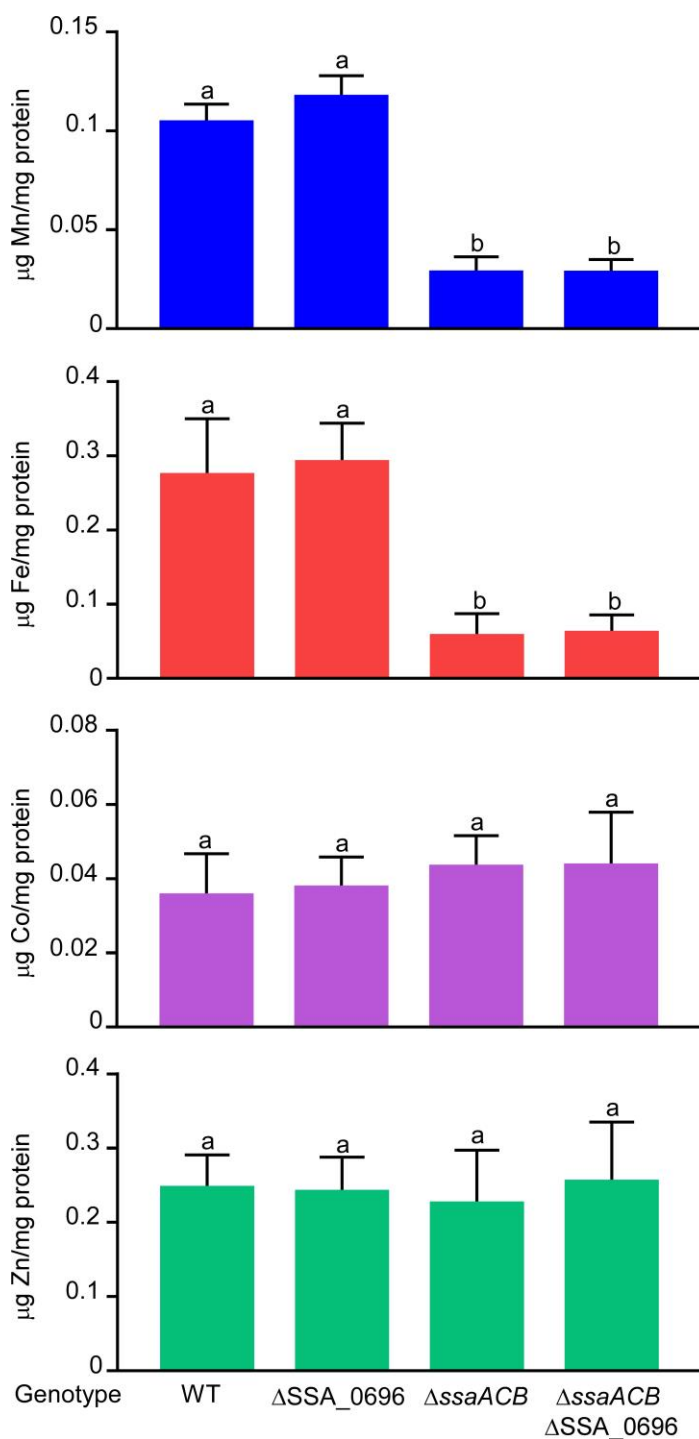


Fig 4.7 Metal analysis by ICP-OES. All strains were grown in BHI in 12% O₂. The means and standard deviations of a minimum of 3 independent experiments are indicated. Statistical significance was assessed by ANOVA with a Tukey-Kramer post-hoc test. Samples that do not share a letter are significantly different; $p < 0.001$.

With no discernable change in metal content, we decided to switch strategies and investigate whether SSA_0696 truly belonged to the ECF-family of transporters, as structural homology previously indicated. This recently discovered family is a subgroup of the ABC transport family (194, 195). To date, they have been characterized as micronutrients transporters, bringing vitamins (195-197), certain amino acids (198), and metal ions (199) into the cell. There are two types of these protein complexes, Group I and Group II; both have a conserved energizing module comprised of subunits A, A' and T. The difference lies in the location of the S, or substrate-binding, subunit, which is encoded alongside the other components in the Group I transporters, and distal to the transmembrane substrate-binding protein components in Group II. Additionally, for Group II transporters, the conserved energizing module is shared by numerous S subunits, each with probable unique substrate specificity. Of these two groups, SSA_0696 most resembles the S subunit of the Group II variety of transporters. We hypothesized that if SSA_0696 was a bona-fide ECF transporter, removal of the shared putative ECF-transport components (A, A' and T; SSA_2365-2367) might recreate the suppressor phenotype associated with deletion of SSA_0696; however, deletion of the genes encoding these subunits from an Δ ssaACB mutant did not result in recovery of growth. In fact, proliferation of the strain after 24 h in serum was less than that of its Δ ssaACB parent, indicating a role for this transport system in serum growth (Fig 4.8).

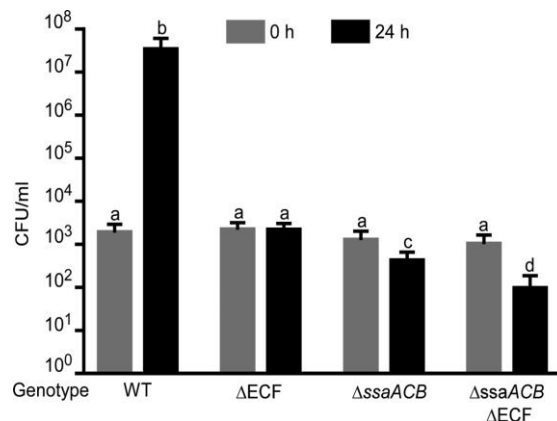


Fig 4.8. The role of an ECF transport system in the suppressor phenotype.

All strains were grown in rabbit serum in 12% O₂. Strains were enumerated by plating serial dilutions and counting resulting colonies. Colony counts are shown for both 0 h and 24 h. The means and standard deviation of 3 independent experiments is indicated. Statistical significance was assessed by repeated measures ANOVA with a Tukey-Kramer post-hoc test. Samples that do not share a letter are significantly different; $p < 0.05$.

With our tractable leads diminishing, we decided to pursue RNA-seq to compare the transcriptomes of the $\Delta ssaACB$ and $\Delta ssaACB \Delta SSA_0696$ mutants. We hoped this approach might implicate specific pathway alterations as being responsible for the suppressor phenotype. To evaluate this, both strains were grown in rabbit serum and cultures were collected at 0, 10 and 30 minutes after shifting from low-oxygen to aerobic conditions. The results reveal the fold-changes of most significantly altered genes were quite small, and that many of the significantly altered transcripts were associated with cell envelope synthesis as identified by DAVID (data not shown).

This was, perhaps, not surprising, as previous morphological investigations concluded the ΔSSA_0696 strains formed abnormal chains or clumps in serum and BHI relative to their parent strains. We questioned whether the cell envelope could be adversely affected during manganese limitation; therefore, the suppressor phenotype could be the consequence of a compensatory effect on cell envelope integrity. To test

this, we grew the Δ SSA_0696 strains (Δ SSA_0696 and Δ ssaACB Δ SSA_0696), in both BHI and serum, and then added antibiotics with varying mechanisms of action relating to cell envelope synthesis or regulation. As in *S. pneumoniae*, where sensitivity to penicillin was eliminated by inactivation of the *murMN* operon, important in the creation of branched muopeptides in the cell wall (200), we hypothesized that if the suppressor phenotype were due to alteration of a particular aspect of the cell wall, the mutant might display a higher resistance to one or more of the antibiotics. This assay failed to establish a relationship to cell envelope modifications and antibiotic resistance as growth of both Δ SSA_0696 strains in media containing vancomycin, bacitracin, ampicillin, or nisin was comparable to that of their respective parent strains (data not shown).

In spite of the challenges in characterization of SSA_0696, the implications of this suppressor mutation could not be ignored, thus, we decided to pursue our investigations, transitioning to *in vivo* analyses. Incredibly, co-inoculation of the erythromycin resistance-marked WT (138), kanamycin resistance-marked Δ ssaACB and the spectinomycin-resistant Δ ssaACB Δ SSA_0696 strains into catheterized rabbits did not replicate our *in vitro* serum growth study results. The Δ ssaACB Δ SSA_0696 strain did not suppress the poor-growth phenotype of a Δ ssaACB mutant in this model (Fig 4.9).

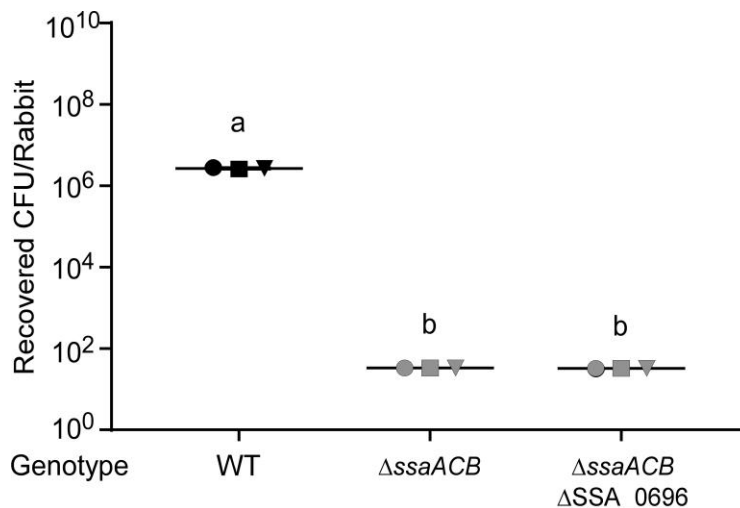


Fig 4.9. Examination of an SSA_0696 deletion mutant in a rabbit model of IE. Rabbits were co-inoculated with the strains indicated and sacrificed at 20 h post-infection. Individual values and geometric means of recovered bacteria from 3 rabbits are shown. Shared symbols indicate strains recovered from the same rabbit. Gray symbols represent the limit of detection for rabbits from which no bacteria were recovered. Statistical significance was determined by repeated-measures ANOVA with a Tukey-Kramer post-hoc test. Samples that do not share a letter are significantly different; $P < 0.001$.

A final component of our knowledge on SSA_0696 was obtained while performing subsequent serum growth studies investigating the possible difference between our *in vivo* and *in vitro* results. Specifically, there were, on several occasions, instances where the suppressor mutant no longer suppressed the poor-growth phenotype as usual. As a matter of due diligence, the Δ SSA_0696 strains were investigated for misidentification or contamination using PCR and sequencing based methods. Removal of SSA_0696 was again confirmed (data not shown). Serendipitously, the cause for this behavior was found to correspond to the age of serum used in the growth studies. Typically, our serum is stored as frozen aliquots, with removal and thawing of aliquots as needed. Once thawed, we consider the serum to have a shelf life of one month, after which, it is discarded. In the case of the Δ SSA_0696 strains, it would appear that month-old serum doesn't support WT levels of

growth. Indeed, we found serum that is more than two weeks old appears to abolish the capacity of SSA_0696 to restore growth to WT levels (Fig 4.10).

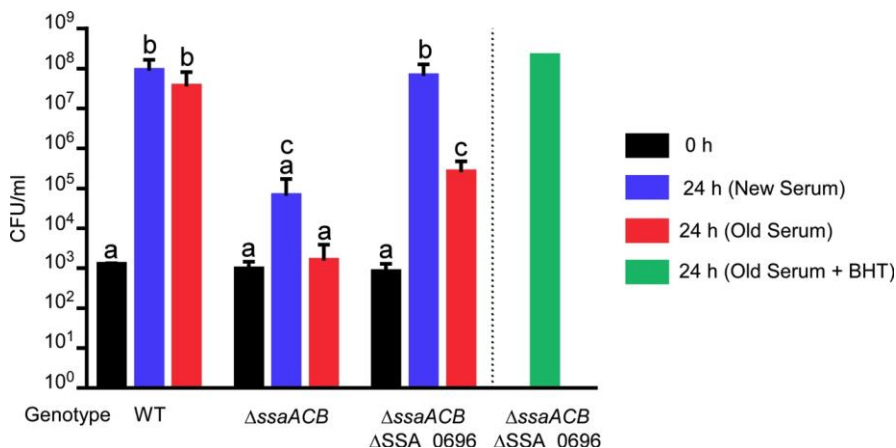


Fig 4.10. Effect of aging serum on suppressor phenotype. (Left panel) All strains were grown for 24 h in rabbit serum in 6% O₂. Strains were enumerated by plating serial dilutions and counting resulting colonies. Colony counts are shown for both 0 h and 24 h, and old and new serum. Serum was considered “old” if it had been thawed for ≥3 weeks. The means and standard deviations of 4 independent experiments are indicated. Statistical significance was assessed by ANOVA with a Tukey-Kramer post-hoc test. Samples that do not share a letter are significantly different; $P < 0.05$. (Right panel) BHT added when serum was inoculated. One replicate demonstrated as reference.

One explanation suggested for these findings was oxidation of the lipids in serum. To test this, serum was aged to three weeks, butylated hydroxytoluene (BHT) was added and strains were inoculated and allowed to grow for 24 hours. BHT, a commonly used food additive since 1947, functions by scavenging free radicals. This, in turn, prevents lipid oxidation and food from becoming rancid. In this context, the BHT would be expected to reverse the oxidation of aging serum lipids; therefore, if changes to the oxidation state of serum lipids were the reason for loss of the suppressor phenotype, adding BHT would be expected to alleviate the problem and thus, restore the SSA_0696-associated suppressor phenotype. As seen in Fig 4.10, when the ΔSSA_0696 mutant was grown in three-week old serum containing BHT, the

suppressor mutant phenotype returned; however, this was also true when BHT was added at the beginning of the serum aging process (data not shown). Whether these results are due to lipid oxidation specifically, as opposed to general antioxidation of serum components, remains to be investigated; however, these findings suggest that the role for SSA_0696 is entwined with serum oxidation and may contribute to the discrepancy in results seen in our two models.

Discussion

Finding manganese-transport deficient mutants that grow well in serum was quite surprising, as to date, these mutants have been uniformly associated with decreased virulence. In fact, it is for this reason that therapeutics aim to target these transport systems (64, 65, 67, 68).

Our investigations concluded that inactivation of SSA_0696 was responsible for the suppressor phenotype. Although annotated as a hypothetical gene, it possesses conserved pfam09529 and TIGR02206 domains. These domains are widely distributed and present in strains including *Bacillus subtilis*, *Treponema pallidum* and *Streptococcus pyogenes*. Additionally, they are associated with integral membrane proteins, a topological result corroborated by the membrane protein topology prediction program TMHMM (171) (<http://www.cbs.dtu.dk/services/TMHMM/>). This program predicts 6 transmembrane domains, with the N and C terminus oriented outside the membrane. Similarly, structural prediction by Phyre (174) found similarity between SSA_0696 and the S subunit of a subclass of ABC transporters. Beyond this, any information —structural, mechanistic, phenotypic or otherwise—is sparse; however, a graphical representation of SSA_0696 (Fig 4.11) obtained utilizing Protter (175) may

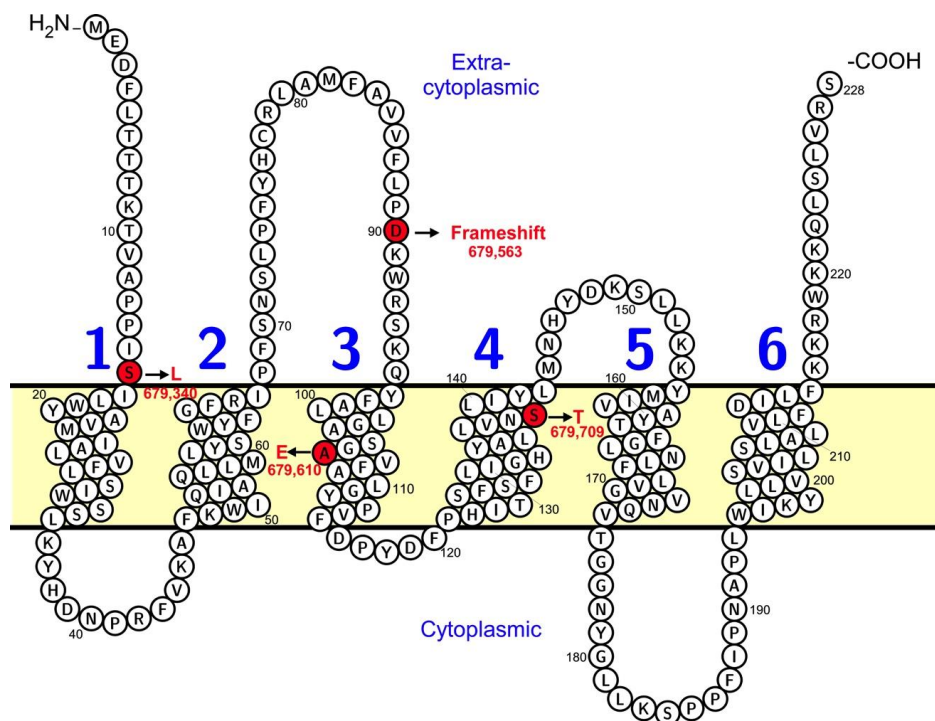


Fig 4.11. Predicted topology and location of suppressing mutations in SSA_0696. Blue numbers indicate successive transmembrane domains. The location and position of each SNP is indicated by red shading; the corresponding amino acid change is indicated in red text.

provide insight on functional residues in SSA_0696. Interestingly, all of the SNPs identified fully restored growth except the SNP at position 679,340, which is also the only SNP that is not within a transmembrane domain or putative ribosomal binding site. As these are sites where mutations could easily result in loss of function, through inhibition of either expression or insertion into the membrane, it is, perhaps, not surprising that the phenotype of the SNP at position 679,340 was less robust. In contrast, the SNP at position 679,563, a frame shift mutation, resulted in the greatest restoration of growth. Excluding the frame shift mutation where much of the protein was likely lost, these results suggest these SNPs may regularly play important functional roles and alterations may impair substrate binding or prevent insertion of the protein into the membrane. Disruption in either manner results in the suppressor phenotype.

Although not mentioned previously in the results, a rabbit polyclonal antibody was generated against a C-terminal peptide sequence of SSA_0696 as a mechanism to investigate SSA_0696 expression. The C-terminus was chosen as it had the highest degree of difference from the paralog, SSA_0695, and therefore had the lowest risk of cross-reactivity. Unfortunately, although the antibody gave a robust signal when used against purified peptide, it failed to react with any protein from cells grown in BHI or serum under aerobic or anaerobic conditions. Efforts to detect an added C-terminal 3X FLAG-tag also failed. In conjunction with the SNP-based graphic, this may indicate that transport and insertion of SSA_0696 into the membrane is extremely intolerant of change and that any changes destabilize and inactivate the protein. However, it is worth mentioning that despite its annotation as a “conserved hypothetical protein” and our inability to detect it by antibody, the number and nature of the suppressing mutations and the fact that precise replacement of the gene with the *aad9* gene produced a spectinomycin-resistant mutant suggest the gene is normally transcribed and translated into a functional protein.

Additional studies investigating the role of the SSA_0696 paralog and the role of SSA_0696 within another *S. sanguinis* strain were surprising. For the former, deletion of the upstream paralog, SSA_0695 restored growth, although only partially. A possible explanation for this result is that deletion of SSA_0695 causes a polar effect on SSA_0696 by reducing, but not eliminating expression. For the latter study, removal of SSA_0696 from the *ssaACB*-devoid SK49 did not beget the suppressor phenotype. Instead, the mutant grew no differently than the SK49 Δ *ssaACB* parent strain. This

suggests a role for SSA_0696 in metabolism that may be specific to certain strains, and at least, is not shared by SK49.

SSA_0696 has predicted structural homology to the S component of ECF-type transporters, and as it is not encoded alongside any other detectable ECF core components, it may be inferred that if it is in fact an S component, then it is part of the Group II subset of ECF transporters. Additionally, a BLASTP search for the Q-helix motif common to the core energizing components (201), indicative of Group I ECF transporters, was unsuccessful. To verify its membership in the ECF transport family, we identified and removed the three core components, which would be shared by the diverse S subunits within a Group II system. In effect, we hypothesized that deletion of the core components would be tantamount to deletion of the entire S subunit repertoire, SSA_0696 included. Restoration of growth would implicate SSA_0696 as a bona-fide S component of an ECF transport system. Future studies could then focus on identifying the specific substrate that SSA_0696 transports. This outcome was not seen. Instead, deletion of the core components resulted in poorer growth than even the Δ ssaACB strain; however, this does not rule out the possibility that SSA_0696 is part of an ECF transport system. Instead, it indicates that one or more substrates transported by the other S subunits that were presumably inactivated could be necessary for growth. Determining which S subunit and substrate is required for growth is challenging. Recent studies predict the presence of numerous S subunits that could have been affected by this approach; however, their identification is difficult due to low sequence similarity (202).

As the results from our mutagenesis studies were inconclusive, we transitioned to studies that focused on roles for manganese in the cell. The simplest explanation for the suppressor phenotype was that total manganese levels had been somehow restored, or that the concentration of another metal had been altered that reduced the cellular requirement for manganese. Interestingly, no significant changes in the cell-associated metal content were identified for any metal tested. Therefore, neither of these hypotheses was supported.

Regardless of the outcome of these early investigations, we can consider possible explanations for our findings. For example, if we maintain the hypothesis that SSA_0696 is an ECF transporter then perhaps there are alternative enzymes or pathways for producing a metabolite that is unavailable in serum, with one pathway being manganese-dependent and the other manganese-independent. A metabolic precursor transported by SSA_0696 might upregulate expression of the manganese-dependent pathway and downregulate expression of the manganese-independent pathway. Therefore, decreased transport of this precursor, due to an inactivating mutation within SSA_0696, could therefore alleviate the manganese requirement for synthesis of the required metabolite. Alternative explanations may reside in the RNA-seq data, where modifications to the cell envelope are overwhelming, but more information is needed to resolve and clarify these data. In an effort to do just that, we began collaborating with the Center on Membrane Protein Production and Analysis (COMPPÅ) to overexpress and purify SSA_0696, so that future studies could focus on a biochemical characterization of the protein. COMPPÅ group members have recently succeeded in overproducing a tagged version of this protein in *Escherichia coli*.

Preliminary experiments to crystallize the protein and investigate putative interacting partners are underway. A search of the protein database in NCBI for the term “TIGR02206,” the family to which SSA_0696 belongs, returns more than 10,000 hits, with more than 3,500 hits to the RefSeq database. These proteins are therefore widespread. Yet, we have been unable to locate a single structure for any member of this family. Thus, these studies could prove valuable for numerous investigators.

Studies of SSA_0696 may be particularly informative as previously, growth in serum in 12% O₂ was found to predict the virulence of *ssaB*- and *sodA*-related mutants in our rabbit model (90). For this study, however, growth in serum did not accurately replicate *in vivo* results. Reasons for this will require further investigation, but may be explained by differences in serum metabolic content related to the diets of the rabbits, presence/absence of host mediators such as calprotectin, or perhaps, attachment deficits that could be assessed by examining rabbits shortly after infection, as has been done previously (90).

It is encouraging to see that suppression did not occur *in vivo*, as this finding maintains metal transporters as promising targets for prevention of streptococcal-related diseases, including IE. Clinical implementation of these drugs may also lower the risk for antibiotic resistance and oral dysbiosis by decreasing antibiotic dependence. In fact, this is supported by a previous study that demonstrated mutation of *sloC*, which encodes the SsaB ortholog in *S. mutans*, reduced IE virulence in a rat model, but had no effect on oral colonization in rats in an experiment lasting more than 60 days (116). Therefore, theoretically, a drug against SloC would be active in the blood, as desired, but not in the mouth, where activity could have undesirable effects. Recent drug

screens searching for inhibitors of these metal-transport systems have emerged; however, success has been mixed in the streptococci (67, 68). Additionally, our study suggests that ECF transport systems may prove to be promising new targets for inhibition, especially if used in combination with drugs against metal transporters.

Chapter 5

General Discussion

Although IE has never been among the most common diseases, it is remarkably persistent. Indeed, in spite of advances in diagnostics methods, antimicrobial and surgical therapies, and complication management (49), the incidence has remained stable. This may be attributed to changing dynamics in the populations that are routinely vulnerable to IE. Historically, those most at risk had chronic rheumatic heart disease, a risk factor that is all but eliminated in the industrialized world (203). This group has been replaced by the elderly, as increased cardiac complications become more likely with age, and intravenous drug users. As always, streptococci comprise a large portion of reported cases of IE. Currently, antibiotic prophylaxis is prescribed for those with a known predisposition for IE; however, a limited number of cases are preventable by this strategy (204) and routine prophylaxis comes at the cost of antibiotic resistance. Therefore, alternative mechanisms to combat streptococcal-mediated IE will likely remain an area of interest.

One such area of interest is antimicrobial therapy, although penetration of the vegetation by antimicrobial compounds is a noted obstacle (205, 206). Regardless, vaccination and small-molecule inhibitor-based approaches have continued to garner attention. One target of these strategies is the well-established Lral family ABC-type metal transporter, which is conserved among the streptococci and is important in streptococcal virulence. Of these transport systems, FimA of *S. parasanguinis* has shown the most promise as a vaccinogen, providing protection against *S. parasanguinis* and other noted streptococci, including *S. mitis*, *S. mutans*, and *S. salivarius* (64, 65).

For *S. sanguinis*, however, targeting of the Lral family protein, SsaB, by vaccination has been less successful. Alternative vaccination attempts have been made more difficult as few other proteins have been identified that are required for virulence, and those that have been identified are intracellular and are less attractive drug targets. An alternative to vaccination entirely—small-molecule inhibitors—have the potential to target intracellular components and may be more readily diffusible throughout the vegetation. With this approach, the target pool is widened, and perhaps, may include the class Ib aerobic ribonucleotide reductase components, NrdHEKF and NrdI. This is significant for IE pathogenesis as previous studies demonstrated the cardiac vegetation is sufficiently aerobic to completely inactivate NrdD, the anaerobic ribonucleotides reductase; however, the aerobic ribonucleotide reductase NrdEF and the NrdI-dependent $Mn^{III}_2\text{-Y}^{\cdot}$ -cofactor remain essential for virulence (106). Even though possible targets have been identified, an added caveat of finding a successful method for targeting an infected vegetation is ensuring that *S. sanguinis* remains unaffected in the oral cavity. *S. sanguinis* is argued to have a beneficial role within the oral cavity, its native habitat; therefore, designing or identifying an antimicrobial therapy that will prevent or inhibit its opportunistic infection of the endocardium, but not eliminate or disrupt its position within the oral cavity, is a uniquely challenging undertaking. Although dental caries are certainly more easily treated than endocarditis, exchanging one disease state for another is not an acceptable outcome for an antimicrobial therapy.

With the publication of the SK36 *S. sanguinis* genome sequence in 2007 (70) and subsequent characterization of this strain, the groundwork was laid for future studies to expand upon the genetic characterization of *S. sanguinis* through sequencing

of additional strains. This expansion would broaden understanding of virulence within the species and would contribute to future antimicrobial drug design. To this end, Chapter 3 reports our bioinformatic and phenotypic interrogation of a collection of *S. sanguinis* strains that consisted of oral and blood isolates. Although a bioinformatic comparison of the strains did not identify any genes with known relationships to virulence, it was successful in identifying the “core” or conserved genome of *S. sanguinis*. Additionally, this study was able to identify a conserved locus for targeted genetic manipulation of these strains. Taken together, the bioinformatic results, along with virulence testing in a rabbit model of endocarditis and phenotypic assays, demonstrated that, in all cases, a productive infection was established and there was a wide and unpredictable range of strain responses to the other various challenges. This highlights that a one-approach practice for treatment of all organisms, even those within a species, may not be the most efficacious. This may be especially true for some strains of *S. sanguinis* that have redundancy in manganese transport systems and would therefore be less susceptible to SsaB-targeted therapies. Of additional note, an unintended, yet crucial, finding of this study was the misidentification of several strains in GenBank. For future studies, like ours, that may seek to include increasing strain numbers, the need for careful appropriation of sequence information is absolute. Misidentifications persist in the public databases, waste funds, lead to erroneous conclusions and delay progress. The identification of wrongly identified strains and their subsequent clarification by this study are therefore of significant benefit to the streptococcal community.

Chapter 4 continued the investigation into the role of SsaB in virulence. Specifically, this study highlighted the possibility that *S. sanguinis* could overcome the barrier imposed by loss of SsaB through spontaneous mutation of the gene SSA_0696. Surprisingly, the recovery in growth was not due to manganese accumulation by an alternative method, as might be expected. In spite of significant effort, the mechanism by which growth was restored remained elusive. Although this phenotype did not persist upon examination in our rabbit model of endocarditis, it does demonstrate that our knowledge of the roles of manganese within the cell is incomplete and it also serves as a precautionary consideration for SsaB and other single-target therapies.

In contrast to studies that seek to eliminate *S. sanguinis* pathogenesis, Chapter 3 engendered results that, in the future, could be used to exploit the attributes associated with the role of *S. sanguinis* as an oral commensal. Specifically, the antagonistic relationship of *S. sanguinis* and caries-causing *S. mutans* provide inspiration for the potential use of *S. sanguinis* as a probiotic. Although preliminary results were obtained in this study, future experiments may consider incorporating information concerning multiple phenotypes, including arginine deaminase activity, hydrogen peroxide production, biofilm formation, and manganese acquisition, to identify a strain that would be a robust oral defender, while abolishing its pathogenic potential. This may be an exciting new area for future research.

Literature Cited:

1. Segata N, Haake SK, Mannon P, Lemon KP, Waldron L, Gevers D, Huttenhower C, Izard J. 2012. Composition of the adult digestive tract bacterial microbiome based on seven mouth surfaces, tonsils, throat and stool samples. *Genome Biology* 13:R42.
2. Dewhirst FE, Chen T, Izard J, Paster BJ, Tanner ACR, Yu W-H, Lakshmanan A, Wade WG. 2010. The human oral microbiome. *J Bacteriol* 192:5002-5017.
3. Gillings MR, Paulsen IT, Tetu SG. 2015. Ecology and Evolution of the Human Microbiota: Fire, Farming and Antibiotics. *Genes (Basel)* 6:841-57.
4. Kilian M, Chapple IL, Hannig M, Marsh PD, Meuric V, Pedersen AM, Tonetti MS, Wade WG, Zaura E. 2016. The oral microbiome - an update for oral healthcare professionals. *Br Dent J* 221:657-666.
5. John E. Bennett RDMJB. 2015. Mandell, Douglas, and Bennett's principles and practice of infectious diseases. Eighth edition. Philadelphia, PA : Elsevier/Saunders, [2015].
6. Geddes DA, Jenkins GN. 1974. Intrinsic and extrinsic factors influencing the flora of the mouth. *Soc Appl Bacteriol Symp Ser* 3:85-100.
7. Socransky SS, Haffajee AD, Cugini MA, Smith C, Kent RL, Jr. 1998. Microbial complexes in subgingival plaque. *J Clin Periodontol* 25:134-44.
8. Huang X, Palmer SR, Ahn S-J, Richards VP, Williams ML, Nascimento MM, Burne RA. 2016. A highly arginolytic *Streptococcus* species that potently antagonizes *Streptococcus mutans*. *Appl Environ Microbiol* 82:2187-2201.
9. Kreth J, Merritt J, Shi W, Qi F. 2005. Competition and coexistence between *Streptococcus mutans* and *Streptococcus sanguinis* in the dental biofilm. *J Bacteriol* 187:7193-7203.
10. Kreth J, Zhang Y, Herzberg MC. 2008. Streptococcal antagonism in oral biofilms: *Streptococcus sanguinis* and *Streptococcus gordonii* interference with *Streptococcus mutans*. *J Bacteriol* 190:4632-4640.
11. Loesche WJ. 1986. Role of *Streptococcus mutans* in human dental decay. *Microbiol Rev* 50:353-380.
12. Aas JA, Paster BJ, Stokes LN, Olsen I, Dewhirst FE. 2005. Defining the normal bacterial flora of the oral cavity. *J Clin Microbiol* 43:5721-32.
13. Palmer RJ, Jr. 2014. Composition and development of oral bacterial communities. *Periodontol* 2000 64:20-39.
14. Kreth J, Merritt J, Qi F. 2009. Bacterial and host interactions of oral streptococci. *DNA Cell Biol* 28:397-403.
15. Pearce C, Bowden GH, Evans M, Fitzsimmons SP, Johnson J, Sheridan MJ, Wientzen R, Cole MF. 1995. Identification of pioneer viridans streptococci in the oral cavity of human neonates. *J Med Microbiol* 42:67-72.
16. Facklam R. 2002. What happened to the streptococci: overview of taxonomic and nomenclature changes. *Clin Microbiol Rev* 15:613-30.
17. Barnard J, Stinson M. 1996. The alpha-hemolysin of *Streptococcus gordonii* is hydrogen peroxide. *Infect Immun* 64:3853-3857.
18. Lancefield RC. 1934. A serological differentiation of specific types of bovine hemolytic streptococci (Group B). *J Exp Med* 59:441-58.

19. Suzuki N, Seki M, Nakano Y, Kiyoura Y, Maeno M, Yamashita Y. 2005. Discrimination of *Streptococcus pneumoniae* from viridans group streptococci by genomic subtractive hybridization. *J Clin Microbiol* 43:4528-34.
20. Bishop C, Aanensen D, Jordan G, Kilian M, Hanage W, Spratt B. 2009. Assigning strains to bacterial species via the internet. *BMC Biology* 7:3.
21. Thompson CC, Emmel VE, Fonseca EL, Marin MA, Vicente ACP. 2013. Streptococcal taxonomy based on genome sequence analyses. *F1000Res* 2:67.
22. De Gheldre Y, Vandamme P, Goossens H, Struelens MJ. 1999. Identification of clinically relevant viridans streptococci by analysis of transfer DNA intergenic spacer length polymorphism. *Int J Syst Bacteriol* 49 Pt 4:1591-8.
23. Jacobs JA, Schot CS, Bunschoten AE, Schouls LM. 1996. Rapid species identification of "*Streptococcus milleri*" strains by line blot hybridization: identification of a distinct 16S rRNA population closely related to *Streptococcus constellatus*. *J Clin Microbiol* 34:1717-21.
24. Hardie JM, Whiley RA. 1997. Classification and overview of the genera *Streptococcus* and *Enterococcus*. *J Appl Microbiol* 83:1S-11S.
25. Poveda-Roda R, Jimenez Y, Carbonell E, Gavalda C, Margaix-Munoz MM, Sarrion-Perez G. 2008. Bacteremia originating in the oral cavity. A review. *Med Oral Patol Oral Cir Bucal* 13:E355-62.
26. Lockhart PB, Brennan MT, Sasser HC, Fox PC, Paster BJ, Bahrani-Mougeot FK. 2008. Bacteremia associated with toothbrushing and dental extraction. *Circulation* 117:3118-3125.
27. Guntheroth WG. 1984. How important are dental procedures as a cause of infective endocarditis? *Am J Cardiol* 54:797-801.
28. Forner L, Larsen T, Kilian M, Holmstrup P. 2006. Incidence of bacteremia after chewing, tooth brushing and scaling in individuals with periodontal inflammation. *J Clin Periodontol* 33:401-407.
29. Maharaj B, Coovadia Y, Vayej AC. 2012. An investigation of the frequency of bacteraemia following dental extraction, tooth brushing and chewing. *Cardiovasc J Afr* 23:340-4.
30. Silver JG, Martin AW, McBride BC. 1977. Experimental transient bacteraemias in human subjects with varying degrees of plaque accumulation and gingival inflammation. *J Clin Periodontol* 4:92-9.
31. Silver JG, Martin AW, McBride BC. 1979. Experimental transient bacteraemias in human subjects with clinically healthy gingivae. *J Clin Periodontol* 6:33-6.
32. Di Filippo S. 2012. Prophylaxis of infective endocarditis in patients with congenital heart disease in the context of recent modified guidelines. *Archives of Cardiovascular Diseases* 105:454-460.
33. Nagpal A, Sohail MR, M Steckelberg J. 2012. Prosthetic valve endocarditis: State of the heart, vol 2.
34. Mani V, Cartwright K, Dooley J, Swarbrick E, Fairclough P, Oakley C. 1997. Antibiotic prophylaxis in gastrointestinal endoscopy: a report by a Working Party for the British Society of Gastroenterology Endoscopy Committee. *Endoscopy* 29:114-9.
35. Harding D, Prendergast B. 2018. Advanced imaging improves the diagnosis of infective endocarditis. *F1000Res* 7.

36. Cresti A, Chiavarelli M, Scalese M, Nencioni C, Valentini S, Guerrini F, D'Aiello I, Picchi A, De Sensi F, Habib G. 2017. Epidemiological and mortality trends in infective endocarditis, a 17-year population-based prospective study. *Cardiovasc Diagn Ther* 7:27-35.
37. Thuny F, Avierinos JF, Tribouilloy C, Giorgi R, Casalta JP, Milandre L, Brahim A, Nadji G, Riberi A, Collart F, Renard S, Raoult D, Habib G. 2007. Impact of cerebrovascular complications on mortality and neurologic outcome during infective endocarditis: a prospective multicentre study. *Eur Heart J* 28:1155-61.
38. Vilacosta I, Graupner C, San Roman JA, Sarria C, Ronderos R, Fernandez C, Mancini L, Sanz O, Sanmartin JV, Stoermann W. 2002. Risk of embolization after institution of antibiotic therapy for infective endocarditis. *J Am Coll Cardiol* 39:1489-95.
39. Dickerman SA, Abrutyn E, Barsic B, Bouza E, Cecchi E, Moreno A, Doco-Lecompte T, Eisen DP, Fortes CQ, Fowler VG, Jr., Lerakis S, Miro JM, Pappas P, Peterson GE, Rubinstein E, Sexton DJ, Suter F, Tornos P, Verhagen DW, Cabell CH, Investigators ICE. 2007. The relationship between the initiation of antimicrobial therapy and the incidence of stroke in infective endocarditis: an analysis from the ICE Prospective Cohort Study (ICE-PCS). *Am Heart J* 154:1086-94.
40. Bor DH, Woolhandler S, Nardin R, Bruschi J, Himmelstein DU. 2013. Infective endocarditis in the U.S., 1998-2009: a nationwide study. *PLoS ONE* 8:e60033.
41. Paterick TE, Paterick TJ, Nishimura RA, Steckelberg JM. 2007. Complexity and subtlety of infective endocarditis. *Mayo Clin Proc* 82:615-21.
42. Steckelberg JM, Melton LJ, 3rd, Ilstrup DM, Rouse MS, Wilson WR. 1990. Influence of referral bias on the apparent clinical spectrum of infective endocarditis. *Am J Med* 88:582-8.
43. Mylonakis E, Calderwood SB. 2001. Infective endocarditis in adults. *N Engl J Med* 345:1318-1330.
44. Gilleece A, Fenelon L. 2000. Nosocomial infective endocarditis. *J Hosp Infect* 46:83-8.
45. McDonald JR. 2009. Acute infective endocarditis. *Infect Dis Clin North Am* 23:643-64.
46. Sadaka M, ElSharkawy E, Soliman M, El-Din AN, El-Hay MAA. 2013. Study of infective endocarditis in Alexandria main university hospitals. *The Egyptian Heart Journal* 65:307-317.
47. Vikram HR. 2007. The long and short of vegetations in infective endocarditis. *Expert Rev Anti Infect Ther* 5:529-33.
48. Shebuski RJ, Kilgore KS. 2002. Role of inflammatory mediators in thrombogenesis. *J Pharmacol Exp Ther* 300:729-35.
49. Moreillon P, Que YA. 2004. Infective endocarditis. *Lancet* 363:139-49.
50. Moreillon P, Que YA, Bayer AS. 2002. Pathogenesis of streptococcal and staphylococcal endocarditis. *Infect Dis Clin North Am* 16:297-318.
51. Thuny F, Di Salvo G, Belliard O, Avierinos JF, Pergola V, Rosenberg V, Casalta JP, Gouvernet J, Derumeaux G, Iarussi D, Ambrosi P, Calabro R, Riberi A, Collart F, Metras D, Lepidi H, Raoult D, Harle JR, Weiller PJ, Cohen A, Habib G.

2005. Risk of embolism and death in infective endocarditis: prognostic value of echocardiography: a prospective multicenter study. *Circulation* 112:69-75.
52. Garcia-Granja PE, Lopez J, Vilacosta I, Ortiz-Bautista C, Sevilla T, Olmos C, Sarria C, Ferrera C, Gomez I, Roman JA. 2015. Polymicrobial Infective Endocarditis: Clinical Features and Prognosis. *Medicine (Baltimore)* 94:e2000.
53. Vogkou CT, Vlachogiannis NI, Palaiodimos L, Kousoulis AA. 2016. The causative agents in infective endocarditis: a systematic review comprising 33,214 cases. *Eur J Clin Microbiol Infect Dis* 35:1227-1245.
54. Di Filippo S, Delahaye F, Semiond B, Celard M, Henaine R, Ninet J, Sassolas F, Bozio A. 2006. Current patterns of infective endocarditis in congenital heart disease. *Heart* 92:1490-1495.
55. Netzer RO, Zollinger E, Seiler C, Cerny A. 2000. Infective endocarditis: clinical spectrum, presentation and outcome. An analysis of 212 cases 1980-1995. *Heart* 84:25-30.
56. Durack DT, Lukes AS, Bright DK. 1994. New criteria for diagnosis of infective endocarditis: utilization of specific echocardiographic findings. Duke Endocarditis Service. *Am J Med* 96:200-9.
57. Li JS, Sexton DJ, Mick N, Nettles R, Fowler VG, Jr., Ryan T, Bashore T, Corey GR. 2000. Proposed modifications to the Duke criteria for the diagnosis of infective endocarditis. *Clin Infect Dis* 30:633-8.
58. Thuny F, Grisoli D, Collart F, Habib G, Raoult D. 2012. Management of infective endocarditis: challenges and perspectives. *The Lancet* 379:965-975.
59. Rasmussen TB, Zwisler A-D, Thygesen LC, Bundgaard H, Moons P, Berg SK. 2017. High readmission rates and mental distress after infective endocarditis — Results from the national population-based CopenHeart IE survey. *Int J Cardiol* 235:133-140.
60. Durack DT, Beeson PB. 1972. Experimental bacterial endocarditis. II. Survival of a bacteria in endocardial vegetations. *Br J Exp Pathol* 53:50-3.
61. Durack DT, Starkebaum MK, Petersdorf RG. 1977. Chemotherapy of experimental streptococcal endocarditis. VI. Prevention of enterococcal endocarditis. *J Lab Clin Med* 90:171-9.
62. Wilson WR, Geraci JE, Wilkowske CJ, Washington JA, 2nd. 1978. Short-term intramuscular therapy with procaine penicillin plus streptomycin for infective endocarditis due to viridans streptococci. *Circulation* 57:1158-61.
63. Habib G, Hoen B, Tornos P, Thuny F, Prendergast B, Vilacosta I, Moreillon P, de Jesus Antunes M, Thilen U, Lekakis J, Lengyel M, Muller L, Naber CK, Nihoyannopoulos P, Moritz A, Zamorano JL. 2009. Guidelines on the prevention, diagnosis, and treatment of infective endocarditis (new version 2009): the Task Force on the Prevention, Diagnosis, and Treatment of Infective Endocarditis of the European Society of Cardiology (ESC). Endorsed by the European Society of Clinical Microbiology and Infectious Diseases (ESCMID) and the International Society of Chemotherapy (ISC) for Infection and Cancer. *Eur Heart J* 30:2369-413.
64. Kitten T, Munro CL, Wang A, Macrina FL. 2002. Vaccination with FimA from *Streptococcus parasanguis* protects rats from endocarditis caused by other viridans streptococci. *Infect Immun* 70:422-425.

65. Briles DE, Ades E, Paton JC, Sampson JS, Carlone GM, Huebner RC, Virolainen A, Swiatlo E, Hollingshead SK. 2000. Intranasal immunization of mice with a mixture of the pneumococcal proteins PsaA and PspA is highly protective against nasopharyngeal carriage of *Streptococcus pneumoniae*. *Infect Immun* 68:796-800.
66. Viscount HB, Munro CL, Burnette-Curley D, Peterson DL, Macrina FL. 1997. Immunization with FimA protects against *Streptococcus parasanguis* endocarditis in rats. *Infect Immun* 65:994-1002.
67. Obaidullah AJ, Ahmed MH, Kitten T, Kellogg GE. 2018. Inhibiting pneumococcal surface antigen A (PsaA) with small molecules discovered through virtual screening: steps toward validating a potential target for *Streptococcus pneumoniae*. *Chemistry & Biodiversity* 0.
68. Bajaj M, Mamidyala SK, Zuegg J, Begg SL, Ween MP, Luo Z, Huang JX, McEwan AG, Kobe B, Paton JC, McDevitt CA, Cooper MA. 2015. Discovery of novel pneumococcal surface antigen A (PsaA) inhibitors using a fragment-based drug design approach. *ACS Chem Biol* 10:1511-20.
69. Wilson W, Taubert KA, Gewitz M, Lockhart PB, Baddour LM, Levison M, Bolger A, Cabell CH, Takahashi M, Baltimore RS, Newburger JW, Strom BL, Tani LY, Gerber M, Bonow RO, Pallasch T, Shulman ST, Rowley AH, Burns JC, Ferrieri P, Gardner T, Goff D, Durack DT. 2007. Prevention of infective endocarditis. Guidelines from the American Heart Association. *Circulation* 116:1736-1754.
70. Xu P, Alves JM, Kitten T, Brown A, Chen Z, Ozaki LS, Manque P, Ge X, Serrano MG, Puiu D, Hendricks S, Wang Y, Chaplin MD, Akan D, Paik S, Peterson DL, Macrina FL, Buck GA. 2007. Genome of the opportunistic pathogen *Streptococcus sanguinis*. *J Bacteriol* 189:3166-3175.
71. Baker SP, Nulton TJ, Kitten T. 2018. Genomic, phenotypic, and virulence analysis of *Streptococcus sanguinis* oral and infective endocarditis isolates. *Infect Immun* doi:10.1128/iai.00703-18:IAI.00703-18.
72. Caufield PW, Dasanayake AP, Li Y, Pan Y, Hsu J, Hardin JM. 2000. Natural history of *Streptococcus sanguinis* in the oral cavity of infants: evidence for a discrete window of infectivity. *Infect Immun* 68:4018-4023.
73. Gross EL, Beall CJ, Kutsch SR, Firestone ND, Leys EJ, Griffen AL. 2012. Beyond *Streptococcus mutans*: dental caries onset linked to multiple species by 16S rRNA community analysis. *PLoS ONE* 7:e47722.
74. Seoudi N, Bergmeier LA, Drobniowski F, Paster B, Fortune F. 2015. The oral mucosal and salivary microbial community of Behcet's syndrome and recurrent aphthous stomatitis. *J Oral Microbiol* 7:27150.
75. Francavilla R, Ercolini D, Piccolo M, Vannini L, Siragusa S, De Filippis F, De Pasquale I, Di Cagno R, Di Toma M, Gozzi G, Serrazanetti DI, De Angelis M, Gobbetti M. 2014. Salivary microbiota and metabolome associated with celiac disease. *Appl Environ Microbiol* 80:3416-25.
76. Gong K, Mailloux L, Herzberg MC. 2000. Salivary film expresses a complex, macromolecular binding site for *Streptococcus sanguis*. *J Biol Chem* 275:8970-8974.

77. Becker MR, Paster BJ, Leys EJ, Moeschberger ML, Kenyon SG, Galvin JL, Boches SK, Dewhirst FE, Griffen AL. 2002. Molecular analysis of bacterial species associated with childhood caries. *J Clin Microbiol* 40:1001-1009.
78. Mikx FH, van der Hoeven JS, Plasschaert AJ, Konig KG. 1976. Establishment and symbiosis of *Actinomyces viscosus*, *Streptococcus sanguis* and *Streptococcus mutans* in germ-free Osborne-Mendel rats. *Caries Res* 10:123-32.
79. Kohler B, Andreen I, Jonsson B. 1988. The earlier the colonization by mutans streptococci, the higher the caries prevalence at 4 years of age. *Oral Microbiol Immunol* 3:14-7.
80. Herzberg MC, Brintzenhofe KL, Clawson CC. 1983. Aggregation of human platelets and adhesion of *Streptococcus sanguis*. *Infect Immun* 39:1457-69.
81. Nobbs AH, Lamont RJ, Jenkinson HF. 2009. *Streptococcus* adherence and colonization. *Microbiol Mol Biol Rev* 73:407-450.
82. Turner LS, Kanamoto T, Unoki T, Munro CL, Wu H, Kitten T. 2009. Comprehensive evaluation of *Streptococcus sanguinis* cell wall-anchored proteins in early infective endocarditis. *Infect Immun* 77:4966-4975.
83. Bensing BA, Loukachevitch LV, McCulloch KM, Yu H, Vann KR, Wawrzak Z, Anderson S, Chen X, Sullam PM, Iverson TM. 2016. Structural basis for sialoglycan binding by the *Streptococcus sanguinis* SrpA adhesin. *J Biol Chem* 291:7230-40.
84. Sullam PM, Bayer AS, Foss WM, Cheung AL. 1996. Diminished platelet binding in vitro by *Staphylococcus aureus* is associated with reduced virulence in a rabbit model of infective endocarditis. *Infect Immun* 64:4915-4921.
85. Herzberg MC, Nobbs A, Tao L, Kilic A, Beckman E, Khammanivong A, Zhang Y. 2005. Oral streptococci and cardiovascular disease: searching for the platelet aggregation-associated protein gene and mechanisms of *Streptococcus sanguis*-induced thrombosis. *J Periodontol* 76:2101-5.
86. Erickson PR, Herzberg MC. 1987. A collagen-like immunodeterminant on the surface of *Streptococcus sanguis* induces platelet aggregation. *J Immunol* 138:3360-6.
87. Erickson PR, Herzberg MC. 1990. Purification and partial characterization of a 65-kDa platelet aggregation-associated protein antigen from the surface of *Streptococcus sanguis*. *J Biol Chem* 265:14080-7.
88. Herzberg MC, Erickson PR, Kane PK, Clawson DJ, Clawson CC, Hoff FA. 1990. Platelet-interactive products of *Streptococcus sanguis* protoplasts. *Infect Immun* 58:4117-25.
89. Herzberg MC, MacFarlane GD, Gong K, Armstrong NN, Witt AR, Erickson PR, Meyer MW. 1992. The platelet interactivity phenotype of *Streptococcus sanguis* influences the course of experimental endocarditis. *Infect Immun* 60:4809-18.
90. Crump KE, Bainbridge B, Brusko S, Turner LS, Ge X, Stone V, Xu P, Kitten T. 2014. The relationship of the lipoprotein SsaB, manganese, and superoxide dismutase in *Streptococcus sanguinis* virulence for endocarditis. *Mol Microbiol* 92:1243-1259.
91. Das S, Kanamoto T, Ge X, Xu P, Unoki T, Munro CL, Kitten T. 2009. Contribution of lipoproteins and lipoprotein processing to endocarditis virulence in *Streptococcus sanguinis*. *J Bacteriol* 191:4166-4179.

92. Jenkinson HF. 1994. Cell surface protein receptors in oral streptococci. *FEMS Microbiol Lett* 121:133-40.
93. Claverys J. 2001. A new family of high-affinity ABC manganese and zinc permeases. *Res Microbiol* 152:231-243.
94. Dintilhac A, Alloing G, Granadel C, Claverys JP. 1997. Competence and virulence of *Streptococcus pneumoniae*: Adc and PsaA mutants exhibit a requirement for Zn and Mn resulting from inactivation of putative ABC metal permeases. *Mol Microbiol* 25:727-739.
95. Kolenbrander PE, Andersen RN, Baker RA, Jenkinson HF. 1998. The adhesion-associated *sca* operon in *Streptococcus gordonii* encodes an inducible high-affinity ABC transporter for Mn²⁺ uptake. *J Bacteriol* 180:290-5.
96. McAllister LJ, Tseng H-J, Ogunniyi AD, Jennings MP, McEwan AG, Paton JC. 2004. Molecular analysis of the *psa* permease complex of *Streptococcus pneumoniae*. *Mol Microbiol* 53:889-901.
97. Berry AM, Paton JC. 1996. Sequence heterogeneity of PsaA, a 37-kilodalton putative adhesin essential for virulence of *Streptococcus pneumoniae*. *Infect Immun* 64:5255-62.
98. Marra A, Lawson S, Asundi JS, Brigham D, Hromockyj AE. 2002. *In vivo* characterization of the *psa* genes from *Streptococcus pneumoniae* in multiple models of infection. *Microbiology* 148:1483-1491.
99. Johnston JW, Myers LE, Ochs MM, Benjamin WH, Jr., Briles DE, Hollingshead SK. 2004. Lipoprotein PsaA in virulence of *Streptococcus pneumoniae*: surface accessibility and role in protection from superoxide. *Infect Immun* 72:5858-5867.
100. Smith AJ, Ward PN, Field TR, Jones CL, Lincoln RA, Leigh JA. 2003. MtuA, a lipoprotein receptor antigen from *Streptococcus uberis*, is responsible for acquisition of manganese during growth in milk and is essential for infection of the lactating bovine mammary gland. *Infect Immun* 71:4842-4849.
101. Janulczyk R, Ricci S, Bjorck L. 2003. MtsABC is important for manganese and iron transport, oxidative stress resistance, and virulence of *Streptococcus pyogenes*. *Infect Immun* 71:2656-2664.
102. Yesilkaya H, Kadioglu A, Gingles N, Alexander JE, Mitchell TJ, Andrew PW. 2000. Role of manganese-containing superoxide dismutase in oxidative stress and virulence of *Streptococcus pneumoniae*. *Infect Immun* 68:2819-2826.
103. Poyart C, Pellegrini E, Gaillot O, Boumaila C, Baptista M, Trieu-Cuot P. 2001. Contribution of Mn-cofactored superoxide dismutase (SodA) to the virulence of *Streptococcus agalactiae*. *Infect Immun* 69:5098-5106.
104. Tang Y, Zhang X, Wu W, Lu Z, Fang W. 2012. Inactivation of the *sodA* gene of *Streptococcus suis* type 2 encoding superoxide dismutase leads to reduced virulence to mice. *Vet Microbiol* 158:360-366.
105. Imlay JA. 2013. The molecular mechanisms and physiological consequences of oxidative stress: lessons from a model bacterium. *Nat Rev Micro* 11:443-454.
106. Rhodes DV, Crump KE, Makhlynets O, Snyder M, Ge X, Xu P, Stubbe J, Kitten T. 2014. Genetic characterization and role in virulence of the ribonucleotide reductases of *Streptococcus sanguinis*. *J Biol Chem* 289:6273-6287.
107. Makhlynets O, Boal AK, Rhodes DV, Kitten T, Rosenzweig AC, Stubbe J. 2014. *Streptococcus sanguinis* class Ib ribonucleotide reductase: high activity with both

- iron and manganese cofactors and structural insights. *J Biol Chem* 289:6259-6272.
108. Cotruvo JA, Stubbe J. 2011. Class I ribonucleotide reductases: metallocofactor assembly and repair in vitro and in vivo. *Annu Rev Biochem* 80:733-767.
 109. Munro CL. 1998. The rat model of endocarditis. *Methods Cell Science* 20:203-207.
 110. Lefort A, Fantin B. 1999. Chapter 72 - Rabbit Model of Bacterial Endocarditis, p 611-617. *In* Zak O, Sande MA (ed), *Handbook of Animal Models of Infection* doi:<https://doi.org/10.1016/B978-012775390-4/50211-6>. Academic Press, London.
 111. Durack DT, Beeson PB, Petersdorf RG. 1973. Experimental bacterial endocarditis. III. Production and progress of the disease in rabbits. *Br J Exp Pathol* 54:142-51.
 112. Durack DT. 1975. Experimental bacterial endocarditis. IV. Structure and evolution of very early lesions. *J Pathol* 115:81-9.
 113. Paik S, Senty L, Das S, Noe JC, Munro CL, Kitten T. 2005. Identification of virulence determinants for endocarditis in *Streptococcus sanguinis* by signature-tagged mutagenesis. *Infect Immun* 73:6064-74.
 114. Meccas J. 2002. Use of signature-tagged mutagenesis in pathogenesis studies. *Curr Opin Microbiol* 5:33-7.
 115. Burnette-Curley D, Wells V, Viscount H, Munro CL, Fenno JC, Fives-Taylor P, Macrina FL. 1995. FimA, a major virulence factor associated with *Streptococcus parasanguis* endocarditis. *Infect Immun* 63:4669-74.
 116. Kitten T, Munro CL, Michalek SM, Macrina FL. 2000. Genetic characterization of a *Streptococcus mutans* Lral family operon and role in virulence. *Infect Immun* 68:4441-4451.
 117. Paik S, Brown A, Munro CL, Cornelissen CN, Kitten T. 2003. The *sloABCR* operon of *Streptococcus mutans* encodes an Mn and Fe transport system required for endocarditis virulence and its Mn-dependent repressor. *J Bacteriol* 185:5967-5975.
 118. Callahan JE, Munro CL, Kitten T. 2011. The *Streptococcus sanguinis* competence regulon is not required for infective endocarditis virulence in a rabbit model. *PLoS One* 6:e26403.
 119. Horton RM. 1995. PCR-mediated recombination and mutagenesis. SOEing together tailor-made genes. *Mol Biotechnol* 3:93-99.
 120. Zhao Y, Wu J, Yang J, Sun S, Xiao J, Yu J. 2012. PGAP: pan-genomes analysis pipeline. *Bioinformatics* 28:416-418.
 121. Okonechnikov K, Golosova O, Fursov M, team U. 2012. Unipro UGENE: a unified bioinformatics toolkit. *Bioinformatics* 28:1166-7.
 122. Arndt D, Grant JR, Marcu A, Sajed T, Pon A, Liang Y, Wishart DS. 2016. PHASTER: a better, faster version of the PHAST phage search tool. *Nucleic Acids Res* 44:W16-W21.
 123. van Heel AJ, de Jong A, Song C, Viel JH, Kok J, Kuipers OP. 2018. BAGEL4: a user-friendly web server to thoroughly mine RiPPs and bacteriocins. *Nucleic Acids Res* 46:W278-W281.

124. Perry JA, Jones MB, Peterson SN, Cvitkovitch DG, Levesque CM. 2009. Peptide alarmone signalling triggers an auto-active bacteriocin necessary for genetic competence. *Mol Microbiol* 72:905-917.
125. Liu J, Stone VN, Ge X, Tang M, Elrami F, Xu P. 2017. TetR family regulator *brpT* modulates biofilm formation in *Streptococcus sanguinis*. *PLoS ONE* 12:e0169301.
126. Schlafer S, Raarup MK, Meyer RL, Sutherland DS, Dige I, Nyengaard JR, Nyvad B. 2011. pH landscapes in a novel five-species model of early dental biofilm. *PLoS One* 6:e25299.
127. Wen Z, Yates D, Ahn S-J, Burne R. 2010. Biofilm formation and virulence expression by *Streptococcus mutans* are altered when grown in dual-species model. *BMC Microbiology* 10:111.
128. Bensing BA, Khedri Z, Deng L, Yu H, Prakobphol A, Fisher SJ, Chen X, Iverson TM, Varki A, Sullam PM. 2016. Novel aspects of sialoglycan recognition by the Siglec-like domains of streptococcal SRR glycoproteins. *Glycobiology* 26:1222-1234.
129. Plummer C, Wu H, Kerrigan SW, Meade G, Cox D, Douglas CWI. 2005. A serine-rich glycoprotein of *Streptococcus sanguis* mediates adhesion to platelets via GPIb. *Br J Haematol* 129:101-9.
130. Yamaguchi M, Terao Y, Ogawa T, Takahashi T, Hamada S, Kawabata S. 2006. Role of *Streptococcus sanguinis* sortase A in bacterial colonization. *Microbes Infect* 8:2791-2796.
131. Camargo TM, Stipp RN, Alves LA, Harth-Chu EN, Höfling JF, Mattos-Graner RO. 2018. Novel two-component system of *Streptococcus sanguinis* affecting functions associated with viability in saliva and biofilm formation. *Infect Immun* 86:e00942-17.
132. Morita C, Sumioka R, Nakata M, Okahashi N, Wada S, Yamashiro T, Hayashi M, Hamada S, Sumitomo T, Kawabata S. 2014. Cell wall-anchored nuclease of *Streptococcus sanguinis* contributes to escape from neutrophil extracellular trap-mediated bacteriocidal activity. *PLoS ONE* 9:e103125.
133. Amin Z, Harvey RM, Wang H, Hughes CE, Paton AW, Paton JC, Trappetti C. 2015. Isolation site influences virulence phenotype of serotype 14 *Streptococcus pneumoniae* strains belonging to multilocus sequence type 15. *Infect Immun* 83:4781-90.
134. Johnston JW, Briles DE, Myers LE, Hollingshead SK. 2006. Mn²⁺-dependent regulation of multiple genes in *Streptococcus pneumoniae* through PsaR and the resultant impact on virulence. *Infect Immun* 74:1171-1180.
135. Hendriksen WT, Bootsma HJ, van Diepen A, Estevao S, Kuipers OP, de Groot R, Hermans PWM. 2009. Strain-specific impact of PsaR of *Streptococcus pneumoniae* on global gene expression and virulence. *Microbiology* 155:1569-1579.
136. Zheng W, Tan MF, Old LA, Paterson IC, Jakubovics NS, Choo SW. 2017. Distinct biological potential of *Streptococcus gordonii* and *Streptococcus sanguinis* revealed by comparative genome analysis. *Sci Rep* 7:2949.

137. Franks SE, Ebrahimi C, Hollands A, Okumura CY, Aroian RV, Nizet V, McGillivray SM. 2014. Novel role for the *yceGH* tellurite resistance genes in the pathogenesis of *Bacillus anthracis*. *Infect Immun* 82:1132-1140.
138. Turner LS, Das S, Kanamoto T, Munro CL, Kitten T. 2009. Development of genetic tools for in vivo virulence analysis of *Streptococcus sanguinis*. *Microbiology* 155:2573-2582.
139. Martin B, Prudhomme M, Alloing G, Granadel C, Claverys JP. 2000. Cross-regulation of competence pheromone production and export in the early control of transformation in *Streptococcus pneumoniae*. *Mol Microbiol* 38:867-78.
140. Ge X, Xu P. 2012. Genome-wide gene deletions in *Streptococcus sanguinis* by high throughput PCR. *J Vis Exp* doi:doi:10.3791/4356:e4356.
141. Atkuri KR, Herzenberg LA, Niemi A-K, Cowan T, Herzenberg LA. 2007. Importance of culturing primary lymphocytes at physiological oxygen levels. *Proc Natl Acad Sci U S A* 104:4547-4552.
142. Smith AM, Heisler LE, Mellor J, Kaper F, Thompson MJ, Chee M, Roth FP, Giaever G, Nislow C. 2009. Quantitative phenotyping via deep barcode sequencing. *Genome Res* 19:1836-1842.
143. Poulsen K, Reinholdt J, Jespersgaard C, Boye K, Brown TA, Hauge M, Kilian M. 1998. A comprehensive genetic study of streptococcal immunoglobulin A1 proteases: evidence for recombination within and between species. *Infect Immun* 66:181-90.
144. Rodriguez AM. 2008. Physiological and molecular characterization of genetic competence in *Streptococcus sanguinis*. M.S. Virginia Commonwealth University, Richmond.
145. Shanker E, Federle MJ. 2017. Quorum sensing regulation of competence and bacteriocins in *Streptococcus pneumoniae* and *mutans*. *Genes (Basel)* 8:15.
146. Ross KF, Ronson CW, Tagg JR. 1993. Isolation and characterization of the lantibiotic salivaricin A and its structural gene *salA* from *Streptococcus salivarius* 20P3. *Appl Environ Microbiol* 59:2014-21.
147. Yonezawa H, Kuramitsu HK. 2005. Genetic analysis of a unique bacteriocin, Smb, produced by *Streptococcus mutans* GS5. *Antimicrob Agents Chemother* 49:541-8.
148. Dawid S, Roche AM, Weiser JN. 2007. The *blp* bacteriocins of *Streptococcus pneumoniae* mediate intraspecies competition both *in vitro* and *in vivo*. *Infect Immun* 75:443-451.
149. Ge X, Kitten T, Chen Z, Lee SP, Munro CL, Xu P. 2008. Identification of *Streptococcus sanguinis* genes required for biofilm formation and examination of their role in endocarditis virulence. *Infect Immun* 76:2551-2559.
150. Kawabata S, Hamada S. 1999. Studying biofilm formation of mutans streptococci. *Methods Enzymol* 310:513-23.
151. Shenoy AT, Brissac T, Gilley RP, Kumar N, Wang Y, Gonzalez-Juarbe N, Hinkle WS, Daugherty SC, Shetty AC, Ott S, Tallon LJ, Deshane J, Tettelin H, Orihuela CJ. 2017. *Streptococcus pneumoniae* in the heart subvert the host response through biofilm-mediated resident macrophage killing. *PLoS Pathog* 13:e1006582.

152. Zhu B, Ge X, Stone V, Kong X, El-Rami F, Liu Y, Kitten T, Xu P. 2017. *ciaR* impacts biofilm formation by regulating an arginine biosynthesis pathway in *Streptococcus sanguinis* SK36. *Sci Rep* 7:17183.
153. Bowen WH. 2002. Do we need to be concerned about dental caries in the coming millennium? *Crit Rev Oral Biol Med* 13:126-131.
154. Koo H, Xiao J, Klein MI. 2009. Extracellular polysaccharides matrix--an often forgotten virulence factor in oral biofilm research. *Int J Oral Sci* 1:229-34.
155. Eijkelkamp BA, McDevitt CA, Kitten T. 2015. Manganese uptake and streptococcal virulence. *Biometals* 28:491-508.
156. Nevo Y, Nelson N. 2006. The NRAMP family of metal-ion transporters. *Biochim Biophys Acta* 1763:609-20.
157. Colomer-Winter C, Flores-Mireles AL, Baker SP, Frank KL, Lynch AJL, Hultgren SJ, Kitten T, Lemos JA. 2018. Manganese acquisition is essential for virulence of *Enterococcus faecalis*. *PLOS Pathogens* 14:e1007102.
158. Manso AS, Chai MH, Atack JM, Furi L, De Ste Croix M, Haigh R, Trappetti C, Ogunniyi AD, Shewell LK, Boitano M, Clark TA, Korlach J, Blades M, Mirkes E, Gorban AN, Paton JC, Jennings MP, Oggioni MR. 2014. A random six-phase switch regulates pneumococcal virulence via global epigenetic changes. *Nature Communications* 5:5055.
159. Oliver MB, Basu Roy A, Kumar R, Lefkowitz EJ, Swords WE. 2017. *Streptococcus pneumoniae* TIGR4 phase-locked opacity variants differ in virulence phenotypes. *mSphere* 2.
160. Li J, Li J-W, Feng Z, Wang J, An H, Liu Y, Wang Y, Wang K, Zhang X, Miao Z, Liang W, Sebra R, Wang G, Wang W-C, Zhang J-R. 2016. Epigenetic switch driven by DNA inversions dictates phase variation in *Streptococcus pneumoniae*. *PLOS Pathogens* 12:e1005762.
161. Blow MJ, Clark TA, Daum CG, Deutschbauer AM, Fomenkov A, Fries R, Froula J, Kang DD, Malmstrom RR, Morgan RD, Posfai J, Singh K, Visel A, Wetmore K, Zhao Z, Rubin EM, Korlach J, Pennacchio LA, Roberts RJ. 2016. The Epigenomic landscape of prokaryotes. *PLOS Genetics* 12:e1005854.
162. Sánchez-Romero MA, Cota I, Casadesús J. 2015. DNA methylation in bacteria: from the methyl group to the methylome. *Curr Opin Microbiol* 25:9-16.
163. Do T, Gilbert SC, Klein J, Warren S, Wade WG, Beighton D. 2011. Clonal structure of *Streptococcus sanguinis* strains isolated from endocarditis cases and the oral cavity. *Mol Oral Microbiol* 26:291-302.
164. Strom BL, Abrutyn E, Berlin JA, Kinman JL, Feldman RS, Stolley PD, Levison ME, Korzeniewski OM, Kaye D. 1998. Dental and cardiac risk factors for infective endocarditis - A population-based, case-control study. *Ann Intern Med* 129:761-769.
165. Gaustad P. 1979. Genetic transformation in *Streptococcus sanguis*. Distribution of competence and competence factors in a collection of strains. *Acta Pathol Microbiol Scand [B]* 87B:123-8.
166. Cotter PD, Hill C, Ross RP. 2005. Bacteriocins: developing innate immunity for food. *Nat Rev Microbiol* 3:777-88.

167. Steinmoen H, Teigen A, Havarstein LS. 2003. Competence-induced cells of *Streptococcus pneumoniae* lyse competence-deficient cells of the same strain during cocultivation. *J Bacteriol* 185:7176-83.
168. Wang M, Schaefer AL, Dandekar AA, Greenberg EP. 2015. Quorum sensing and policing of *Pseudomonas aeruginosa* social cheaters. *Proc Natl Acad Sci USA* 112:2187-2191.
169. Stavrou AA, Mixao V, Boekhout T, Gabaldon T. 2018. Misidentification of genome assemblies in public databases: The case of *Naumovozyma dairenensis* and proposal of a protocol to correct misidentifications. *Yeast* 35:425-429.
170. Ballester AR, Marcet-Houben M, Levin E, Sela N, Selma-Lazaro C, Carmona L, Wisniewski M, Droby S, Gonzalez-Candelas L, Gabaldon T. 2015. Genome, transcriptome, and functional analyses of *Penicillium expansum* provide new insights into secondary metabolism and pathogenicity. *Mol Plant Microbe Interact* 28:232-48.
171. Sonnhammer EL, von Heijne G, Krogh A. 1998. A hidden Markov model for predicting transmembrane helices in protein sequences. *Proc Int Conf Intell Syst Mol Biol* 6:175-82.
172. Krogh A, Larsson B, von Heijne G, Sonnhammer ELL. 2001. Predicting transmembrane protein topology with a hidden Markov model: application to complete genomes. *J Mol Biol* 305:567-580.
173. Bendtsen JD, Nielsen H, von Heijne G, Brunak S. 2004. Improved prediction of signal peptides: SignalP 3.0. *J Mol Biol* 340:783-95.
174. Kelley LA, Mezulis S, Yates CM, Wass MN, Sternberg MJ. 2015. The Phyre2 web portal for protein modeling, prediction and analysis. *Nat Protoc* 10:845-58.
175. Omasits U, Ahrens CH, Muller S, Wollscheid B. 2014. Protter: interactive protein feature visualization and integration with experimental proteomic data. *Bioinformatics* 30:884-6.
176. Andreini C, Bertini I, Cavallaro G, Holliday G, Thornton J. 2008. Metal ions in biological catalysis: from enzyme databases to general principles. *J Biol Inorg Chem* 13:1205-1218.
177. Makthal N, Nguyen K, Do H, Gavagan M, Chandransu P, Helmann JD, Olsen RJ, Kumaraswami M. 2017. A critical role of zinc importer AdcABC in Group A *Streptococcus*-host interactions during infection and its implications for vaccine development. *EBioMedicine* 21:131-141.
178. Kehl-Fie Thomas E, Chitayat S, Hood MI, Damo S, Restrepo N, Garcia C, Munro Kim A, Chazin Walter J, Skaar Eric P. 2011. Nutrient metal sequestration by calprotectin inhibits bacterial ssuperoxide defense, enhancing neutrophil killing of *Staphylococcus aureus*. *Cell Host & Microbe* 10:158-164.
179. Shafeeq S, Kuipers OP, Kloosterman TG. 2013. The role of zinc in the interplay between pathogenic streptococci and their hosts. *Mol Microbiol* 88:1047-1057.
180. Lusitani D, Malawista SE, Montgomery RR. 2003. Calprotectin, an abundant cytosolic protein from human polymorphonuclear leukocytes, inhibits the growth of *Borrelia burgdorferi*. *Infect Immun* 71:4711-6.
181. Sun Y, Lu Y, Engeland CG, Gordon SC, Sroussi HY. 2013. The anti-oxidative, anti-inflammatory, and protective effect of S100A8 in endotoxemic mice. *Mol Immunol* 53:443-9.

182. Aust SD. 1995. Ferritin as a source of iron and protection from iron-induced toxicities. *Toxicol Lett* 82-83:941-944.
183. Spatafora G, Moore M, Landgren S, Stonehouse E, Michalek S. 2001. Expression of *Streptococcus mutans fimA* is iron-responsive and regulated by a DtxR homologue. *Microbiology* 147:1599-610.
184. Oetjen J, Fives-Taylor P, Froeliger EH. 2002. The divergently transcribed *Streptococcus parasanguis* virulence-associated *fimA* operon encoding an Mn²⁺-responsive metal transporter and *pepO* encoding a zinc metallopeptidase are not coordinately regulated. *Infect Immun* 70:5706-5714.
185. Mechold U, Murphy H, Brown L, Cashel M. 2002. Intramolecular regulation of the opposing (p)ppGpp catalytic activities of Rel(Seq), the Rel/Spo enzyme from *Streptococcus equisimilis*. *J Bacteriol* 184:2878-88.
186. Hogg T, Mechold U, Malke H, Cashel M, Hilgenfeld R. 2004. Conformational antagonism between opposing active sites in a bifunctional RelA/SpoT homolog modulates (p)ppGpp metabolism during the stringent response. *Cell* 117:57-68.
187. Nascimento MM, Lemos JA, Abranches J, Lin VK, Burne RA. 2008. Role of RelA of *Streptococcus mutans* in global control of gene expression. *J Bacteriol* 190:28-36.
188. Kehres DG, Zaharik ML, Finlay BB, Maguire ME. 2000. The NRAMP proteins of salmonella typhimurium and escherichia coli are selective manganese transporters involved in the response to reactive oxygen. *Mol Microbiol* 36:1085-100.
189. Anderson AS, Scully IL, Timofeyeva Y, Murphy E, McNeil LK, Mininni T, Nuñez L, Carriere M, Singer C, Dilts DA, Jansen KU. 2012. *Staphylococcus aureus* manganese transport protein C is a highly conserved cell surface protein that elicits protective immunity against *S. aureus* and *Staphylococcus epidermidis*. *J Infect Dis* 205:1688-1696.
190. Ilari A, Pescatori L, Di Santo R, Battistoni A, Ammendola S, Falconi M, Berlutti F, Valenti P, Chiancone E. 2016. Salmonella enterica serovar Typhimurium growth is inhibited by the concomitant binding of Zn(II) and a pyrrolyl-hydroxamate to ZnuA, the soluble component of the ZnuABC transporter. *Biochim Biophys Acta* 1860:534-41.
191. Salvadori G, Junges R, Morrison DA, Petersen FC. 2016. Overcoming the barrier of low efficiency during genetic transformation of *Streptococcus mitis*. *Front Microbiol* 7:1009.
192. Fenno JC, Shaikh A, Spatafora G, Fives-Taylor P. 1995. The *fimA* locus of *Streptococcus parasanguis* encodes an ATP-binding membrane transport system. *Mol Microbiol* 15:849-63.
193. Novak R, Braun JS, Charpentier E, Tuomanen E. 1998. Penicillin tolerance genes of *Streptococcus pneumoniae*: the ABC-type manganese permease complex Psa. *Mol Microbiol* 29:1285-1296.
194. Rodionov DA, Hebbeln P, Eudes A, ter Beek J, Rodionova IA, Erkens GB, Slotboom DJ, Gelfand MS, Osterman AL, Hanson AD, Eitinger T. 2009. A novel class of modular transporters for vitamins in prokaryotes. *J Bacteriol* 191:42-51.

195. Hebbeln P, Rodionov DA, Alfandega A, Eitinger T. 2007. Biotin uptake in prokaryotes by solute transporters with an optional ATP-binding cassette-containing module. *Proc Natl Acad Sci U S A* 104:2909-14.
196. Henderson GB, Zevely EM, Huennekens FM. 1979. Mechanism of folate transport in *Lactobacillus casei*: evidence for a component shared with the thiamine and biotin transport systems. *J Bacteriol* 137:1308-14.
197. Erkens GB, Slotboom DJ. 2010. Biochemical characterization of ThiT from *Lactococcus lactis*: a thiamin transporter with picomolar substrate binding affinity. *Biochemistry* 49:3203-12.
198. Burgess CM, Slotboom DJ, Geertsma ER, Duurkens RH, Poolman B, van Sinderen D. 2006. The riboflavin transporter RibU in *Lactococcus lactis*: molecular characterization of gene expression and the transport mechanism. *J Bacteriol* 188:2752-60.
199. Rodionov DA, Hebbeln P, Gelfand MS, Eitinger T. 2006. Comparative and functional genomic analysis of prokaryotic nickel and cobalt uptake transporters: evidence for a novel group of ATP-binding cassette transporters. *J Bacteriol* 188:317-27.
200. Filipe SR, Severina E, Tomasz A. 2002. The murMN operon: a functional link between antibiotic resistance and antibiotic tolerance in *Streptococcus pneumoniae*. *Proc Natl Acad Sci U S A* 99:1550-5.
201. Karpowich NK, Wang DN. 2013. Assembly and mechanism of a group II ECF transporter. *Proc Natl Acad Sci U S A* 110:2534-9.
202. Josts I, Almeida Hernandez Y, Andreeva A, Tidow H. 2016. Crystal structure of a Group I energy coupling factor vitamin transporter S component in complex with its cognate substrate. *Cell Chem Biol* 23:827-836.
203. Millar BC, Moore JE. 2004. Emerging issues in infective endocarditis. *Emerg Infect Dis* 10:1110-6.
204. Durack DT. 1995. Prevention of infective endocarditis. *N Engl J Med* 332:38-44.
205. Cremieux AC, Maziere B, Vallois JM, Ottaviani M, Azancot A, Raffoul H, Bouvet A, Pocard JJ, Carbon C. 1989. Evaluation of antibiotic diffusion into cardiac vegetations by quantitative autoradiography. *J Infect Dis* 159:938-44.
206. McCormick JK, Hirt H, Waters CM, Tripp TJ, Dunny GM, Schlievert PM. 2001. Antibodies to a surface-exposed, N-terminal domain of aggregation substance are not protective in the rabbit model of *Enterococcus faecalis* infective endocarditis. *Infect Immun* 69:3305-3314.

Vita

Shannon Paige Baker is a native South Carolinian turned Virginian. Born October 13, 1991, in Columbia, SC, she always displayed a passion for science. She continued that passion at Clemson University, where she graduated in the Spring of 2013 with a B.S. in Microbiology. After graduation she took a gap year before applying to graduate school. During that time, she landed her first job as a laboratory assistant in a nanotechnology lab at the Medical University of South Carolina. In 2014, she was accepted into the Biomedical Sciences Doctoral Program at Virginia Commonwealth University in Richmond, Virginia. Upon entry into the program, her second laboratory rotation was in the lab of Dr. Todd Kitten, a placement that she ended up finalizing in early 2015.

Awards and Honors:

Symposium on Membrane Protein Production and Analysis Travel Award (Spring, 2018)
 Phi Kappa Phi Academic Achievement Award (Spring, 2018)
 Best Presentation at Philips Institute Research Day (Spring, 2017)
 Mid-Atlantic Microbial Pathogenesis Meeting Travel Award (Spring, 2017)
 ASM Virginia Travel Award (Fall, 2016)
 Phi Kappa Phi Nomination Award (Spring, 2016)
 Graduated Cum Laude (Spring 2013)
 Palmetto Fellows State Scholarship (Fall 2010-Spring 2013)
 Presidential Scholarship via Clemson (Fall 2010- Spring 2013)

Service Activities and Organizational Affiliations:

AAAS/Science Program for Excellence in Science (Fall 2018- Current)
 Vice President of Communications for Women In Science (Spring 2017- Spring 2018)
 Women in Science Member (Fall 2014- Current)
 President of the Microbiology Student Group (Fall 2016-Spring 2017)
 Student Recruiter for the Biomedical Sciences Doctoral Portal (Spring, 2016)
 Student Recruiter for the Philips Institute for Oral Health Research (Spring, 2017)
 American Society for Microbiology (Fall 2015-Current)
 Gamma Sigma Sigma (Spring 2012- Current)

Publications

1. **Baker SP**, Nulton TJ, Kitten T. 2018. Genomic, phenotypic, and virulence analysis of *Streptococcus sanguinis* oral and infective endocarditis isolates. *Infect Immun* doi:10.1128/iai.00703-18:IAI.00703-18.
2. Colomer-Winter C, Flores-Mireles AL, **Baker SP**, Frank KL, Lynch AJL, Hultgren SJ, Kitten T, Lemos JA. 2018. Manganese acquisition is essential for virulence of *Enterococcus faecalis*. *PLOS Pathogens* 14:e1007102.